Archaeology and Human Evolution

Class Figures

Process of Speciation

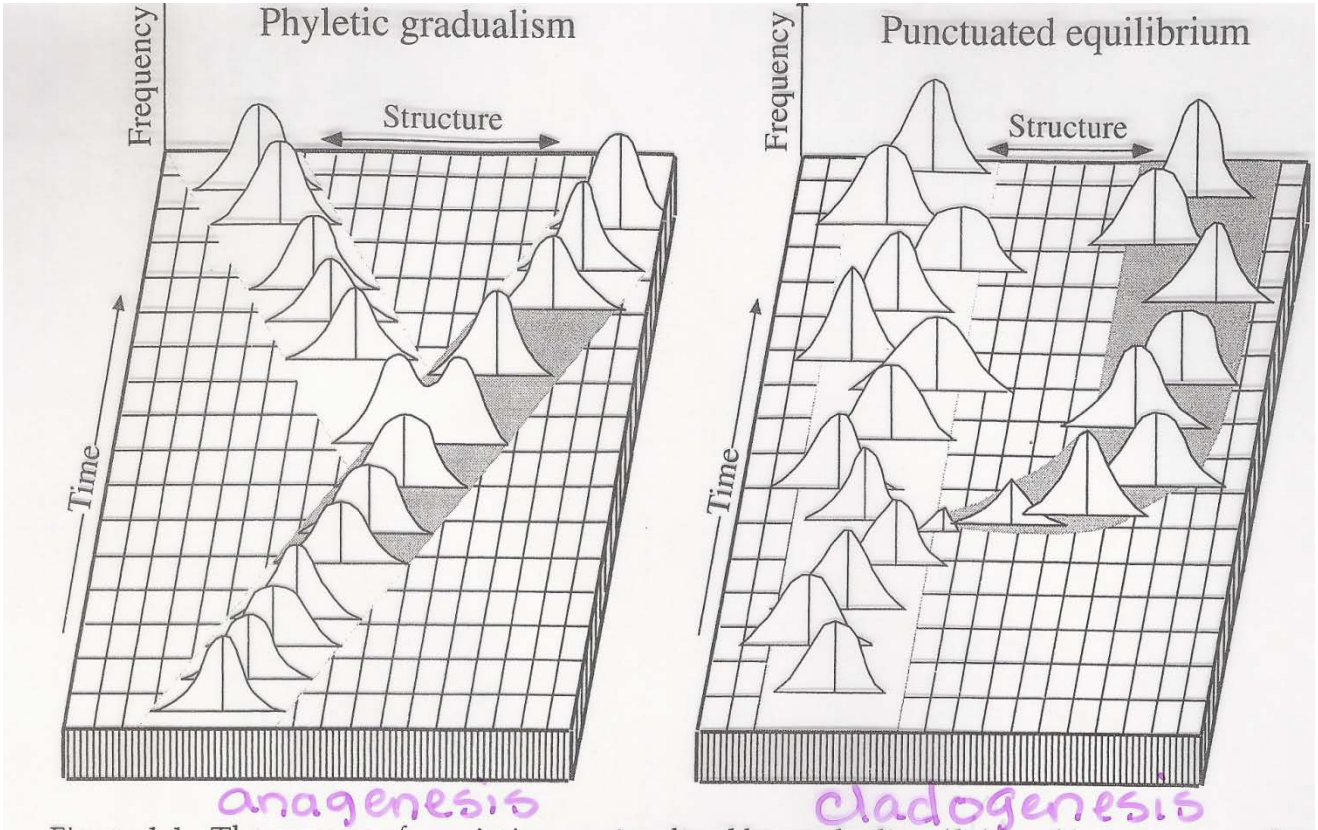

Figure 1.1. The process of speciation as visualized by gradualists (*left*) and by advocates of punctuated equilibrium (*right*) (redrawn after 2343, p. 62). The bell-shaped curves reflect the distribution of one or more morphological traits at different times. Distinct species are indicated by the blank and shaded paths the curves rest on. The gradualist model postulates a steady, continuous shift in modal morphology along branches. When the shift is extensive enough, a new species is born. The punctuationalist model postulates essentially random, noncumulative morphological change through time. A new species emerges only when innovations become fixed in a small peripheral population. This population then diverges rapidly before settling into a conservative mode where change once again tends to be random and noncumulative.

Hominid Phylogeny

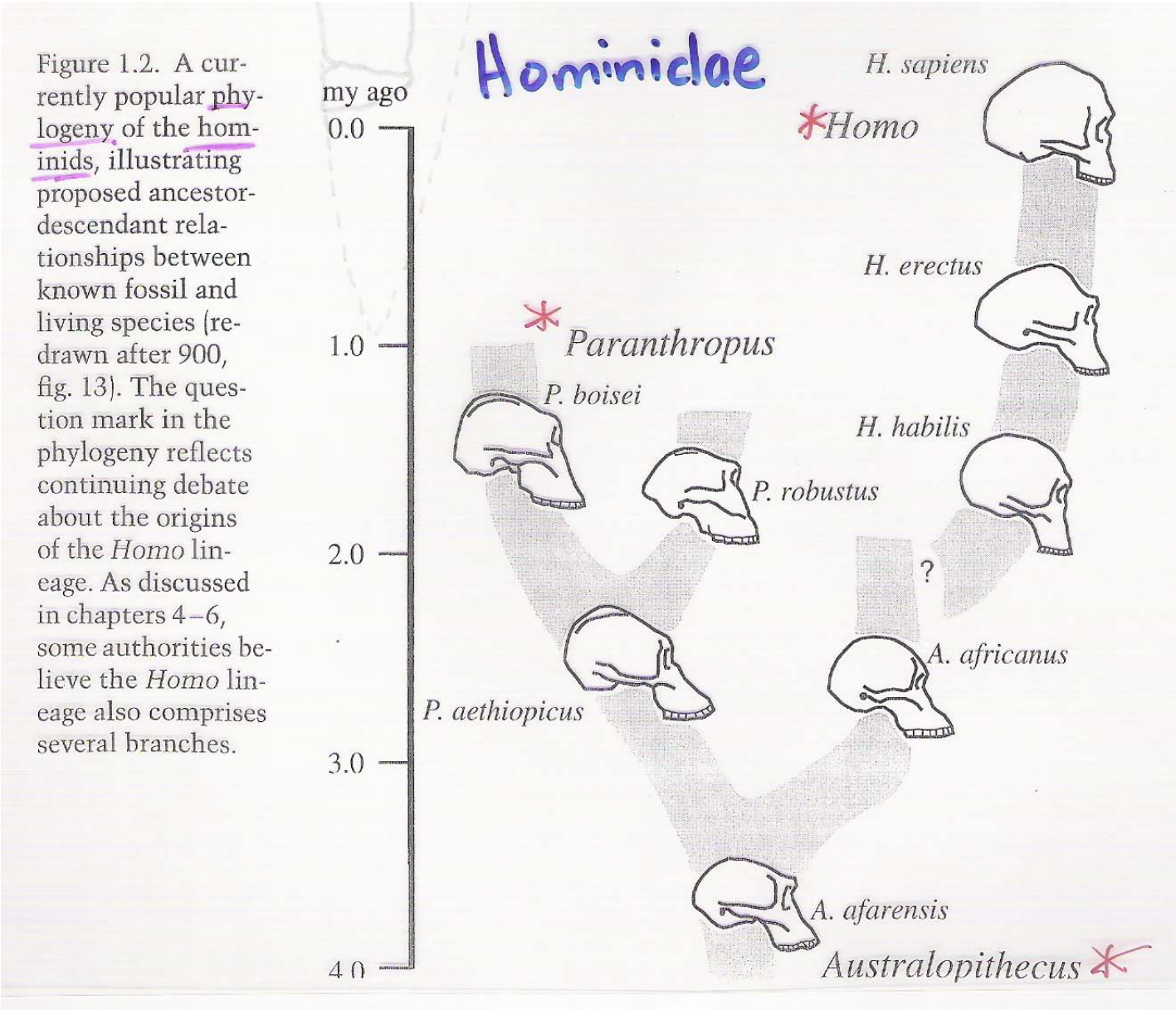

Taxonomy

Table 1.1. A Classification of Living People Involving Twenty-one Potential Levels in the Linnaean Hierarchy

*KINGDOM: Animalia
*PHYLUM: Chordata
SUBPHYLUM: Vertebrata
SUPERCLASS: Tetrapoda
*CLASS: Mammalia
SUBCLASS: Theria
INFRACLASS: Eutheria
COHORT: Unguiculata
SUPERORDER: ———
*ORDER: Primates
SUBORDER: Anthropoidea
INFRAORDER: Catarrhini
SUPERFAMILY: Hominoidea
*FAMILY: Hominidae
SUBFAMILY: Homininae
TRIBE: Hominini
SUBTRIBE: ———
*GENUS: *Homo*
SUBGENUS: (*Homo*)
*SPECIES: *sapiens*
SUBSPECIES: *sapiens*

Note: A dash follows a level for which no taxon is in common use. Asterisks designate the seven obligatory and most basic levels in the Linnaean system.

Classification of Living Primates

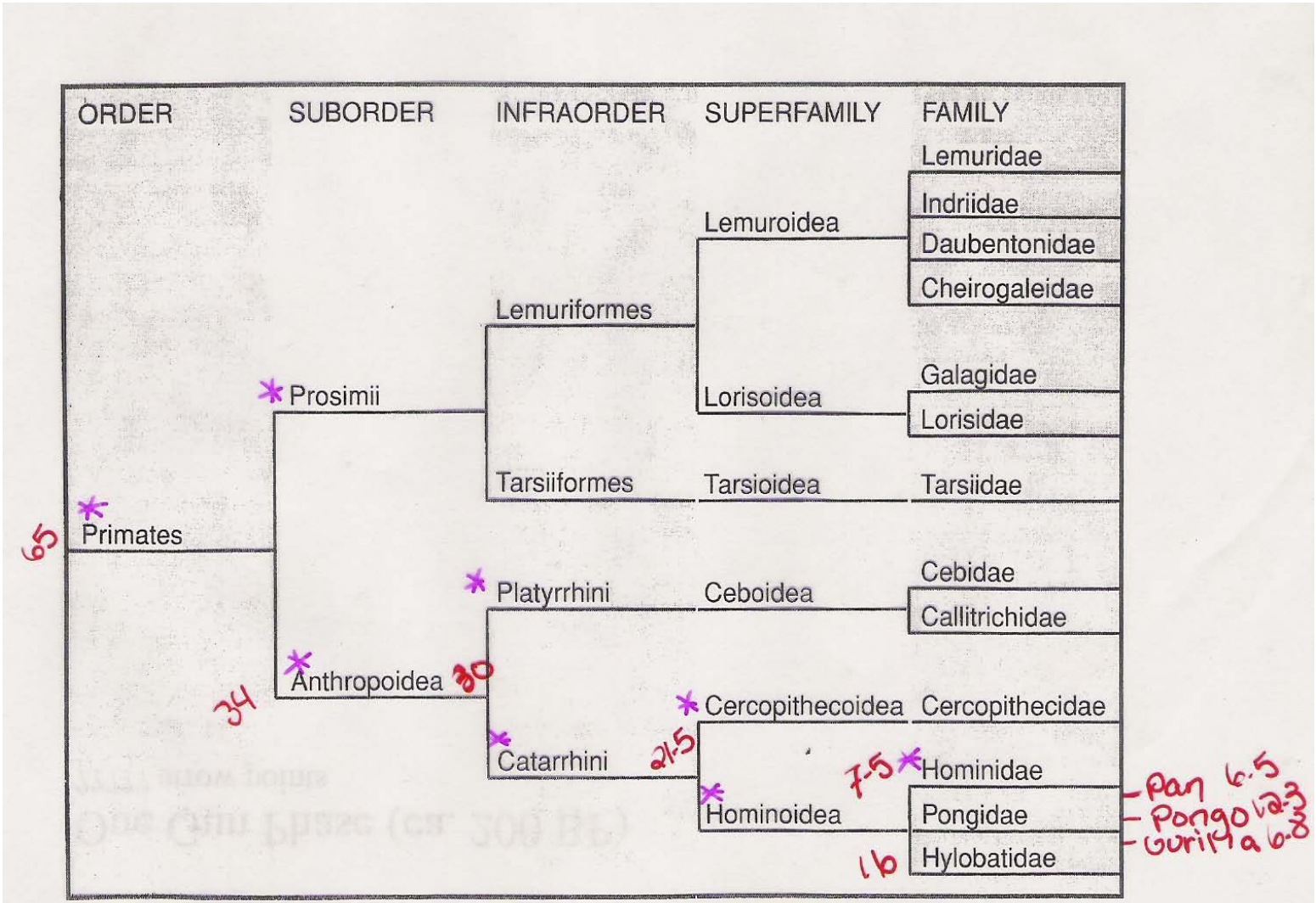

Figure 1.3. A popular hierarchical classification of the living Primates down to the family level. Chapter 2 discusses alternatives.

Cladogram

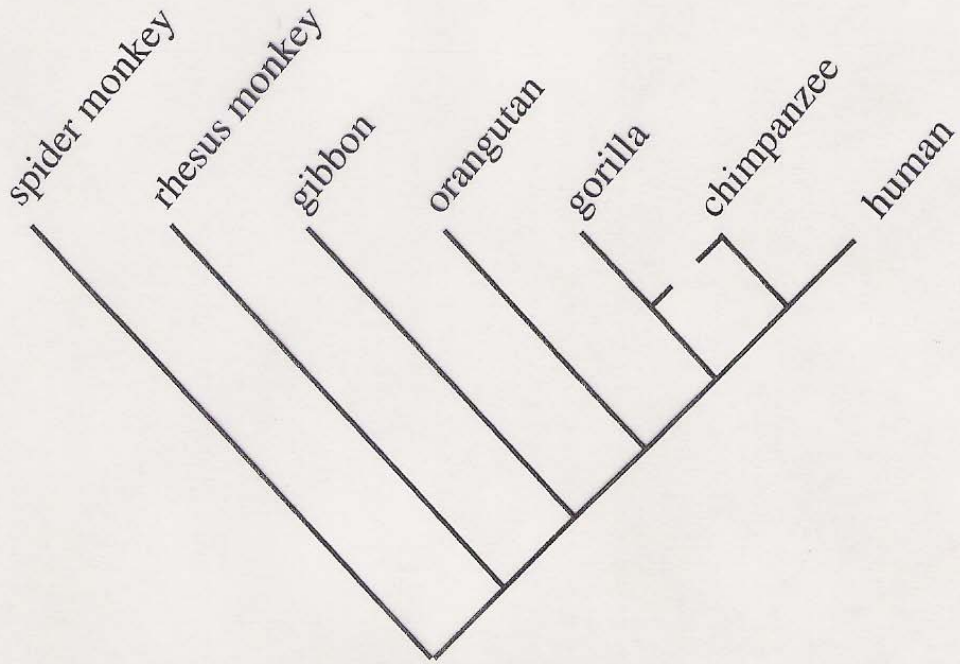

Figure 1.4. A cladogram illustrating the evolutionary relationships among humans (*Homo*), chimpanzees (*Pan*), gorillas (*Gorilla*), orangutans (*Pongo*), gibbons (*Hylobates*), rhesus monkeys (*Macaca*), and spider monkeys (*Ateles*), based on inferred derived similarities in the structure of the beta-globin gene (data in 858). Other biomolecular and morphological analyses produce similar cladograms, except that morphological data often suggest that the chimpanzees and gorilla are more closely related to each other than either is to people. If the chimpanzees and gorilla share a closer common ancestor with each other than either does with people, then the cladogram should be altered, and the broken line should replace the solid line leading to the chimpanzees.

Geologic Time Scale

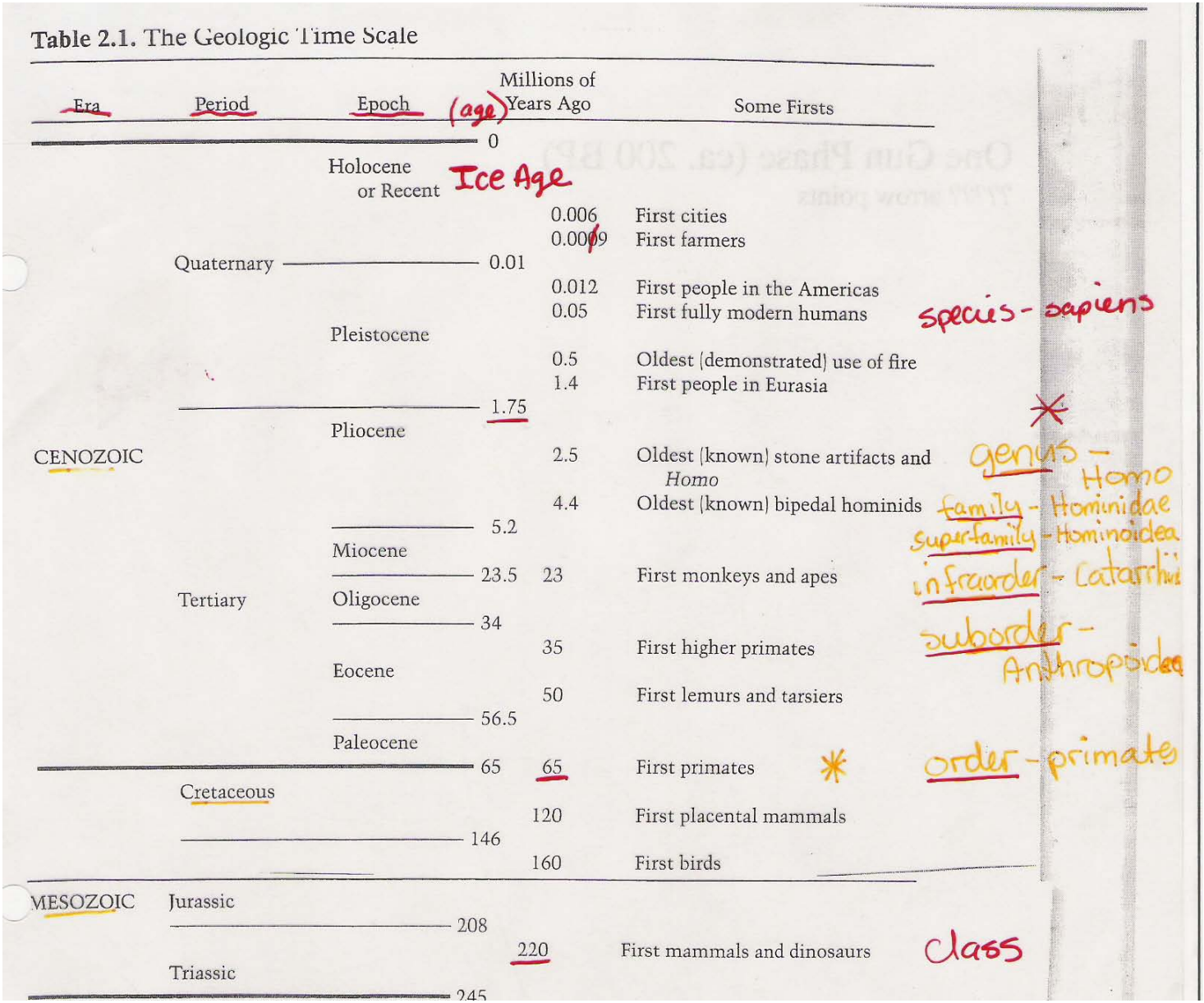

Table 2.1. The Geologic Time Scale

Era	Period	Epoch	Millions of Years Ago (age)		Some Firsts
			0		
		Holocene or Recent			Ice Age
				0.006	First cities
				0.009	First farmers
	Quaternary		0.01		
				0.012	First people in the Americas
				0.05	First fully modern humans
		Pleistocene			
				0.5	Oldest (demonstrated) use of fire
				1.4	First people in Eurasia
			1.75		
		Pliocene			
CENOZOIC				2.5	Oldest (known) stone artifacts and *Homo*
				4.4	Oldest (known) bipedal hominids
			5.2		
		Miocene			
			23.5	23	First monkeys and apes
	Tertiary	Oligocene			
			34		
				35	First higher primates
		Eocene			
				50	First lemurs and tarsiers
			56.5		
		Paleocene			
			65	65	First primates
	Cretaceous				
				120	First placental mammals
			146		
				160	First birds
MESOZOIC	Jurassic				
			208		
				220	First mammals and dinosaurs
	Triassic				
			245		

species - sapiens

genus - Homo

family - Hominidae

superfamily - Hominoidea

infraorder - Catarrhini

suborder - Anthropoidea

order - primates

class

Geologic Time Scale

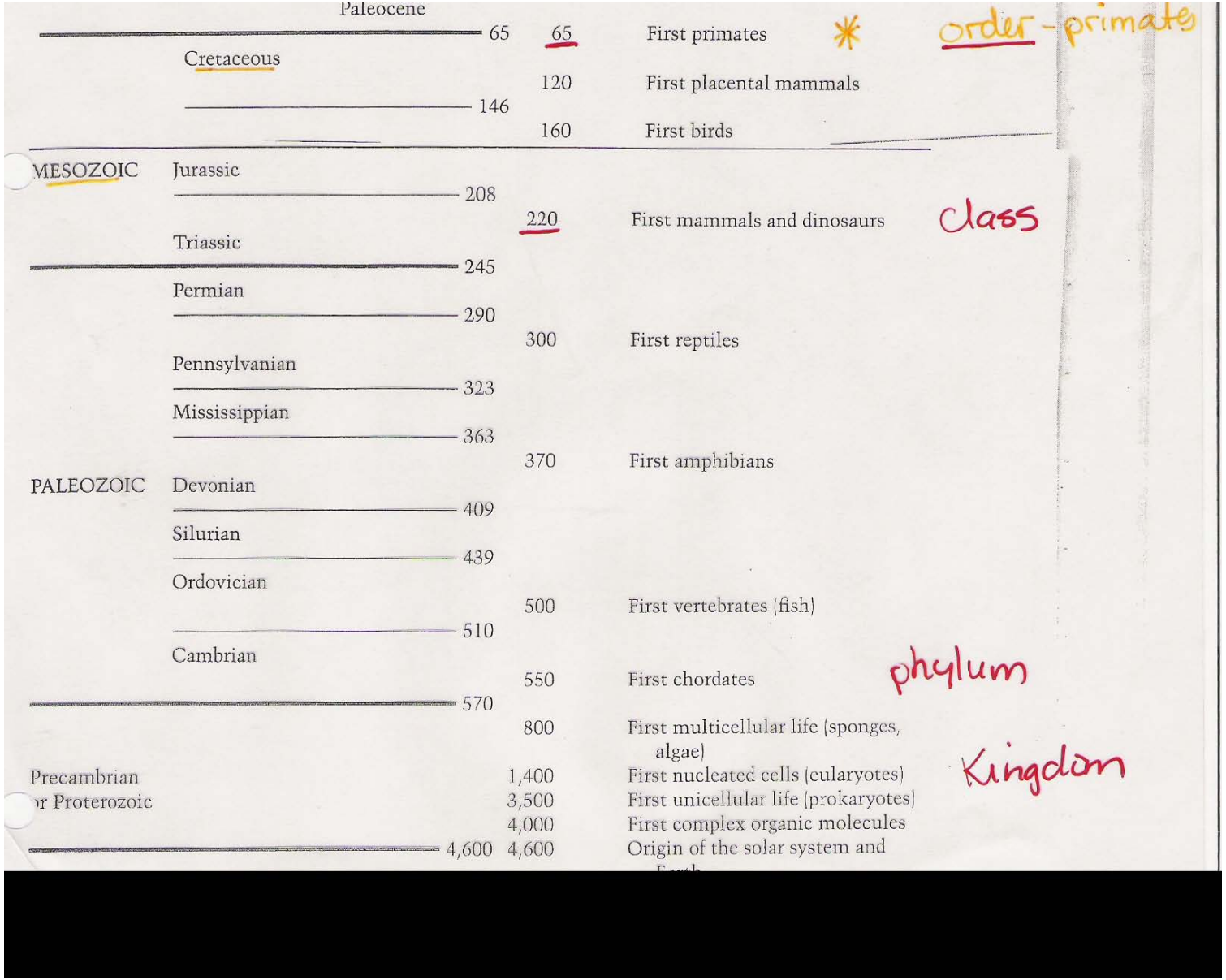

	Paleocene	65	65	First primates * order - primates
	Cretaceous	146	120	First placental mammals
			160	First birds
MESOZOIC	Jurassic	208	220	First mammals and dinosaurs class
	Triassic	245		
	Permian	290	300	First reptiles
	Pennsylvanian	323		
	Mississippian	363	370	First amphibians
PALEOZOIC	Devonian	409		
	Silurian	439		
	Ordovician	510	500	First vertebrates (fish)
	Cambrian	570	550	First chordates phylum
			800	First multicellular life (sponges, algae)
Precambrian or Proterozoic			1,400	First nucleated cells (eularyotes) Kingdom
			3,500	First unicellular life (prokaryotes)
			4,000	First complex organic molecules
		4,600	4,600	Origin of the solar system and

Biostratigraphic Dating

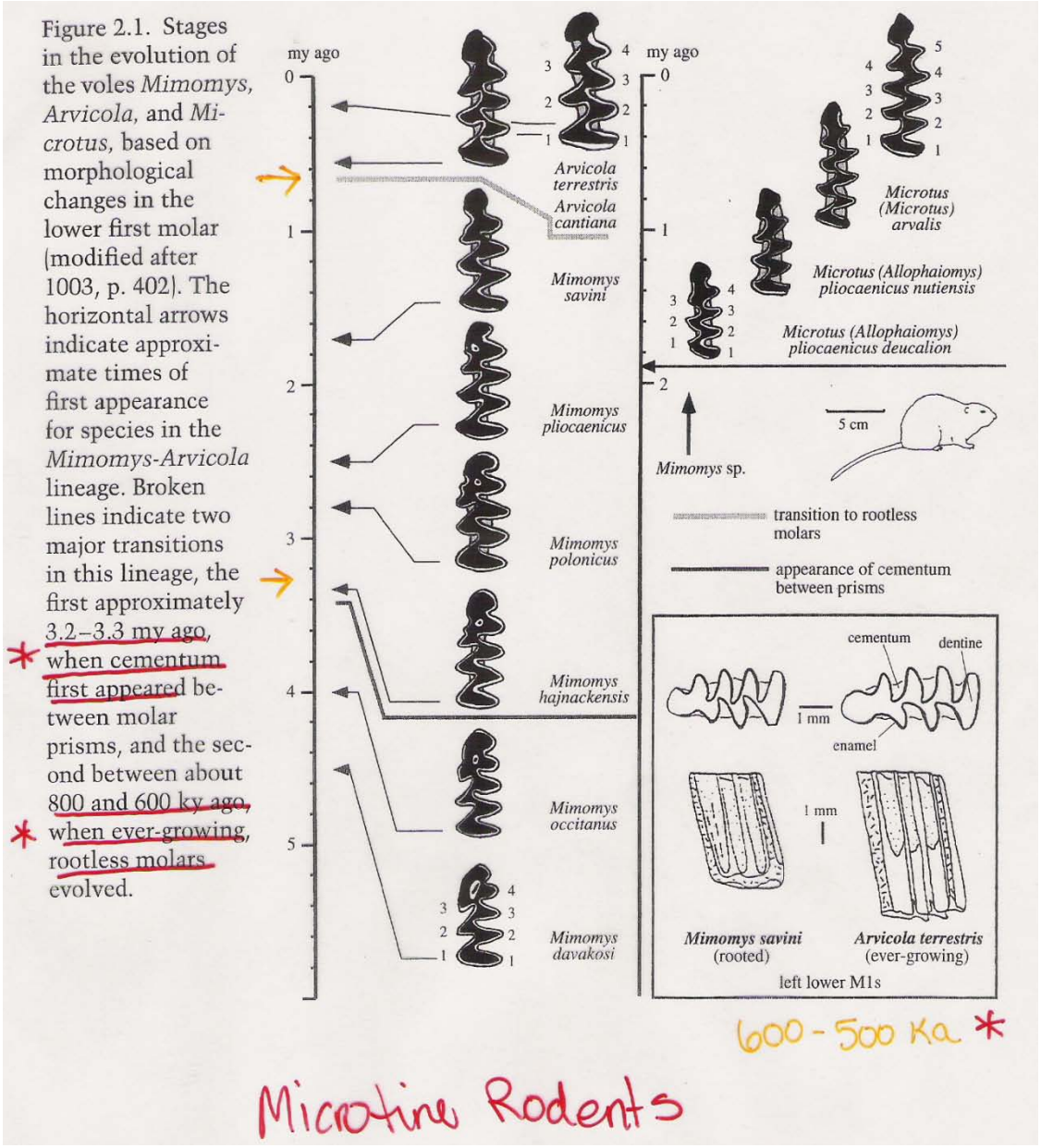

Figure 2.1. Stages in the evolution of the voles *Mimomys*, *Arvicola*, and *Microtus*, based on morphological changes in the lower first molar (modified after 1003, p. 402). The horizontal arrows indicate approximate times of first appearance for species in the *Mimomys-Arvicola* lineage. Broken lines indicate two major transitions in this lineage, the first approximately 3.2–3.3 my ago, when cementum first appeared between molar prisms, and the second between about 800 and 600 ky ago, when ever-growing, rootless molars evolved.

600 - 500 Ka *

Microtine Rodents

Biostratigraphic Dating

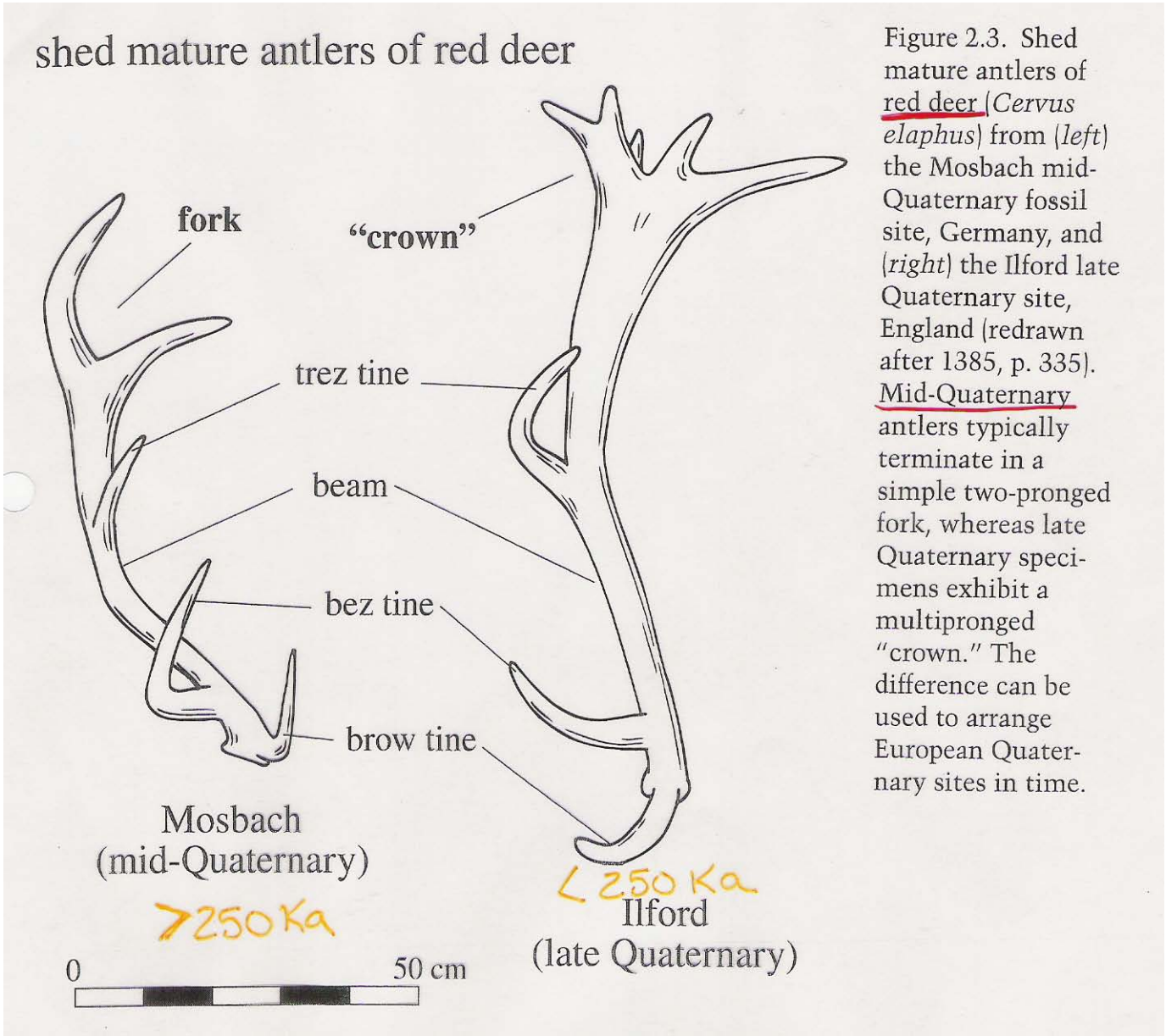

Figure 2.3. Shed mature antlers of red deer (*Cervus elaphus*) from (*left*) the Mosbach mid-Quaternary fossil site, Germany, and (*right*) the Ilford late Quaternary site, England (redrawn after 1385, p. 335). Mid-Quaternary antlers typically terminate in a simple two-pronged fork, whereas late Quaternary specimens exhibit a multipronged "crown." The difference can be used to arrange European Quaternary sites in time.

Biostratigraphic Dating

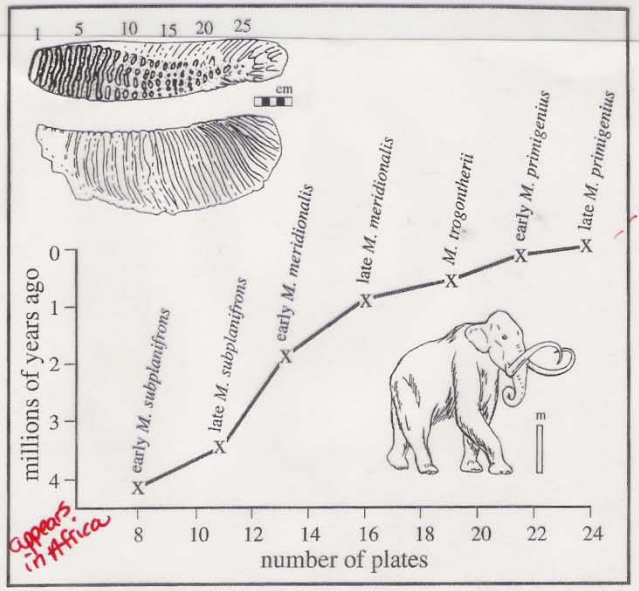

Figure 2.4. The average number of plates on third molars in successive species of *Mammuthus*, from its first appearance in Africa before 4 my ago until its extinction on the Eurasian mainland, roughly 1.5 my ago (redrawn after 1387, p. 150). The earliest species—*M. subplanifrons*—was exclusively African, but later species—*M. meridionalis*, *M. trogontherii*, and *M. primigenius*—were Eurasian. *M. primigenius* is known popularly as the woolly mammoth from its hairy coat, which Paleolithic people depicted in their art and which is sometimes partially preserved in permanently frozen ground. The mammoths can be distinguished from other elephants by their domed braincases and their inwardly curved tusks, shown on a reconstructed woolly mammoth in the figure (redrawn after 2096, p. 44). The molars of mammoths and other elephants comprise a series of subparallel enamel plates that are held together by cementum. Each plate has an enamel shell surrounding dentine. Occlusal and lateral views (*top left*) illustrate the basic structure on an upper third molar of *Mammuthus primigenius* from Last Glacial deposits in Britain (redrawn after 2096, p. 47). The alternation of enamel and dentine produced a rough occlusal surface that helped in grinding vegetal foods. In *Mammuthus* (and *Elephas*, as discussed in the text), natural selection for a more abrasive diet favored an increase in the number of plates through time. In Last Glacial *M. primigenius*, the third molars sometimes had more than twenty-five plates, as illustrated on the occlusal view in the figure.

Climatic Reconstruction

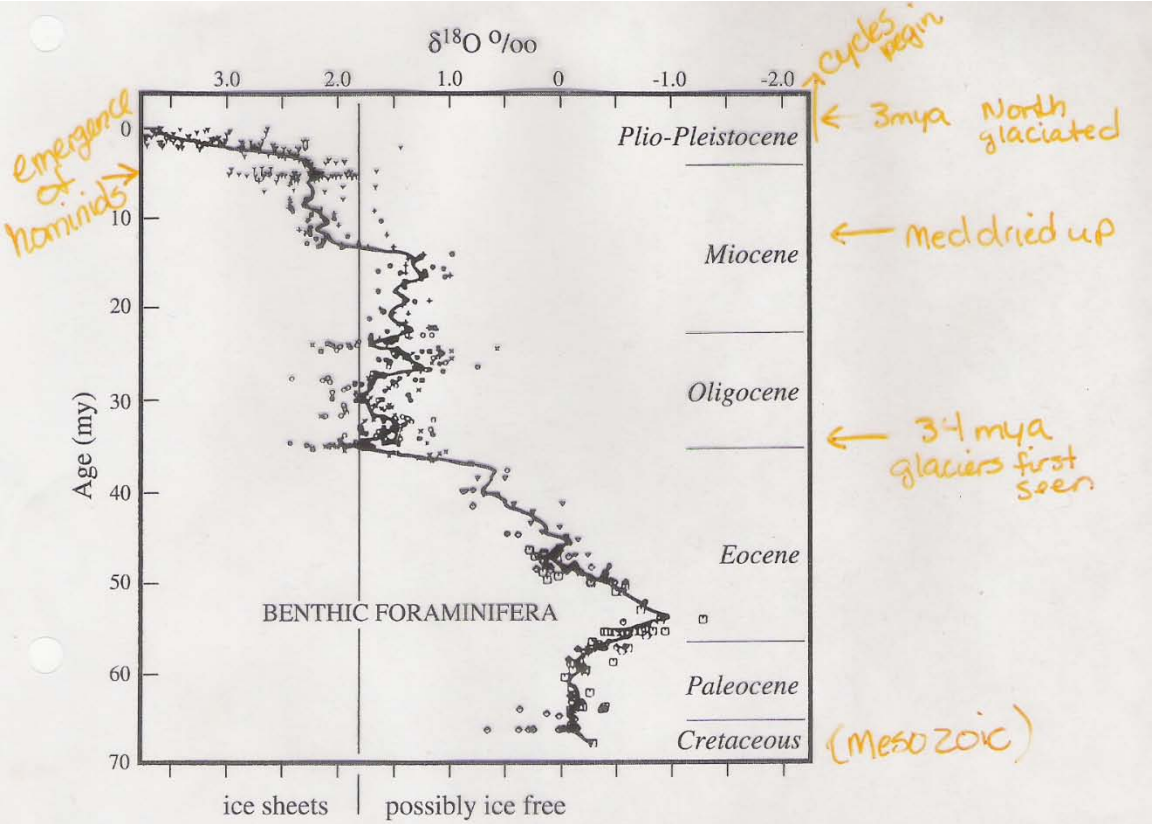

Figure 2.11. Composite δ oxygen-18 ($\delta^{18}O$) record for Atlantic Cenozoic localities (modified after 1561, fig. 1). The vertical scale is time in millions of years before the present. The horizontal scale tracks relative change in the concentration of ^{18}O in deepwater (benthic) foraminifera. Small positive or negative $\delta^{18}O$ values (to the right) indicate a low likelihood for continental ice sheets. Large positive values (to the left) indicate a high probability. The continuous curve is based on individual $\delta^{18}O$ values obtained in different deep-sea cores that cover the entire Cenozoic era. A transient ice sheet probably formed in east Antarctica during the Oligocene, but it became permanent only from the mid-Miocene, beginning about 14 my ago. Ice sheets formed in the Northern Hemisphere only after the mid-Pliocene, beginning about 3.2 my ago.

Climatic Reconstruction

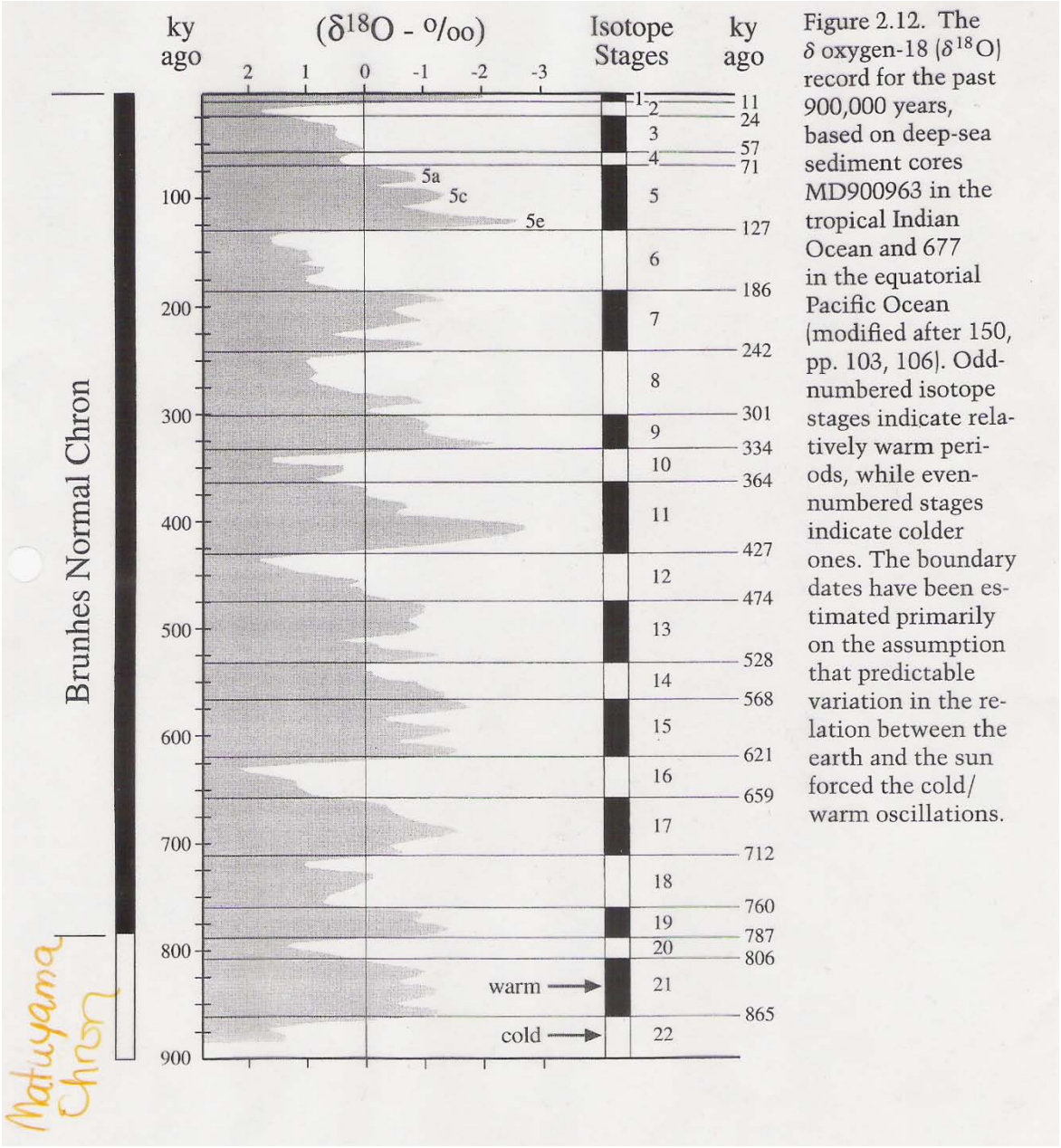

Figure 2.12. The δ oxygen-18 ($\delta^{18}O$) record for the past 900,000 years, based on deep-sea sediment cores MD900963 in the tropical Indian Ocean and 677 in the equatorial Pacific Ocean (modified after 150, pp. 103, 106). Odd-numbered isotope stages indicate relatively warm periods, while even-numbered stages indicate colder ones. The boundary dates have been estimated primarily on the assumption that predictable variation in the relation between the earth and the sun forced the cold/warm oscillations.

The Skeleton

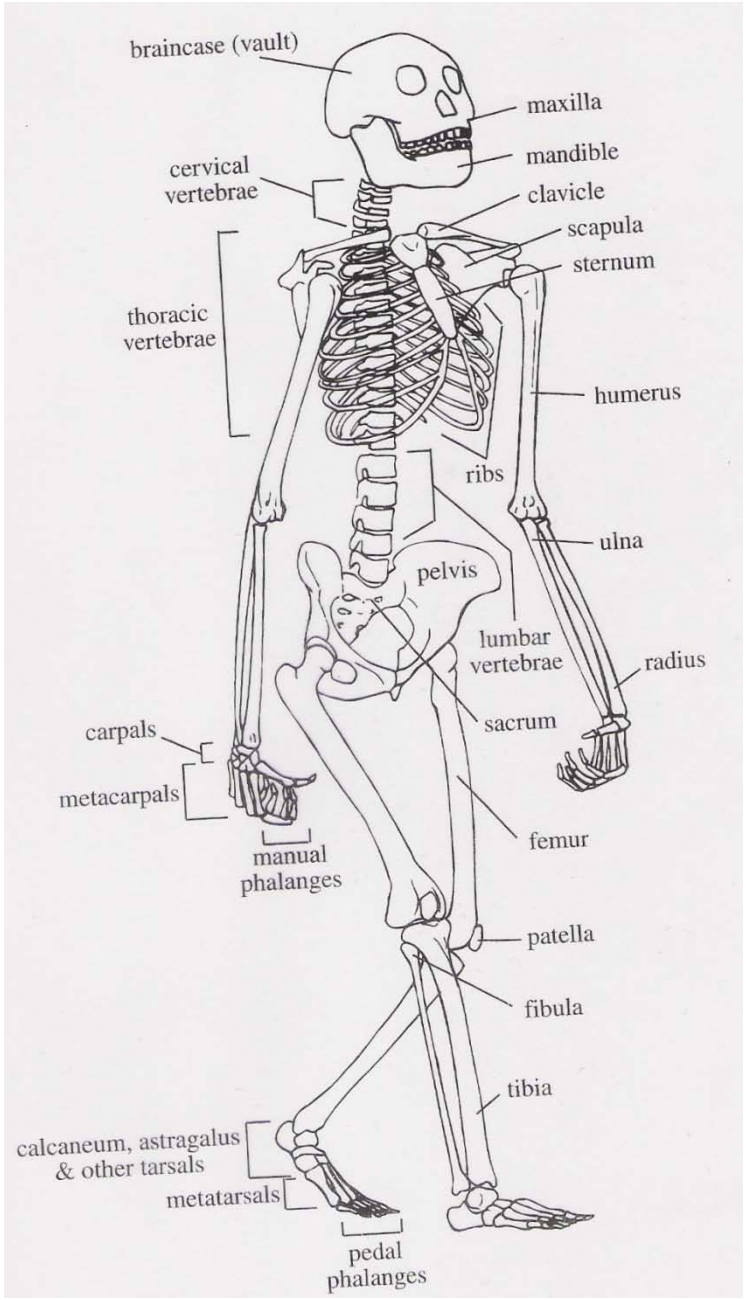

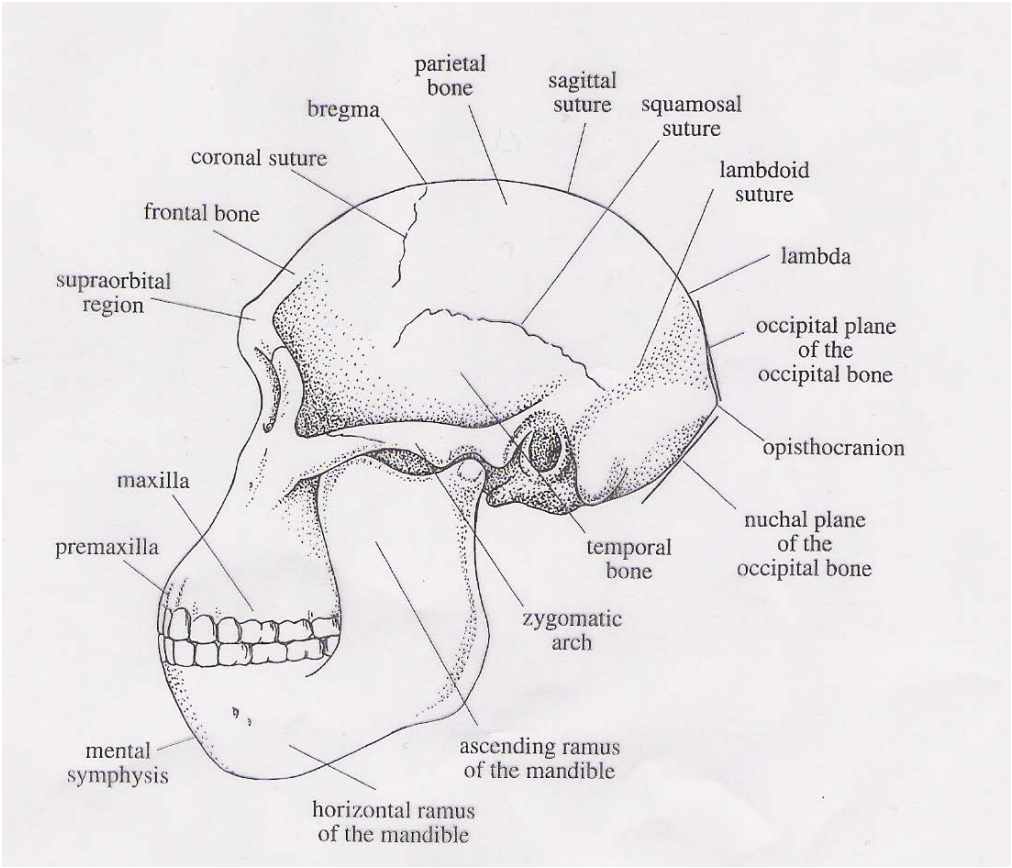

Quadrupedal Postures

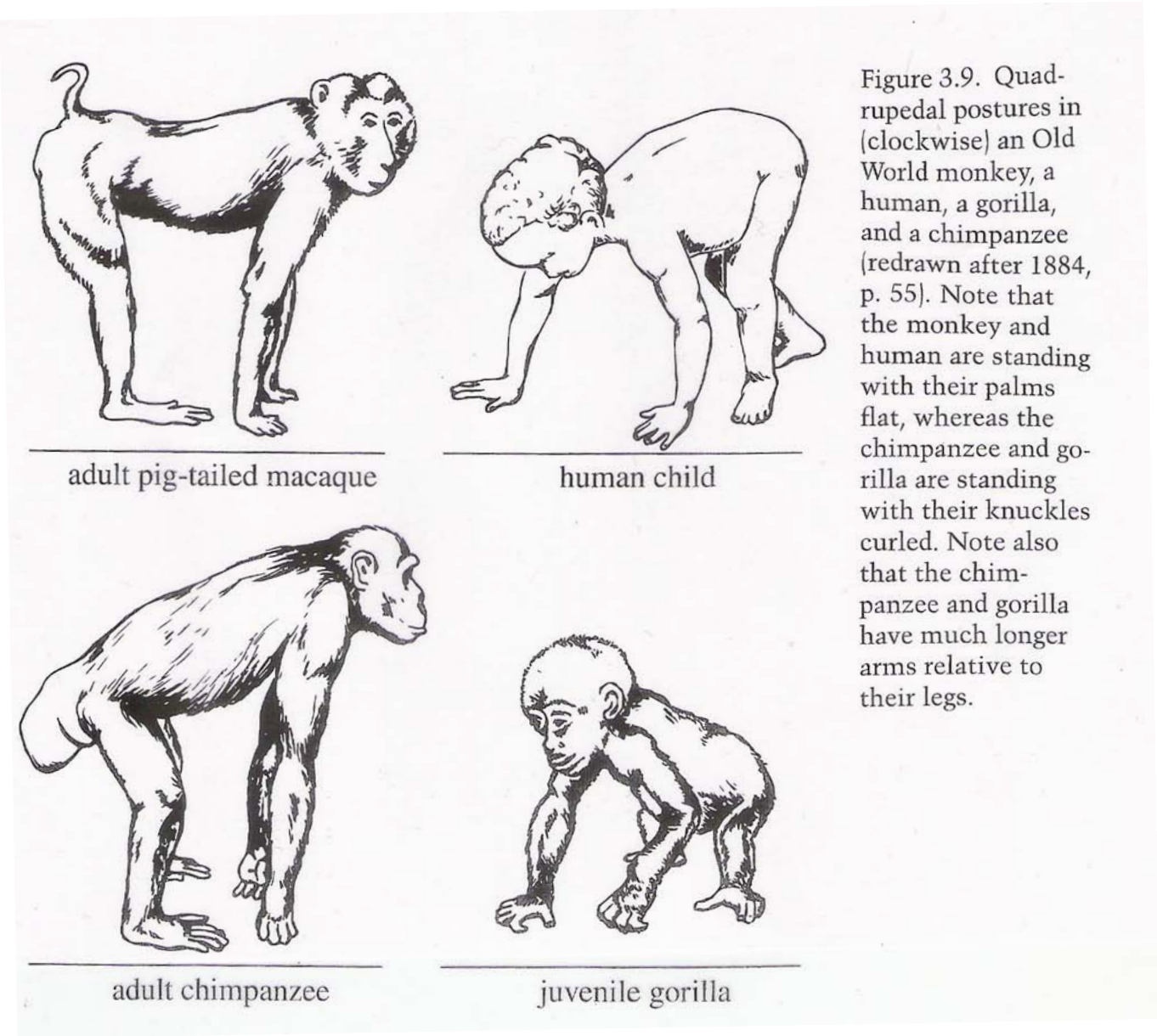

Figure 3.9. Quadrupedal postures in (clockwise) an Old World monkey, a human, a gorilla, and a chimpanzee (redrawn after 1884, p. 55). Note that the monkey and human are standing with their palms flat, whereas the chimpanzee and gorilla are standing with their knuckles curled. Note also that the chimpanzee and gorilla have much longer arms relative to their legs.

Catarrhine Evolution

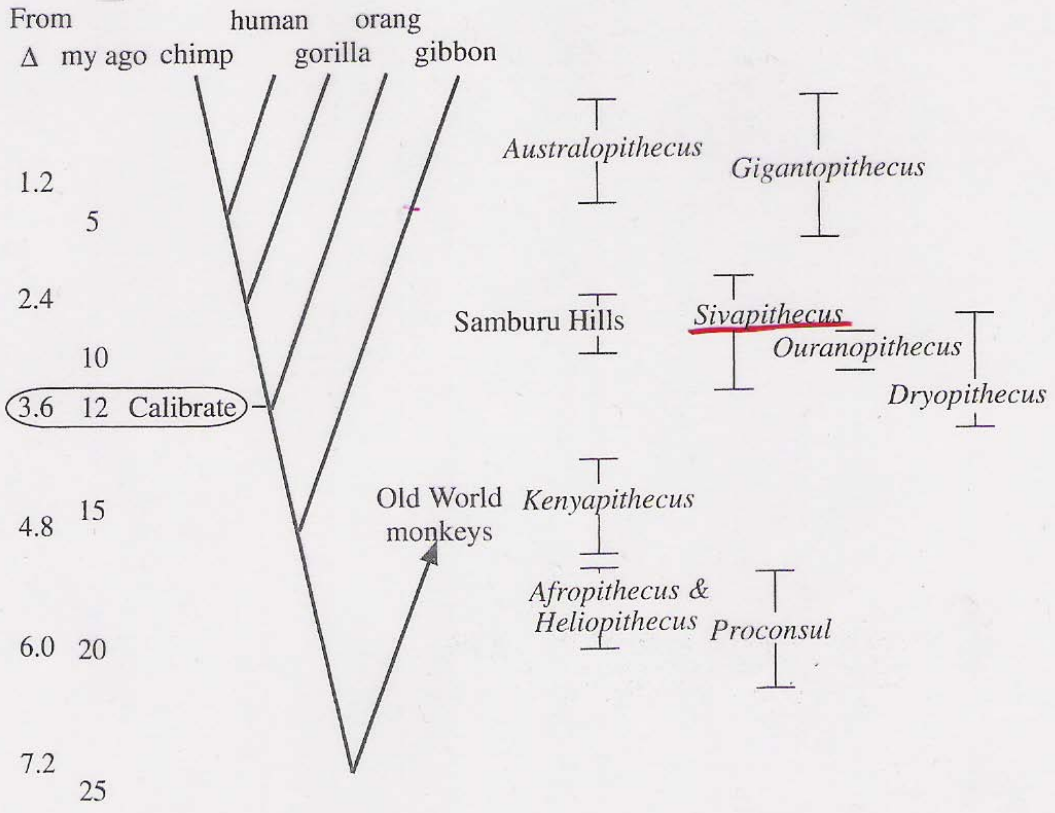

Figure 3.13. Framework of catarrhine evolution as deduced from DNA hybridization data (modified after 1689, fig. 8). The branching times are based on the assumption that DNA differences accumulate at a linear rate, which can be calculated from the branching time of the orangutan "clade," estimated here from the appearance of *Sivapithecus* roughly 12 my ago. The known or probable time ranges of some important fossil hominoids are shown to the right. Dates of divergence based on most other molecular data are broadly similar, and they are broadly consistent with the fossil record.

Nonhuman Primate Distribution

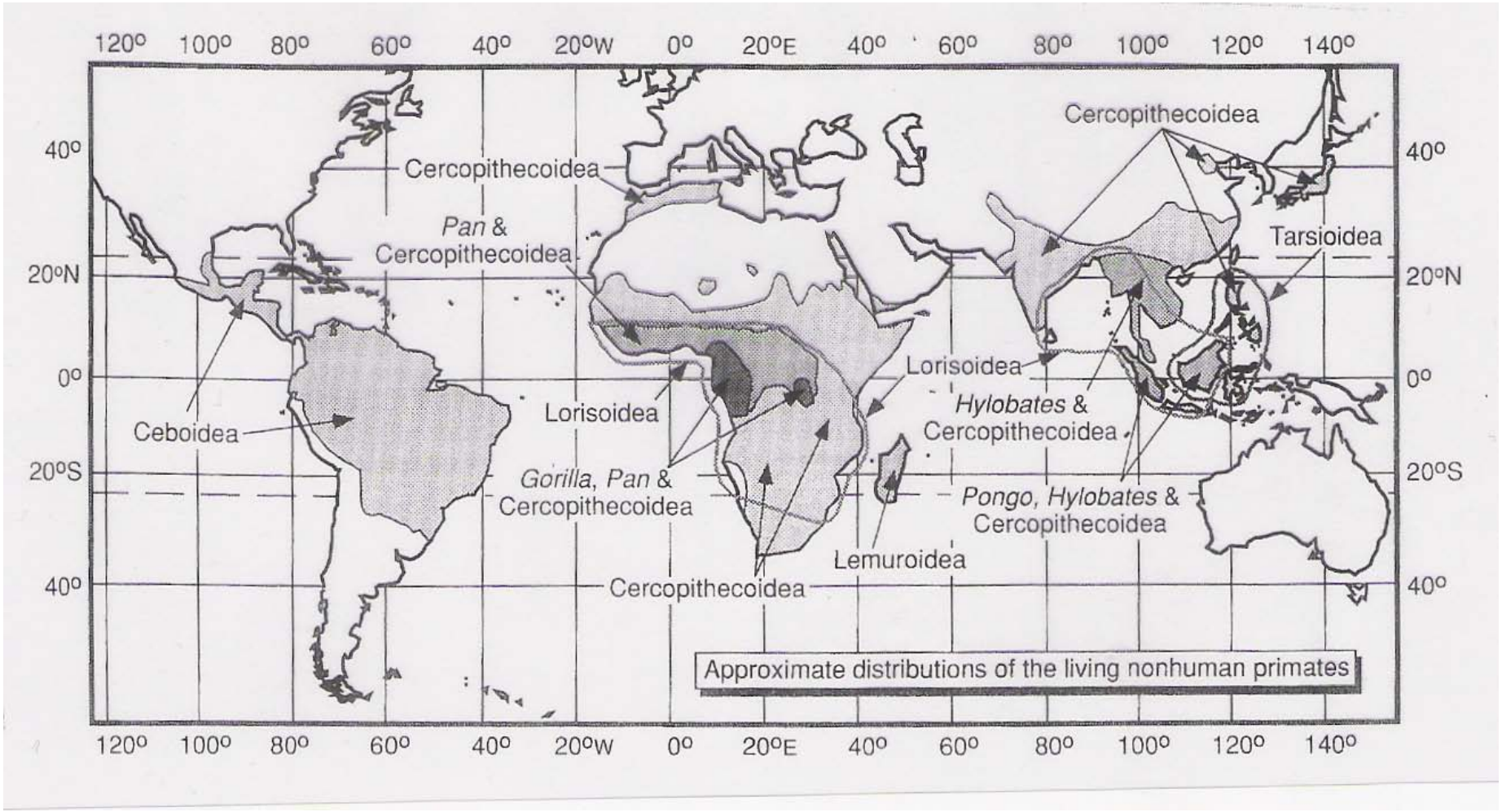

Primate Dentition

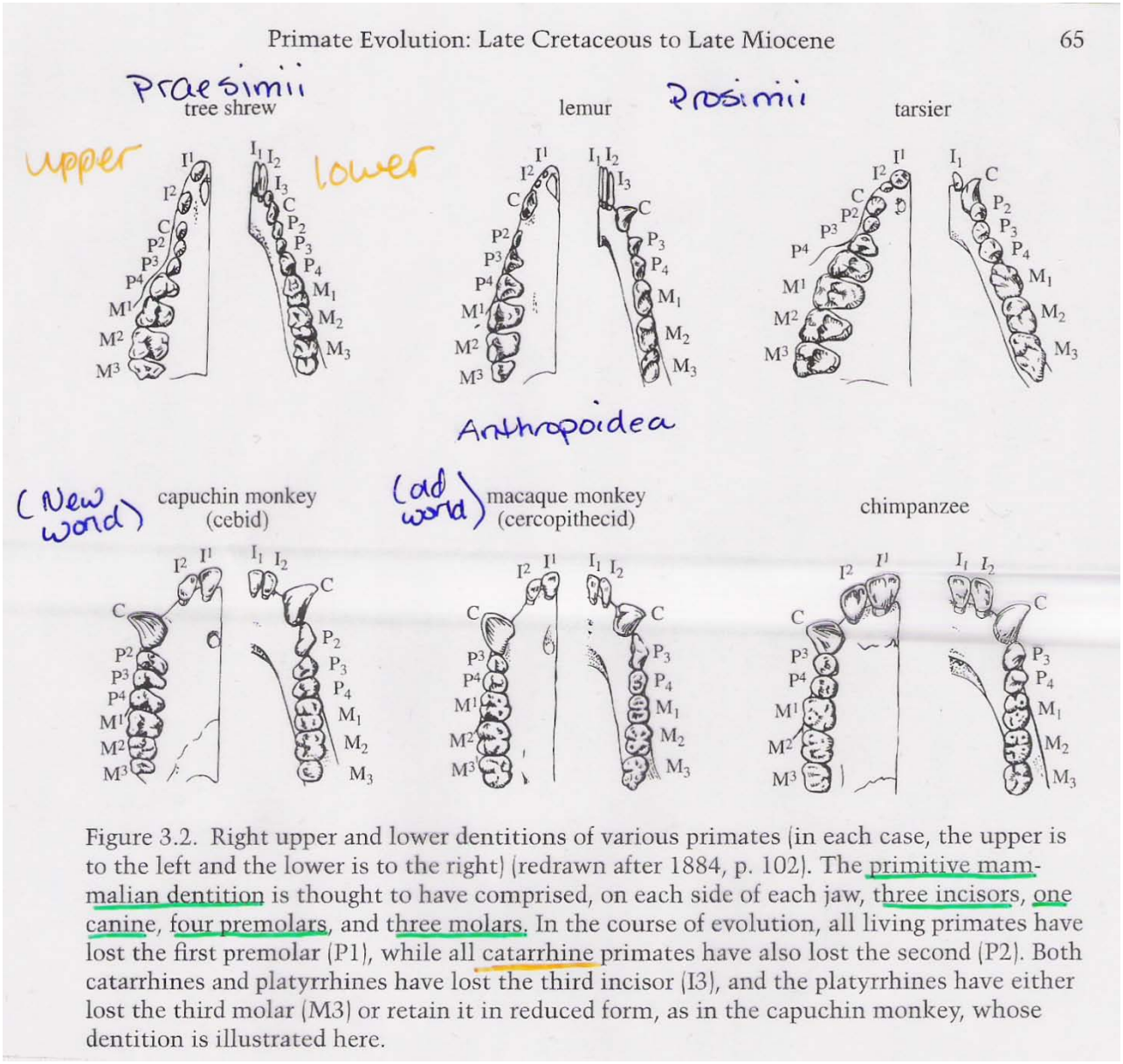

Figure 3.2. Right upper and lower dentitions of various primates (in each case, the upper is to the left and the lower is to the right) (redrawn after 1884, p. 102). The primitive mammalian dentition is thought to have comprised, on each side of each jaw, three incisors, one canine, four premolars, and three molars. In the course of evolution, all living primates have lost the first premolar (P1), while all catarrhine primates have also lost the second (P2). Both catarrhines and platyrrhines have lost the third incisor (I3), and the platyrrhines have either lost the third molar (M3) or retain it in reduced form, as in the capuchin monkey, whose dentition is illustrated here.

Continent Positions

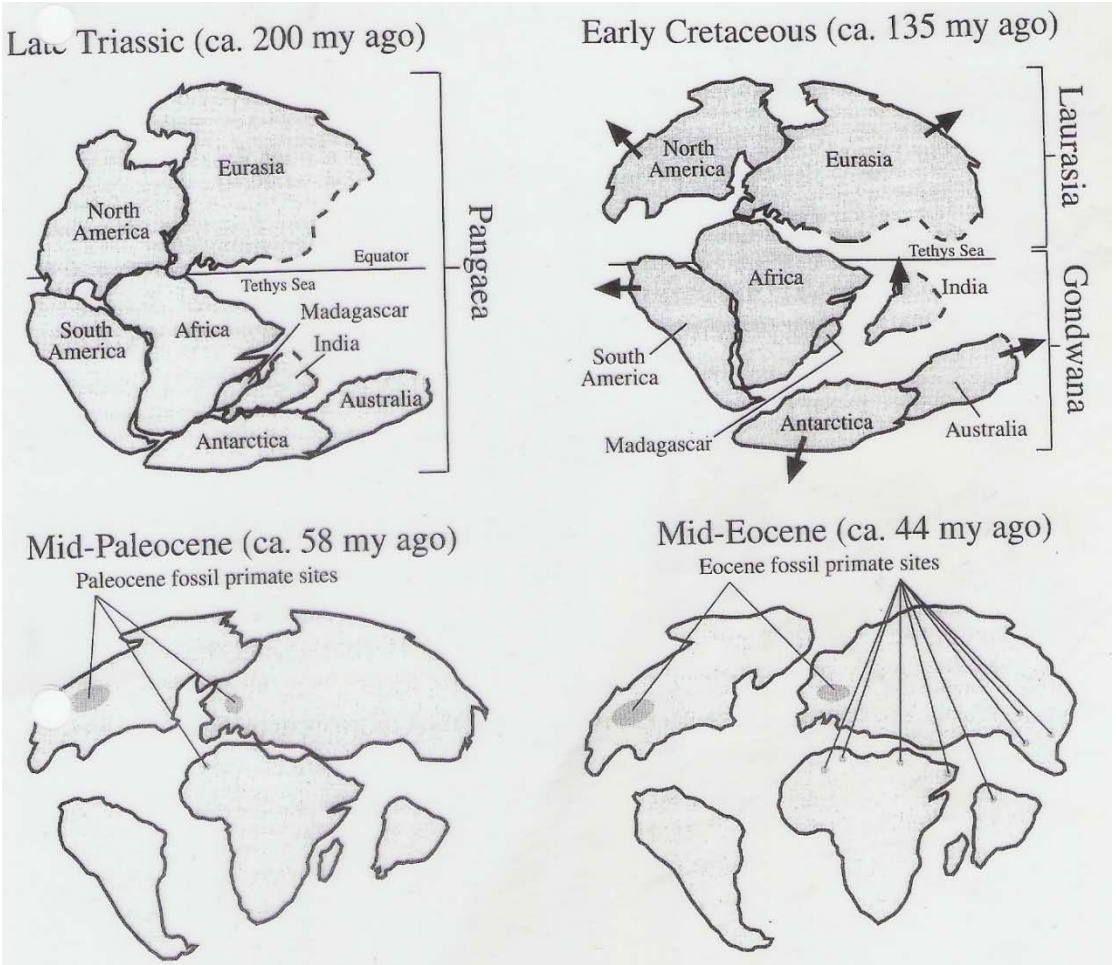

Figure 3.12. Changing positions of the continents from the late Triassic, roughly 200 my ago, to the middle Eocene, roughly 44 my ago (modeled after 2534). In the late Triassic, the modern continents were essentially joined in a single supercontinent known to geophysicists as Pangaea. Subsequent fragmentation (drift) divided Pangaea into a northern hemisphere landmass known as Laurasia and a southern hemisphere mass known as Gondwana. Yet further fragmentation divided Laurasia and Gondwana into separate parts, foreshadowing the modern continents. The conjunction of North America and Eurasia in the Paleocene and early Eocene accounts for the close similarity of their early primate faunas, as discussed in the text.

Early Primate Phylogeny

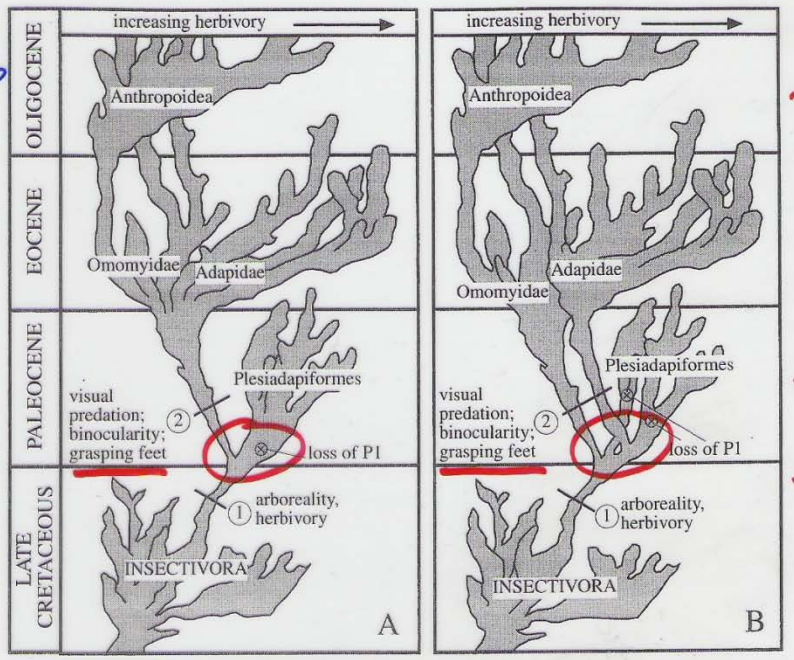

Figure 3.14. Two interpretations of early primate phylogeny (adapted from 430, fig. 8). In both, the earliest primates diverged from their insectivore (or insectivore-like) ancestors by a greater emphasis on arboreality and herbivory. In both, the evolution of the omomyids and adapids (Eocene prosimians) involved a subsequent shift back toward insectivory, based now on binocular vision and grasping extremities. Finally, in both, increasing emphasis on herbivory is a crucial element in the evolution of the anthropoids. The main difference between the two interpretations is that in A (*left*), the omomyids and adapids share a single Paleocene ancestor, whereas in B (*right*) they have separate ones in which binocular vision and grasping extremities evolved independently. On present evidence, A is more likely. Both interpretations suggest that the omomyids and not the adapids were ancestral to the anthropoids, but this issue remains debatable. The circled xs mark the loss of the first premolar (P1) in the plesiadapiforms. This is one of the specializations that makes them unlikely ancestors for Eocene prosimians.

Amphipithecus mogaungensis Mandible

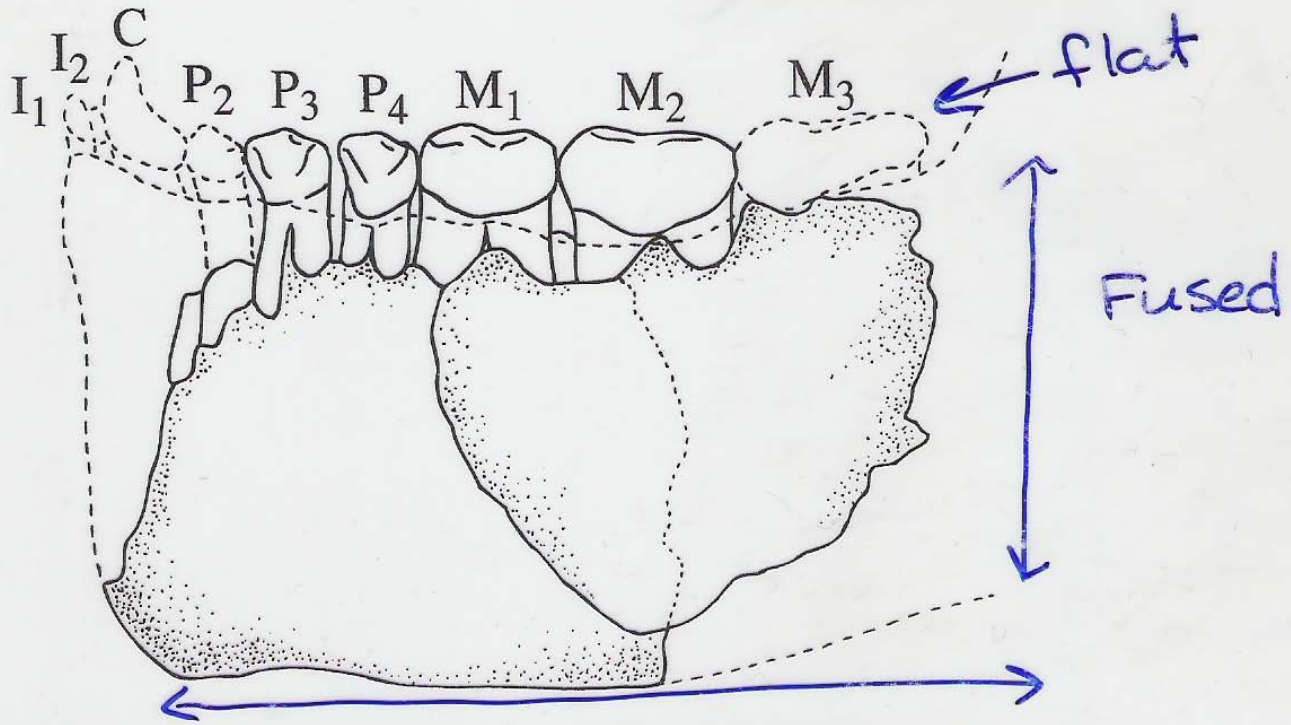

Figure 3.17. Partially reconstructed mandible of *Amphipithecus mogaungensis* (redrawn after 471, p. 30). Dated to about 40 my ago, it is arguably the oldest higher primate fossil yet found. An assignment to the higher (vs. lower) primates is suggested by several features, including the great depth of the jaw relative to the molar crown height and the nearly equal depth of the jaw from back to front. Typically, in lower primates the mandible is shallower overall, and it becomes especially shallow toward the front.

Eocene and Oligocene Fossil Locations

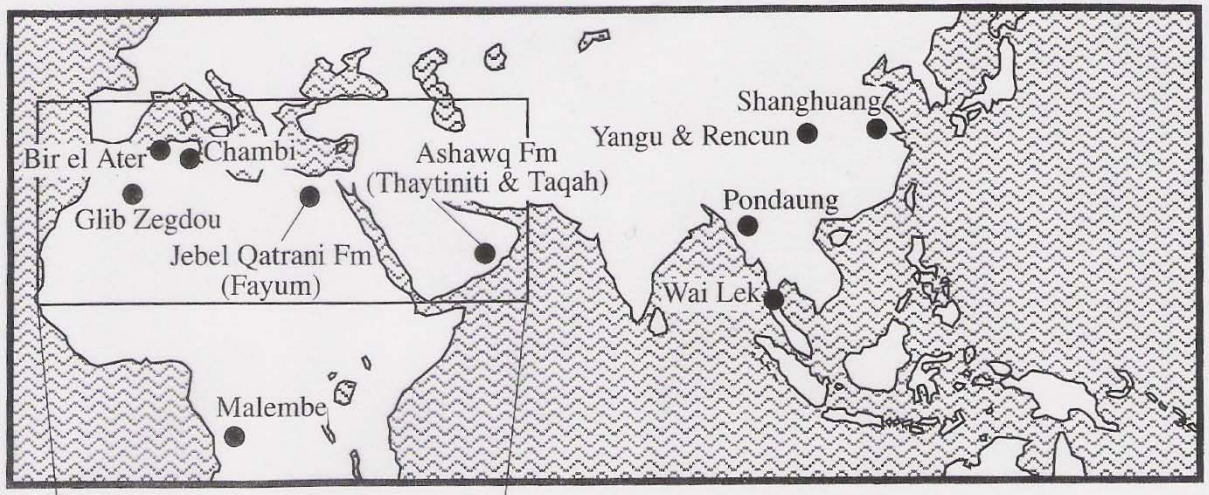

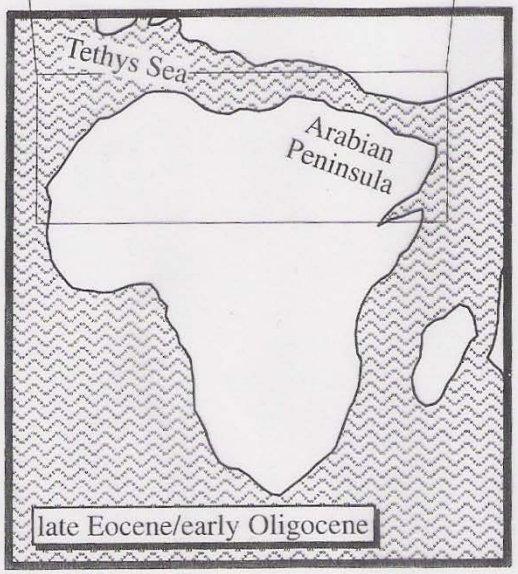

Figure 3.16. *Top:* Eocene and Oligocene localities with fossils that probably or possibly bear on the origins of the higher primates. By far the most important locality is the Fayum, Egypt (redrawn after 1973, p. 130). *Bottom:* Africa during the late Eocene and early Oligocene, before the development of the Red Sea that separates Africa and the Arabian Peninsula today (modeled after 2534).

Eocene and Oligocene of Fayum, Egypt

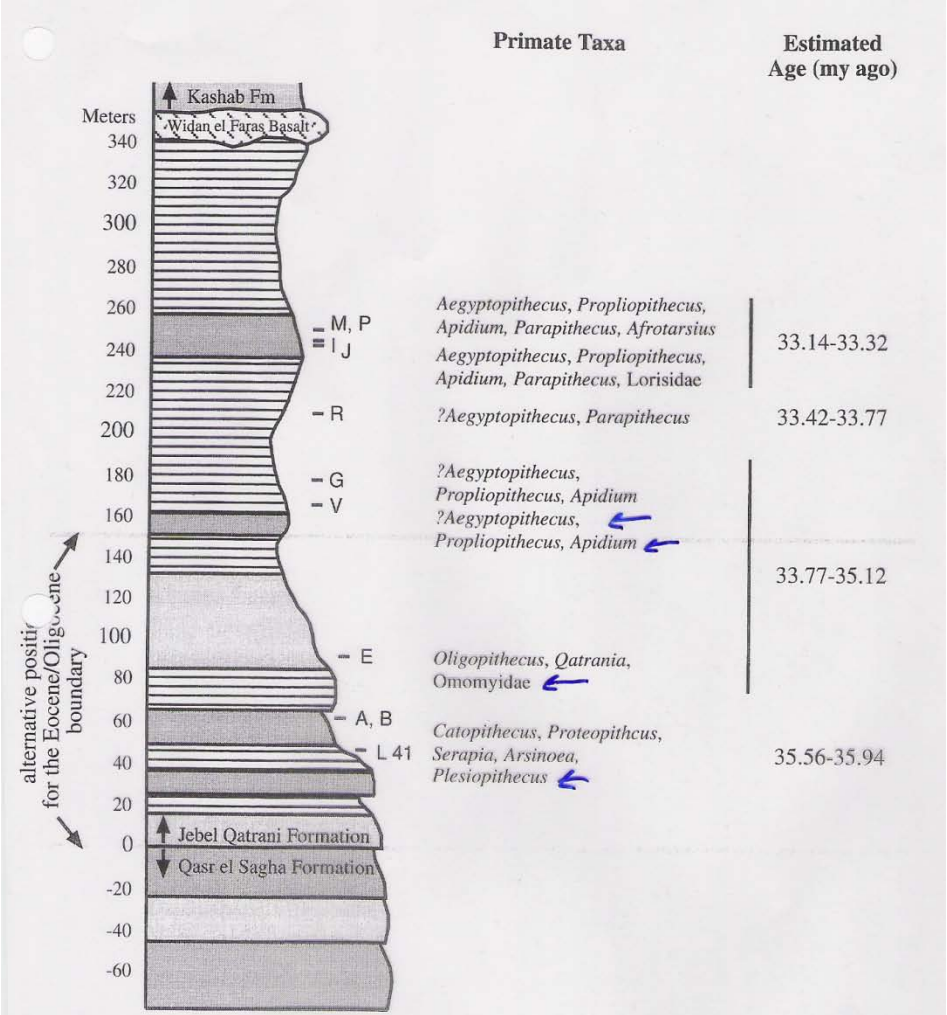

Figure 3.18. Schematic profile through the fossiliferous Eocene and Oligocene deposits in the Fayum Depression, Egypt (redrawn after 1178, fig. 4 and table 1). Gray tones indicate relatively fine sediments; horizontal lines designate coarser ones. The letters immediately to the right of the profile denote collecting localities ("quarries"). The middle column lists the primate taxa recovered at various localities, and the right-hand column shows the ages inferred from correlation between the geomagnetic reversal stratigraphy of the Fayum section and the global geomagnetic reversal time scale. The Eocene/Oligocene boundary may lie within the Jebel Qatrani Formation (1178, 1181), or it may lie at its very base (836).

Eocene and Oligocene Fossils

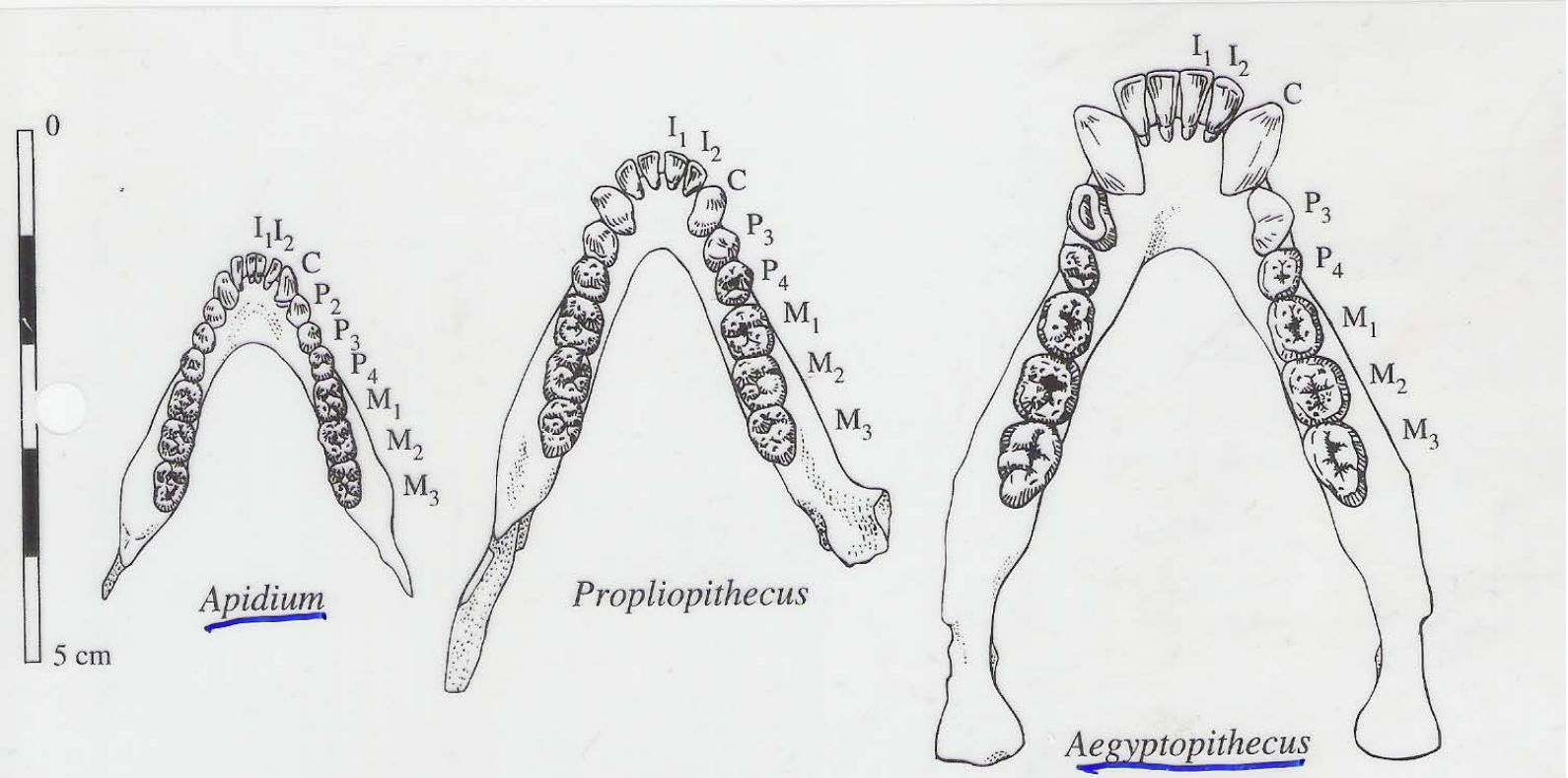

Figure 3.21. Mandibles of *Apidium*, *Propliopithecus*, and *Aegyptopithecus* (partially restored) (drawn by Kathryn Cruz-Uribe from photos in 2126, fig. 156, and 738, figs. 4, 9, 10; © 1999 by Kathryn Cruz-Uribe). Note the presence of three premolars on each side of the jaw in *Apidium*, versus two in *Propliopithecus* and *Aegyptopithecus*. The mandibles and teeth of *Propliopithecus* and *Aegyptopithecus* are strikingly apelike in overall form and differ from each other only in size and some basic proportions, particularly in the relatively larger size of M_1 in *Propliopithecus*. Based on mandibular and dental morphology, either *Aegyptopithecus* or *Propliopithecus* could be ancestral to all later catarrhines.

Aegyptopithecus Skull

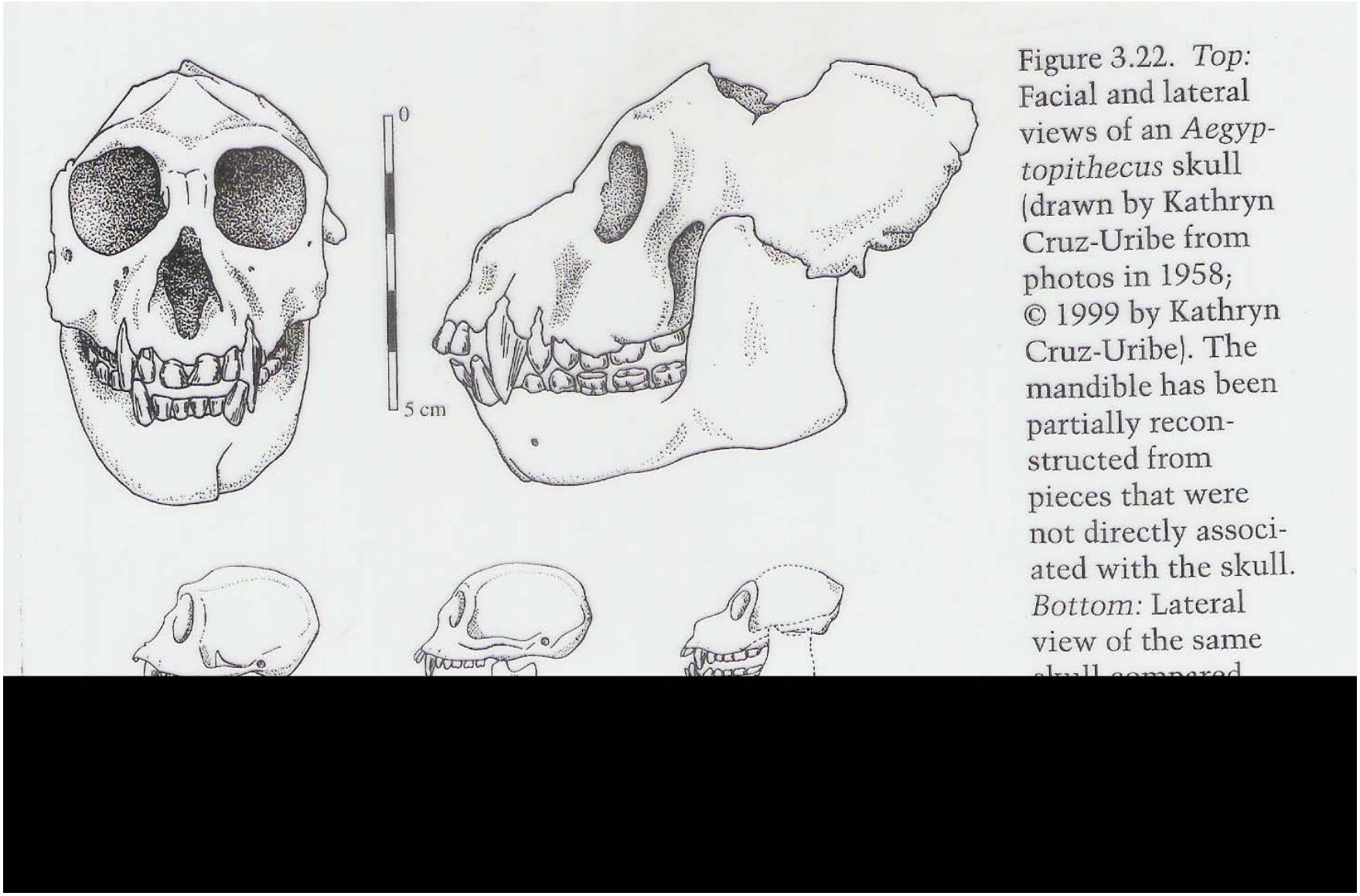

Figure 3.22. *Top:* Facial and lateral views of an *Aegyptopithecus* skull (drawn by Kathryn Cruz-Uribe from photos in 1958; © 1999 by Kathryn Cruz-Uribe). The mandible has been partially reconstructed from pieces that were not directly associated with the skull. *Bottom:* Lateral view of the same

Aegyptopithecus Lower Molars

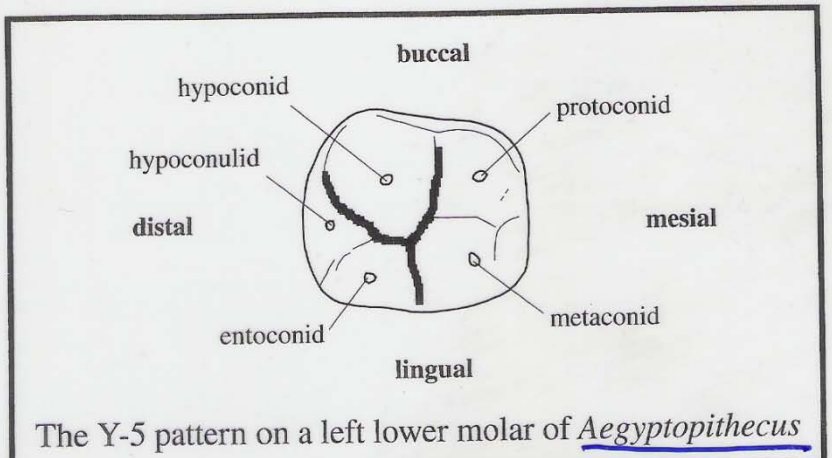

Figure 3.20. Lower molars of the early Oligocene catarrhine *Aegyptopithecus* and of the extant leaf-eating monkey *Colobus* (adapted from 391, figs. 2 and 8). The monkey molar exhibits the typical bilophodonty of all cercopithecoids, with two pairs of cusps linked by shearing crests (lophs). The *Aegyptopithecus* molar shows a pattern of five distinct cusps separated by a Y-shaped fissure system that is broadly characteristic of all Miocene to Recent hominoids. The Y-5 pattern is believed to be primitive in catarrhines, and the bilophodont condition probably evolved from it.

Proconsul heseloni

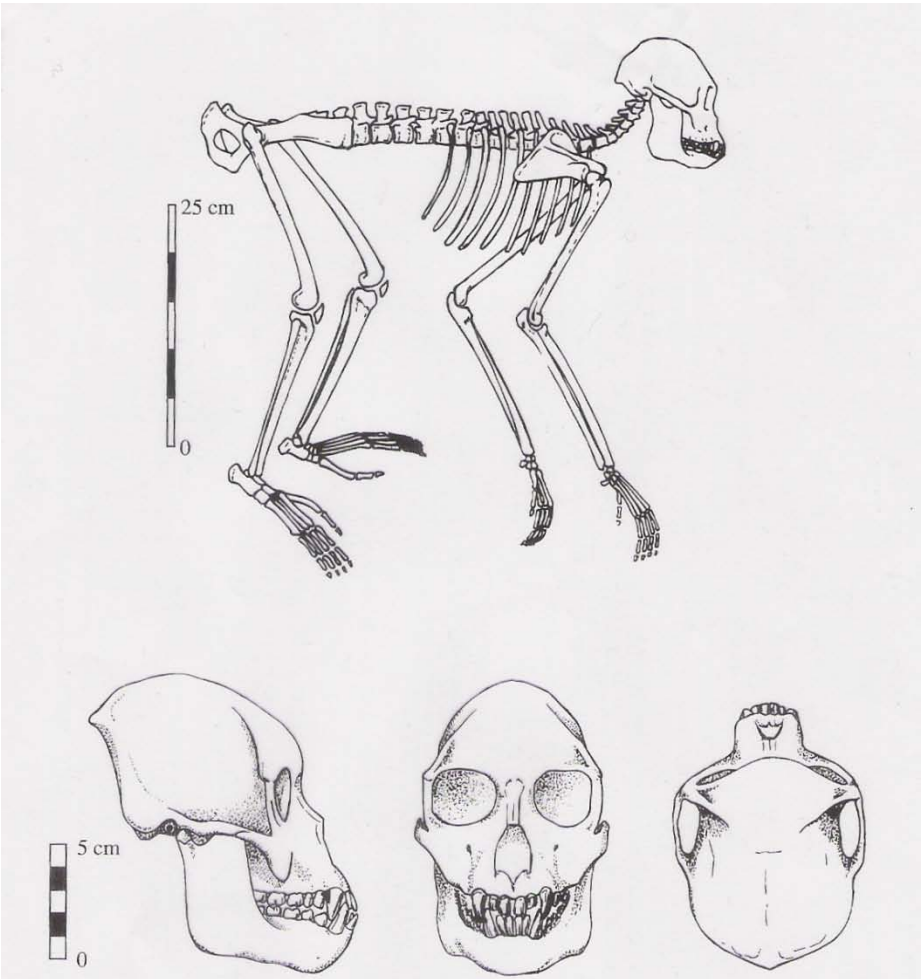

Proconsul heseloni (KNM-RU 2036)

Figure 3.27. *Above:* Reconstruction of *Proconsul heseloni* (Rusinga Island specimen no. 2036 in the collections of the National Museums of Kenya) (redrawn after 2374). *Below:* Reconstructed skull of female *P. heseloni* (redrawn after 2375). The specimens were recently removed from *P. africanus* to *P. heseloni* (2365).

Pliopithecus vindobonensis

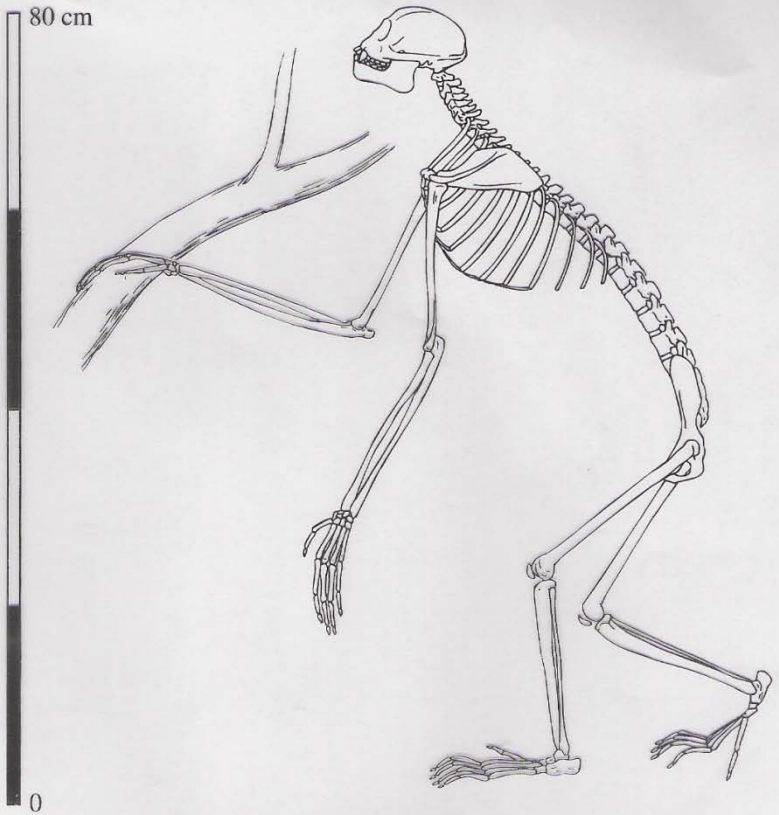

Figure 3.30. Reconstructed skeleton of *Pliopithecus vindobonensis* from mid-Miocene (ca. 15 my old) deposits in Slovakia (redrawn after 2529, fig. 106). In its short, broad face, slender postcranial bones, and other features, *P. vindobonensis* resembled the living gibbons and siamangs, but it lacked their extraordinarily long arms and other morphological specializations for brachiation. It also retained some remarkably primitive features, such as an incompletely ossified external auditory meatus and an epicondylar foramen on the distal humerus. Most authorities now regard it as one of a group of closely related small hominoids that inhabited western and central European forests between roughly 16 and 11 my ago and that bear no relationto any later hominoids.

Early and Mid Miocene Fossil Sites

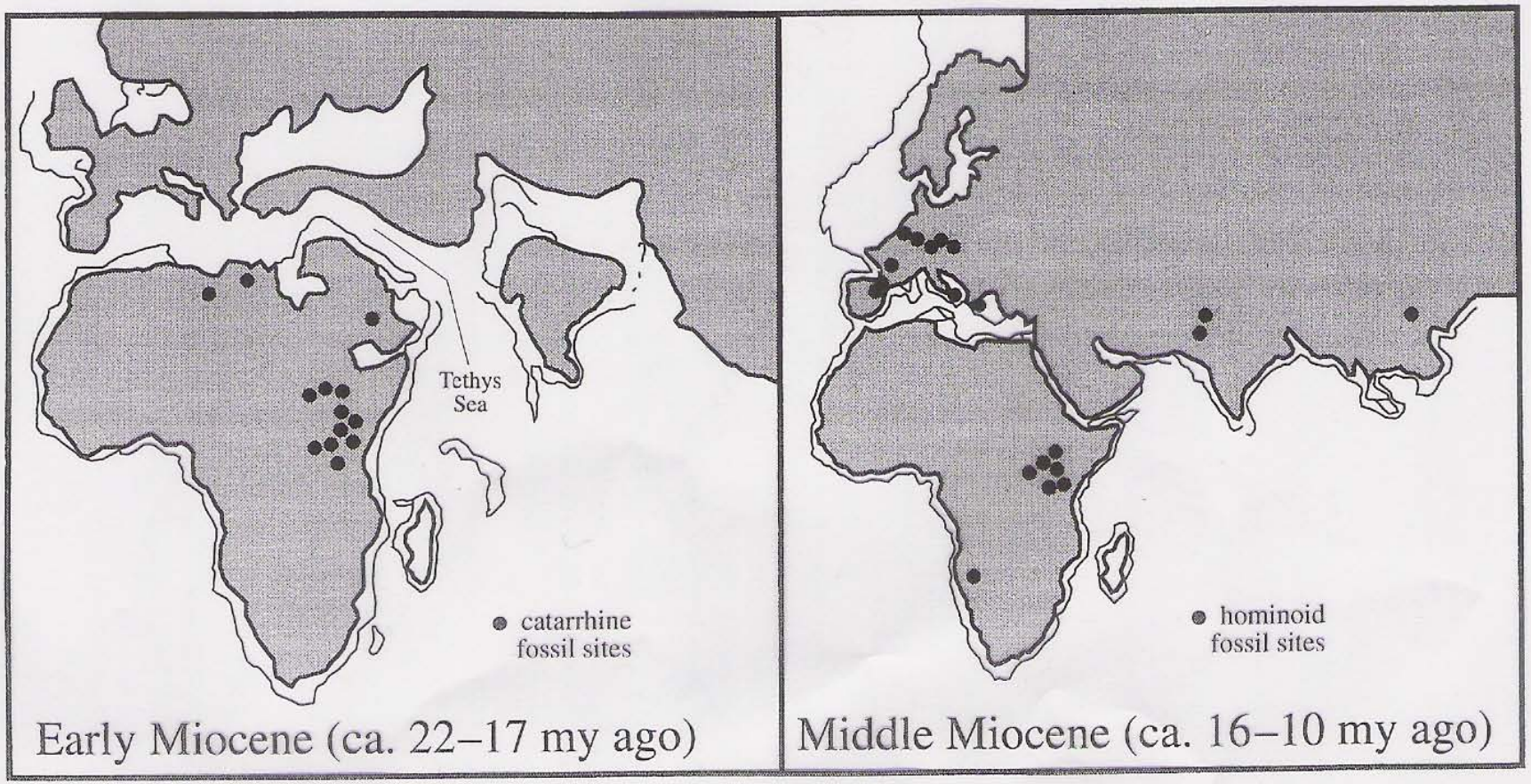

Figure 3.24. Relative positions of Africa and Eurasia in the early and middle Miocene (modified after 1304, figs. 3 and 4). The middle Miocene higher primates of Eurasia probably evolved from African forms that dispersed to Eurasia when the northward drift of the

Mid and Late Miocene Fossil Sites

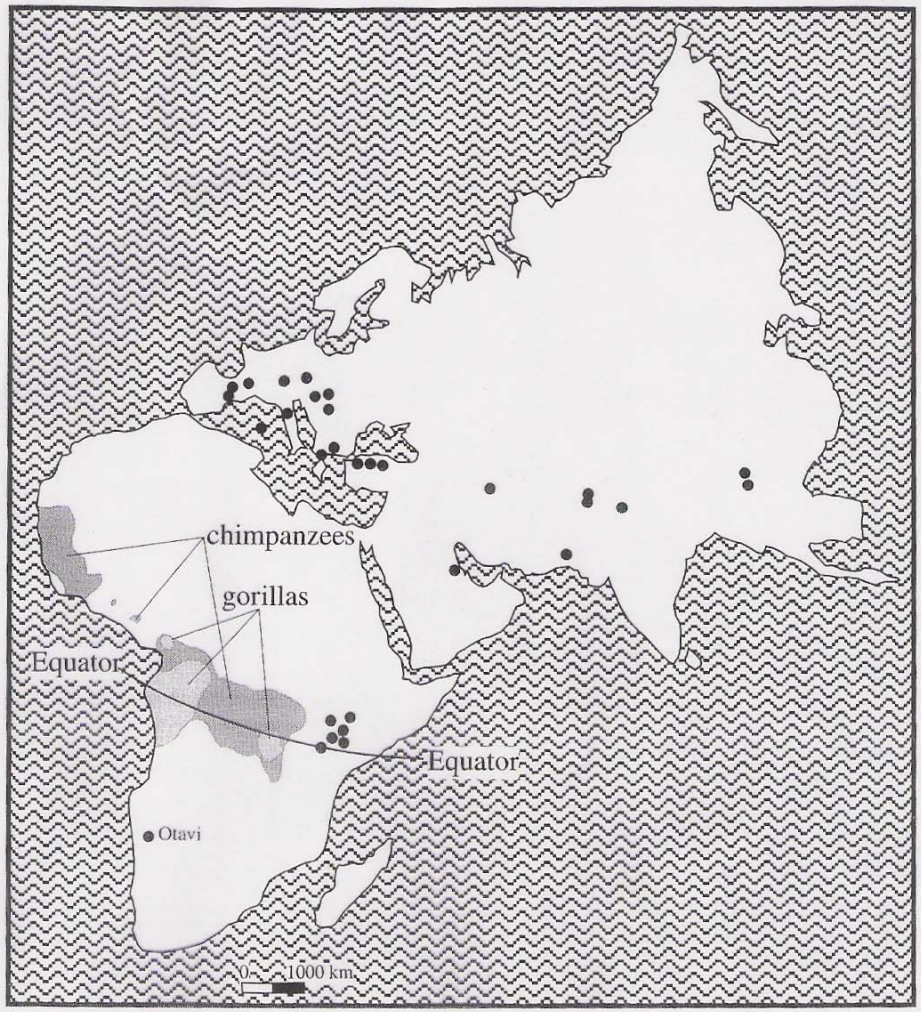

Figure 3.28. Middle and later Miocene (ca. 15–6 my old) fossil hominoid localities in relation to the historic distribution of the chimpanzees and the gorilla (redrawn after 542, p. 356). Note the concentration of fossil sites in equatorial eastern Africa and their spread across midlatitude Europe from Spain to China.

Midsagittal section of Primate Faces

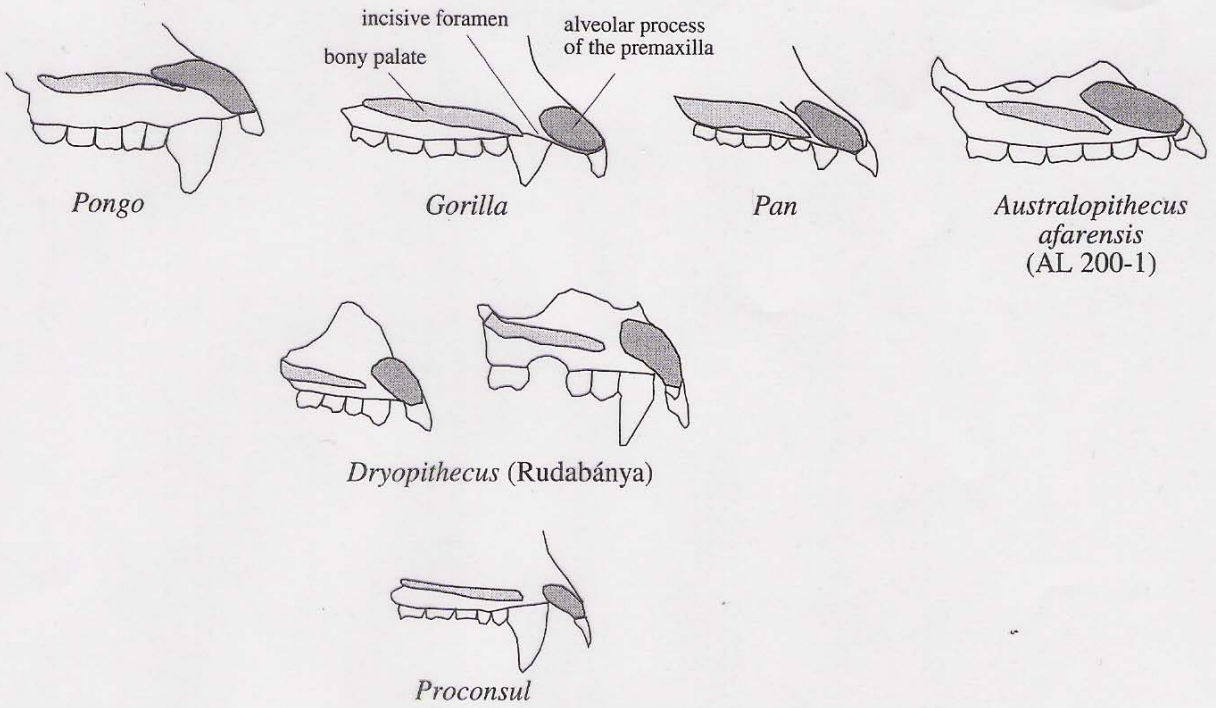

Figure 3.29. Midsagittal sections through the faces of *Pongo* (orangutan), *Gorilla*, *Pan* (chimpanzee), *Australopithecus afarensis* (from Hadar, Ethiopia), an early hominid, *Dryopithecus* (from Rudabánya, Hungary), a mid-Miocene ape, and *Proconsul* (from Kenya), an early Miocene ape (redrawn after 2389 and 172). Light shading outlines the bony (or hard) palate. Dark shading outlines the alveolar (or incisor-bearing) process of the premaxilla. The gap between the two is the incisive canal with the incisive foramen at its base. In *Pongo* the premaxilla tends to be longer and more horizontally oriented than in *Gorilla* and *Pan*, and the incisive canal is very small. It is especially wide in *Gorilla* and narrower in *Pan* and *Australopithecus*. Its great breadth in *Dryopithecus* suggests that *Gorilla* maintains the primitive condition, whereas *Pan* and *Australopithecus* are derived in the same way. If this is accepted, then palatal-premaxillary morphology joins other features suggesting that *Pan* and *Australopithecus* share a more recent common ancestor with each other than either does with *Gorilla*.

Sivapithecus indicus Skull

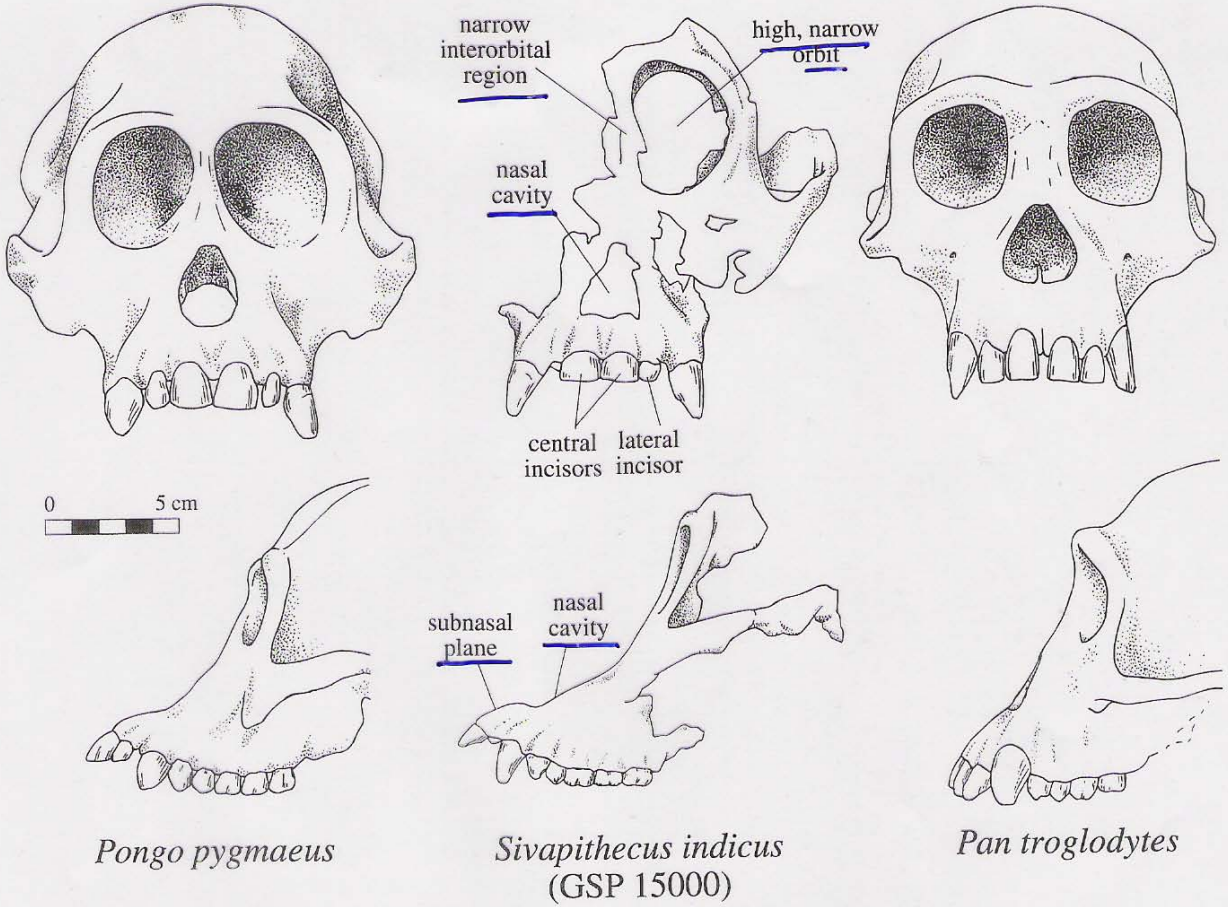

Figure 3.31. Partial skull of *Sivapithecus indicus* (GSP 15000) compared with skulls of an orangutan, *Pongo pygmaeus*, and of a chimpanzee, *Pan troglodytes* (drawn by Kathryn Cruz-Uribe from photographs and casts; © 1999 by Kathryn Cruz-Uribe). In its high, narrow orbits, narrow interorbital region, (nonstepped) continuity between the floor of the nasal cavity and the subnasal plane, and large size of the central incisors compared with the lateral ones, the *Sivapithecus* skull closely resembles that of the orangutan and differs from those of the African great apes. The implication is that *Sivapithecus* is near the ancestry of the orangutan. (GSP = Geological Survey of Pakistan.)

Lufengpithecus

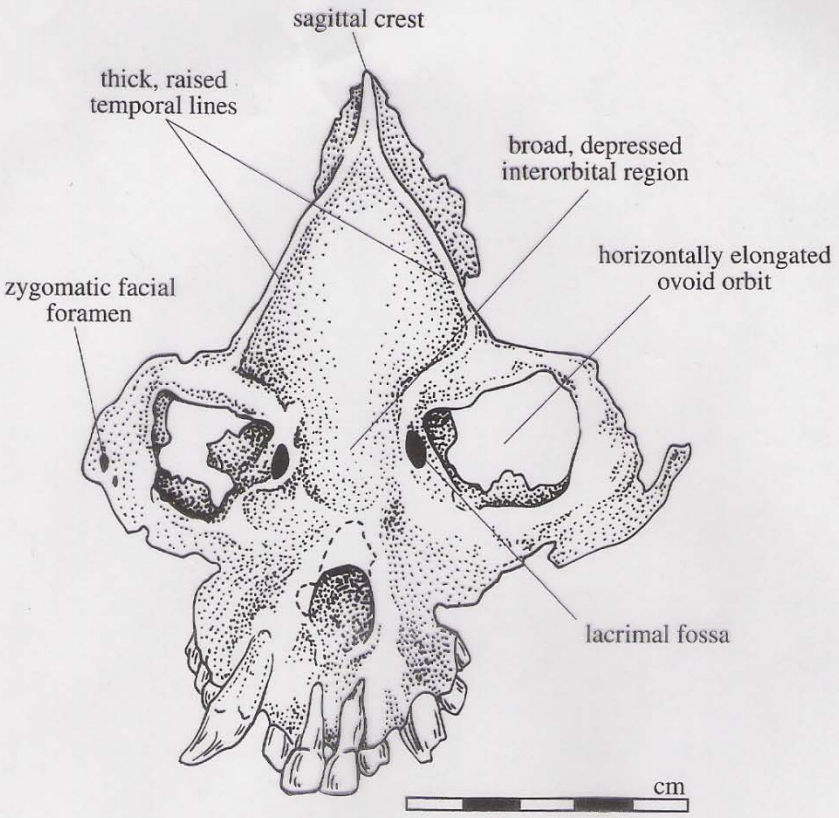

Lufengpithecus PA 644

Figure 3.32. Skull PA 644 of *Lufengpithecus* from Yunnan Province, southern China (redrawn after 1896, fig. 1). *Lufengpithecus* had thick dental enamel like *Sivapithecus* and most other mid- and late-Miocene hominoids, but it was unique in many features, including its thick, upraised temporal lines, its broad, depressed interorbital (glabellar region), and perhaps its extreme sexual dimorphism. It underscores the remarkable diversity of late- and mid-Miocene hominoids in Eurasia. (PA = Paleoanthropology specimen, Institute of Vertebrate Paleontology and Paleoanthropology, Beijing.)

Rib Cages of a Macaque and Human

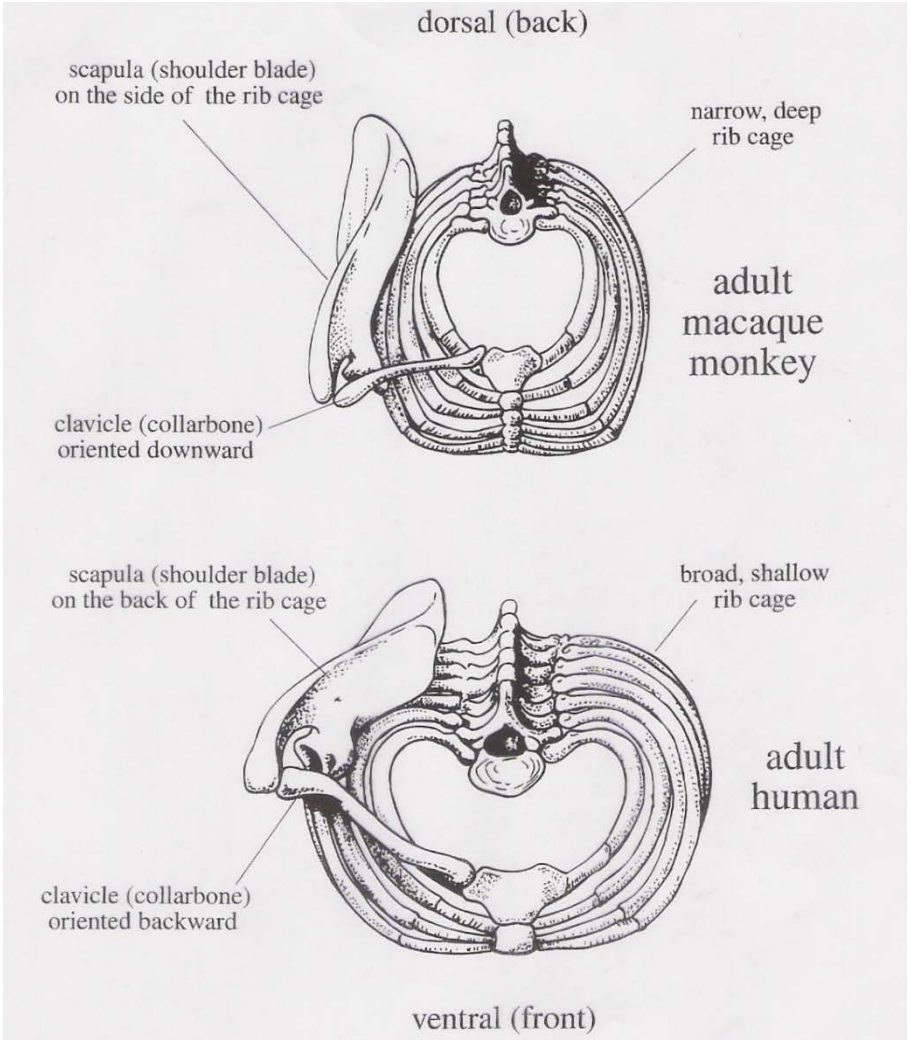

Figure 3.7. Cephalic (top down) views of the rib cage and right shoulder girdle of an adult macaque monkey and of an adult human, showing the deeper, narrower chest of the monkey and the different arrangement of the scapula and clavicle, which limits the monkey's ability to rotate its arm around the shoulder (redrawn after 1884, p. 81).

Primate Phylogeny

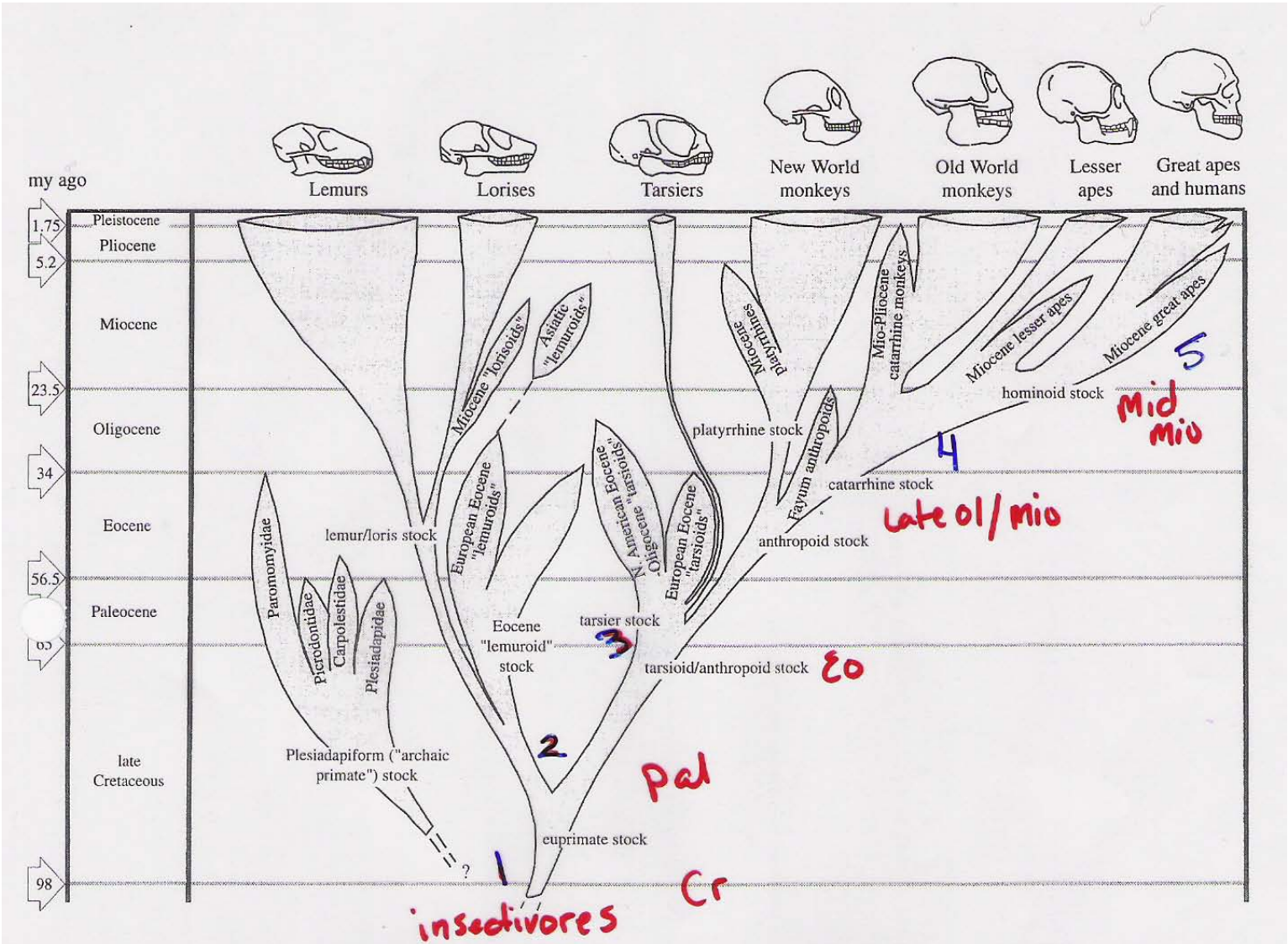

Figure 3.33. A provisional phylogeny of the Primates (modified after 1468, p. 46). The times when major groups diverged are subject to revision, but the order of divergence is reasonably firm.

The Australopithecines

Table 1.1. A Classification of Living People Involving Twenty-one Potential Levels in the Linnaean Hierarchy

*KINGDOM: Animalia
*PHYLUM: Chordata
SUBPHYLUM: Vertebrata
SUPERCLASS: Tetrapoda
*CLASS: Mammalia
SUBCLASS: Theria
INFRACLASS: Eutheria
COHORT: Unguiculata
SUPERORDER: ———
*ORDER: Primates
SUBORDER: Anthropoidea
INFRAORDER: Catarrhini
SUPERFAMILY: Hominoidea
*FAMILY: Hominidae
SUBFAMILY: Homininae
TRIBE: Hominini
SUBTRIBE: ———
*GENUS: *Homo*
SUBGENUS: (*Homo*)
*SPECIES: *sapiens*
SUBSPECIES: *sapiens*

Australopithecinae

Australopithecus

Note: A dash follows a level for which no taxon is in common use. Asterisks designate the seven obligatory and most basic levels in the Linnaean system.

Time Spans of the Hominids

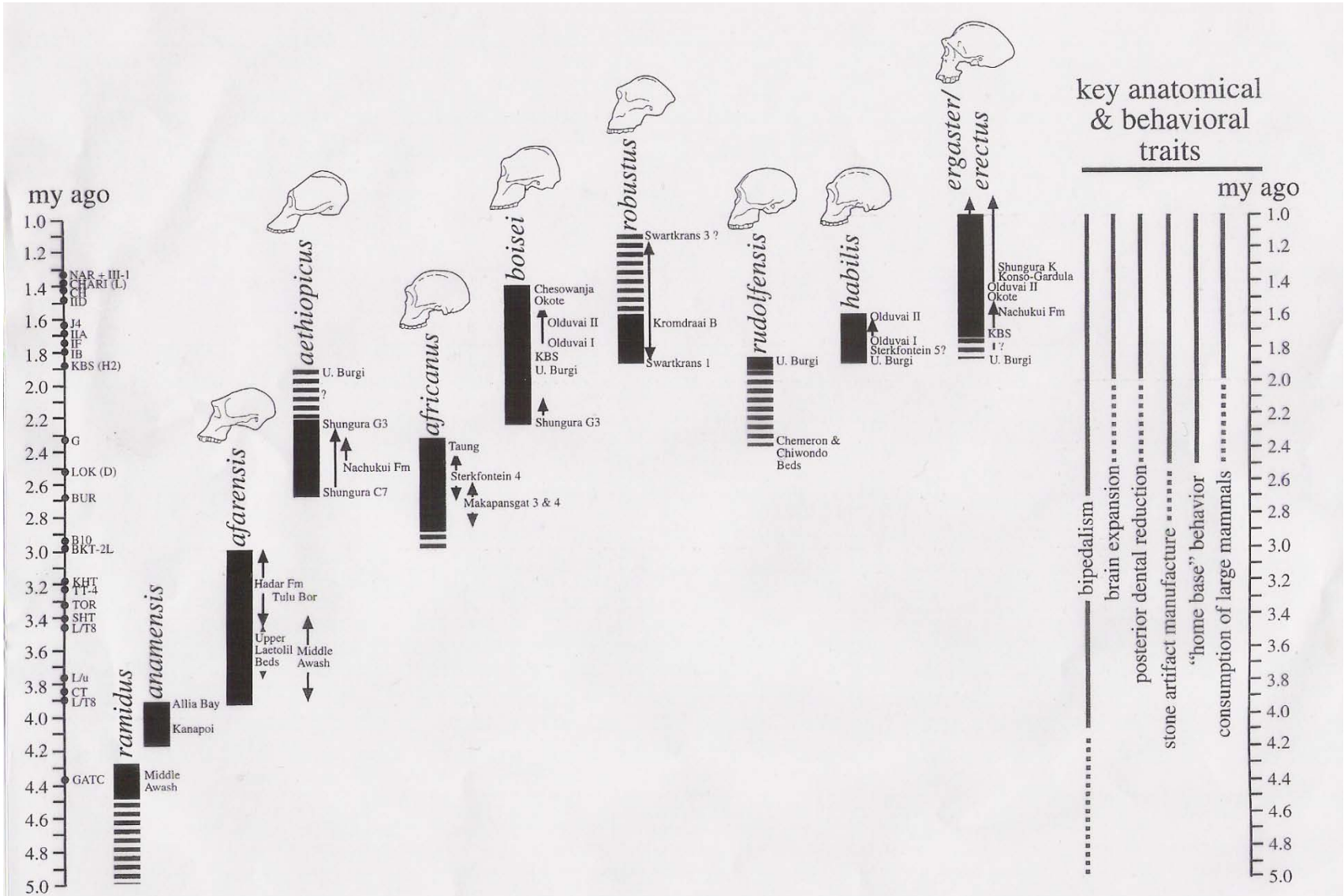

Figure 4.7. *Left:* Time spans of the most commonly recognized hominid species between 4.4 and 1.0 my ago (modified after 1219, p. 428). *Right:* Dating of some key behavioral and anatomical traits (adapted from 959, fig. 1). Broken lines imply uncertain or insecure records. Circles and associated abbreviations on the time scale indicate especially well-dated east African volcanic layers. Names alongside the species bars designate sites or units within sites that have provided key fossils.

Skull Orientations of Gorillas and Humans

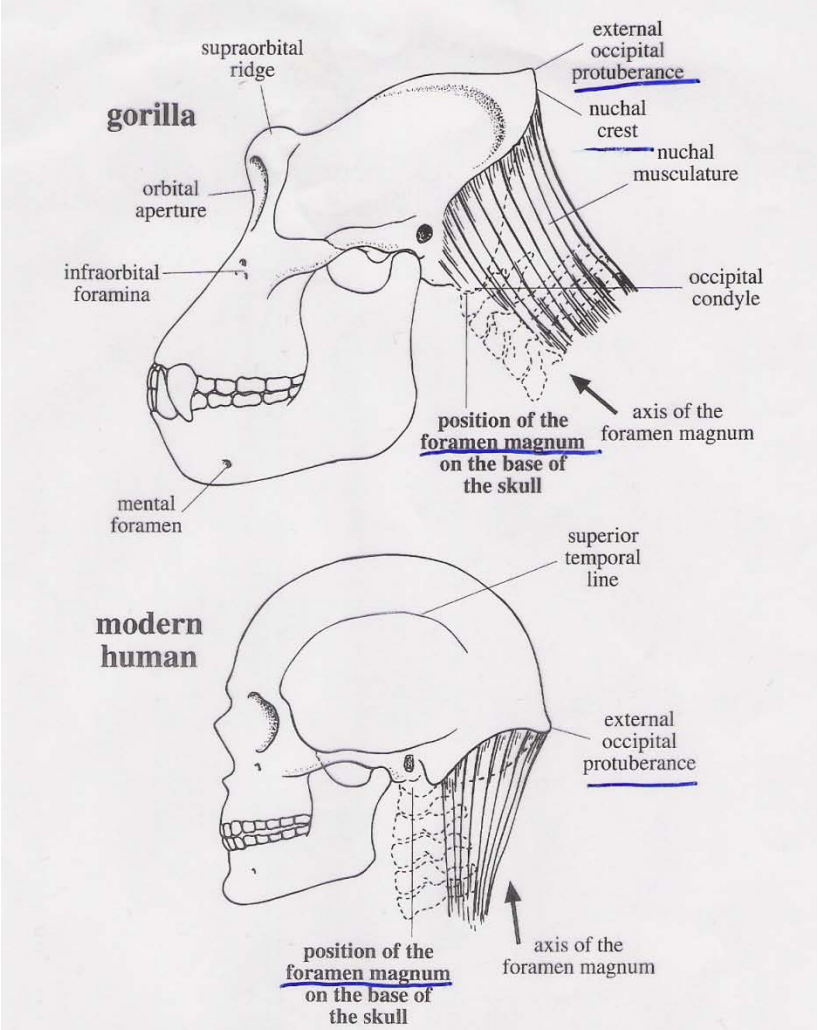

Figure 4.3. Gorilla and modern human skulls, showing the differences in the position of the skull with respect to the spinal column (adapted from 1318, p. 67). In people, the skull is balanced on top of the spinal column, and the foramen magnum consequently lies much farther forward on the base of the skull. The orientation of its axis is also more vertical. The more posterior position of the foramen magnum in the gorilla, together with its larger, more protruding face, also requires larger, more powerful nuchal (neck) muscles to stabilize the head.

Taung Child

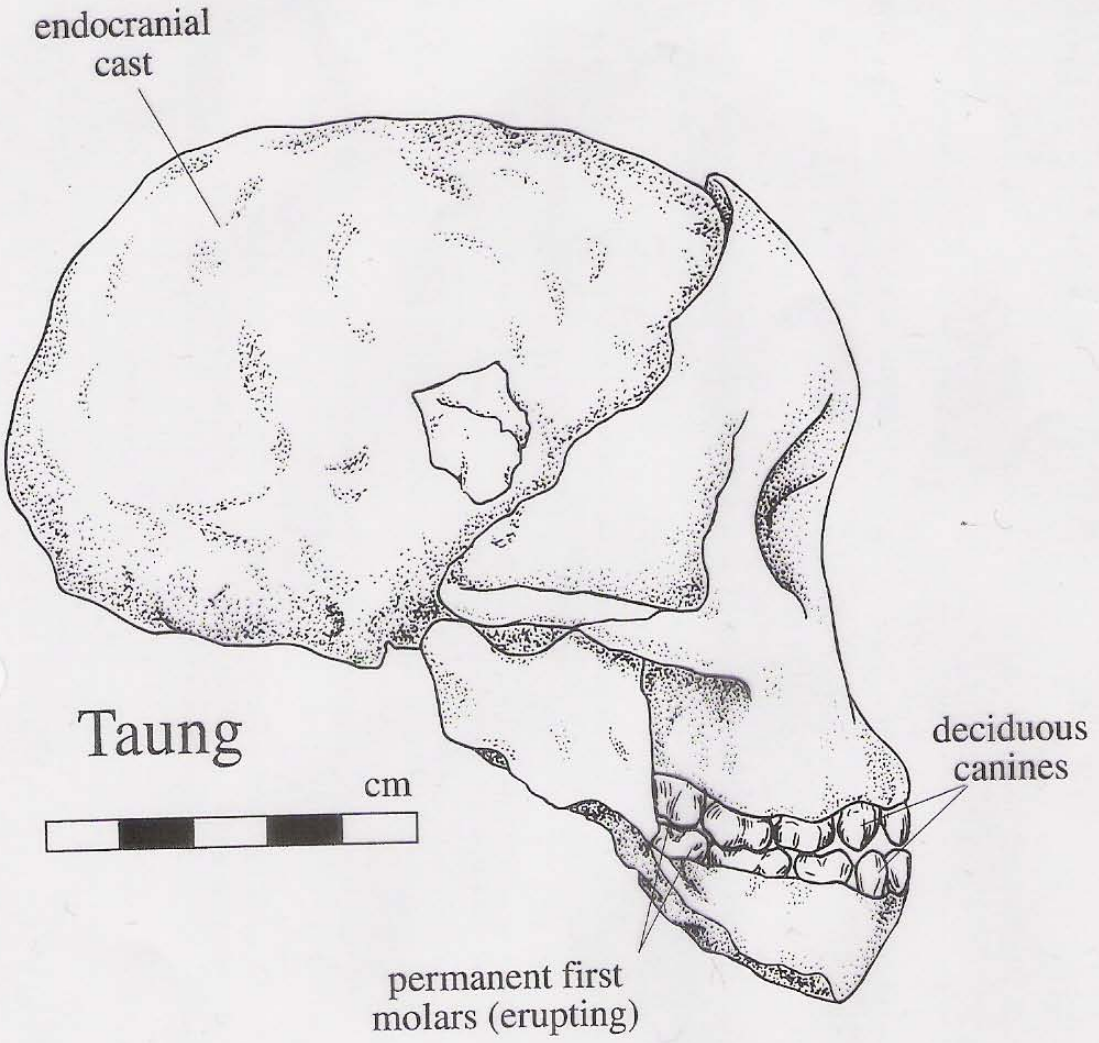

Figure 4.2. Facial skeleton and endocast of *Australopithecus africanus* from Taung, viewed from the right side (drawn by Kathryn Cruz-Uribe from photos and casts; © 1999 by Kathryn Cruz-Uribe).

Mrs. Ples

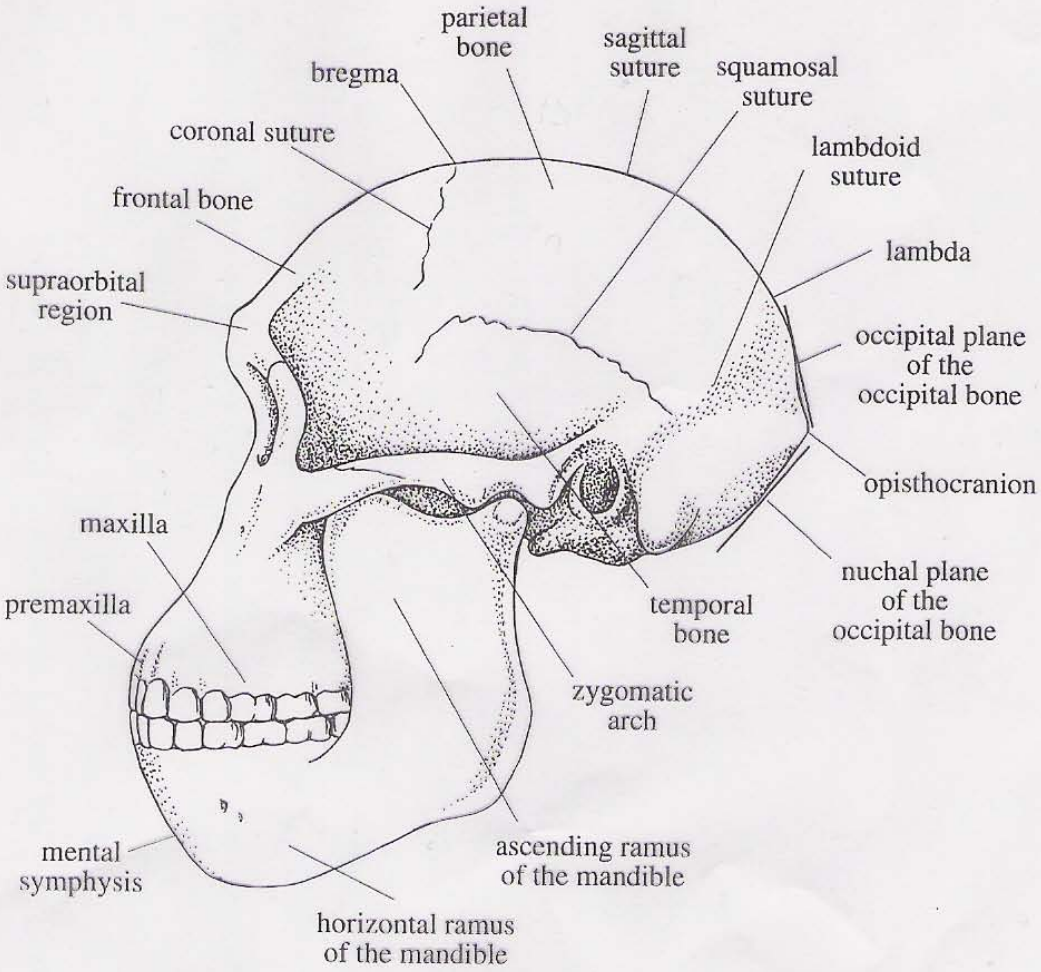

Figure 3.1. Reconstructed skull of *Australopithecus africanus* ("Mrs. Ples"), showing the principal anatomical parts or regions (redrawn after 1317, p. 130).

East African Plio-Pleistocene Fossil Sites

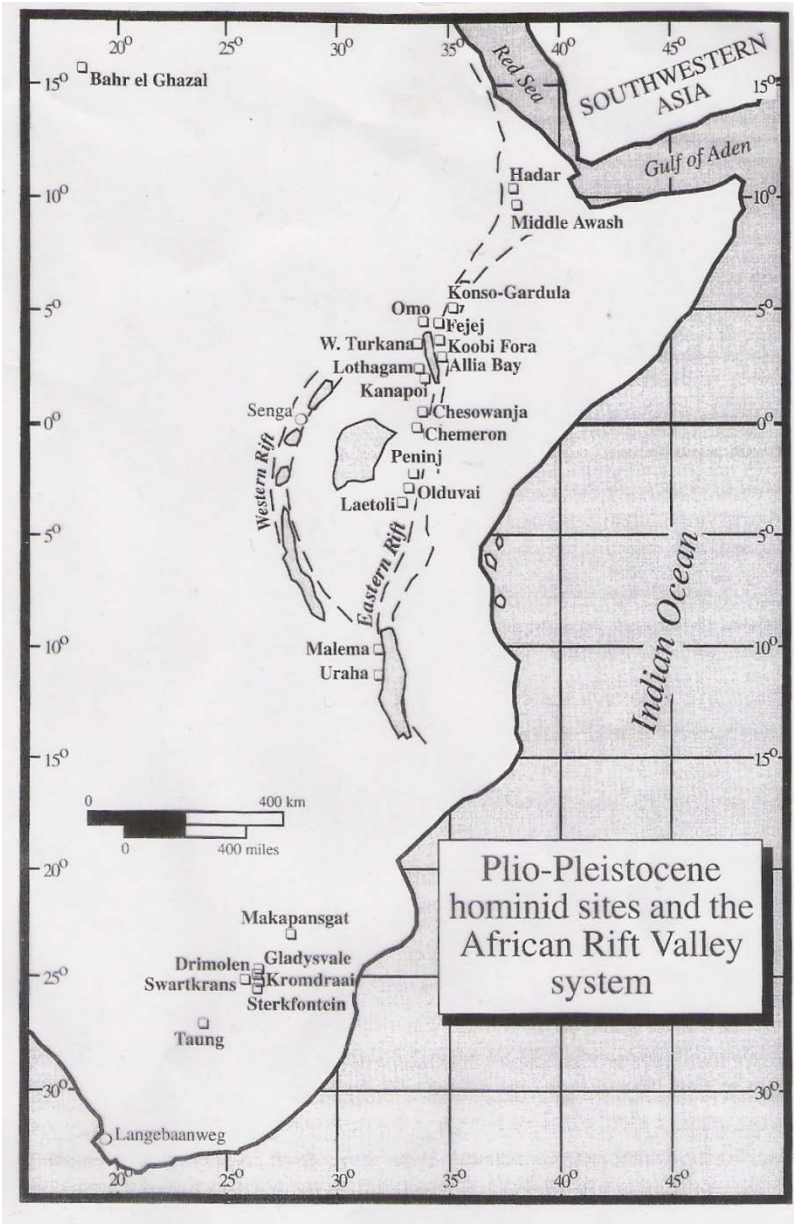

Figure 4.1. Approximate locations of African Plio-Pleistocene hominid fossil sites and of the Langebaanweg early Pliocene faunal site. Tectonic activity associated with the Rift Valley system in eastern Africa created numerous basins that trapped and preserved bones beneath lake and riverine sediments. Volcanoes also linked to rifting provided lavas and ashes that permit radiometric dating. Tectonic activity, often sparse vegetation, and episodic and frequently violent rainfall have promoted gullying that now exposes fossils at the surface. The Rift system does not extend to southern Africa, where sedimentary basins tend to be rare and very shallow. The southern African Plio-Pleistocene hominid sites are all in limestone caves, and they lack volcanic materials for dating. The known caves are clus-

Lake Turkana Basin, East Africa

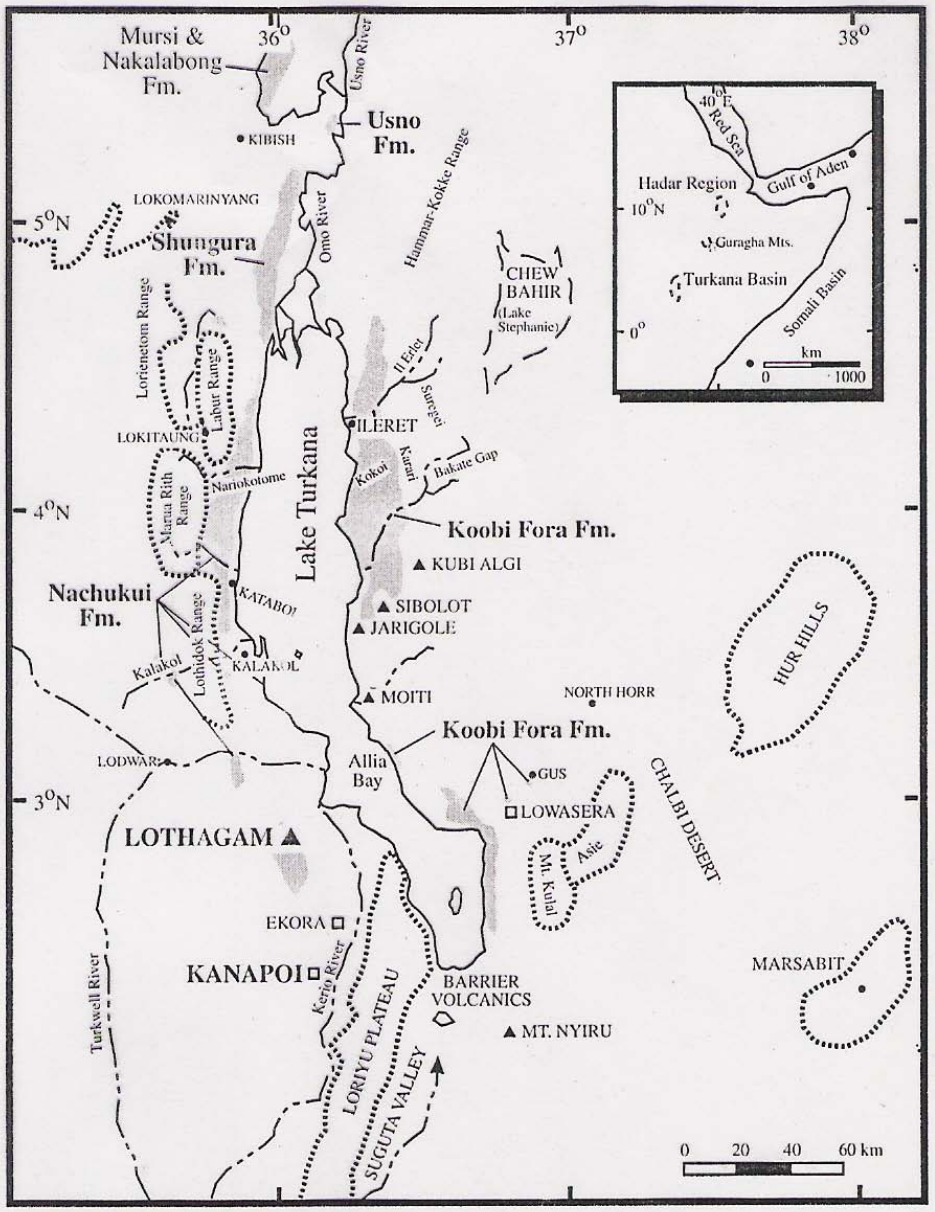

Figure 4.11. The Lake Turkana Basin showing the geological formations (in boldface) that have provided fossils of australopithecines, early *Homo*, or both (redrawn after 370, p. 287). Collectively, localities within the Koobi Fora Formation are often referred to as East Turkana, those within the Nachukui Formation as West Turkana, and those within the Usno and Shungura Formations as Omo or Lower Omo.

Ages of South African Hominid Sites

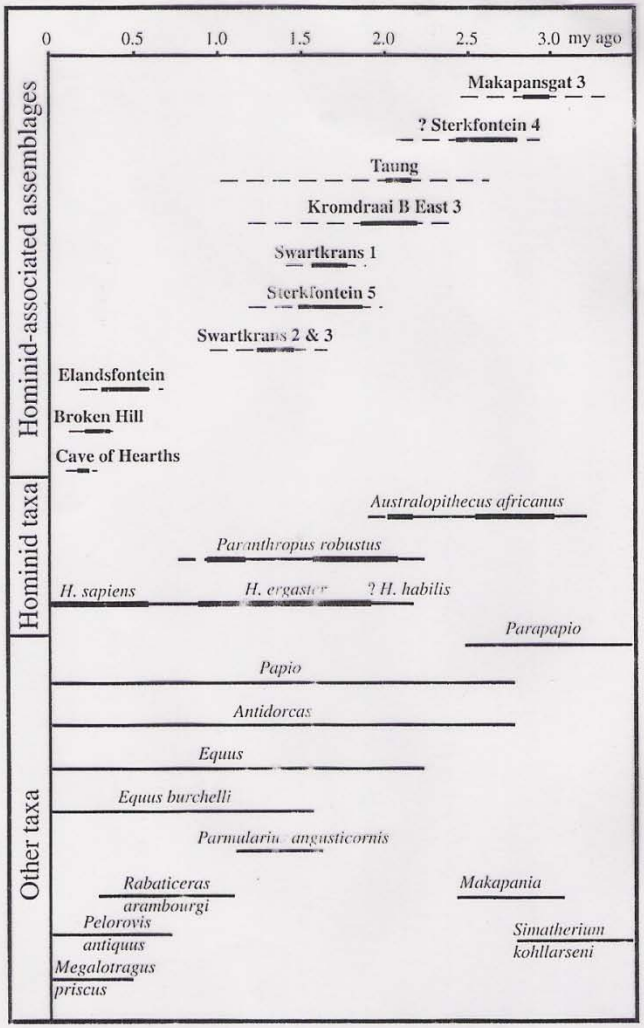

Figure 4.4. Ages (in millions of years ago) of some important South African hominid fossil sites, based on their faunal contents (modified after 2346, p. 741). The numbers following site names are stratigraphic units (members). Also shown are the known time ranges of some important mammalian taxa used in the dating, as well as the inferred time ranges for fossil hominid species. (*Parapapio* and *Papio* are baboons, *Equus* and *Equus burchelli* are zebras, and the remaining species are buffalo or antelopes.)

Swartkrans Cave, South Africa

Figure 4.6. Three stages in the evolution of the Swartkrans australopithecine cave (modified after 328, pp. 31–32). In the first stage, outside sediment has just begun to funnel down a recently formed shaft. In the second, erosion has partly removed earlier sediment, and fresh material has filled the erosional gap. In the third stage, erosion has totally removed the roof, and the complex fill is exposed to the elements.

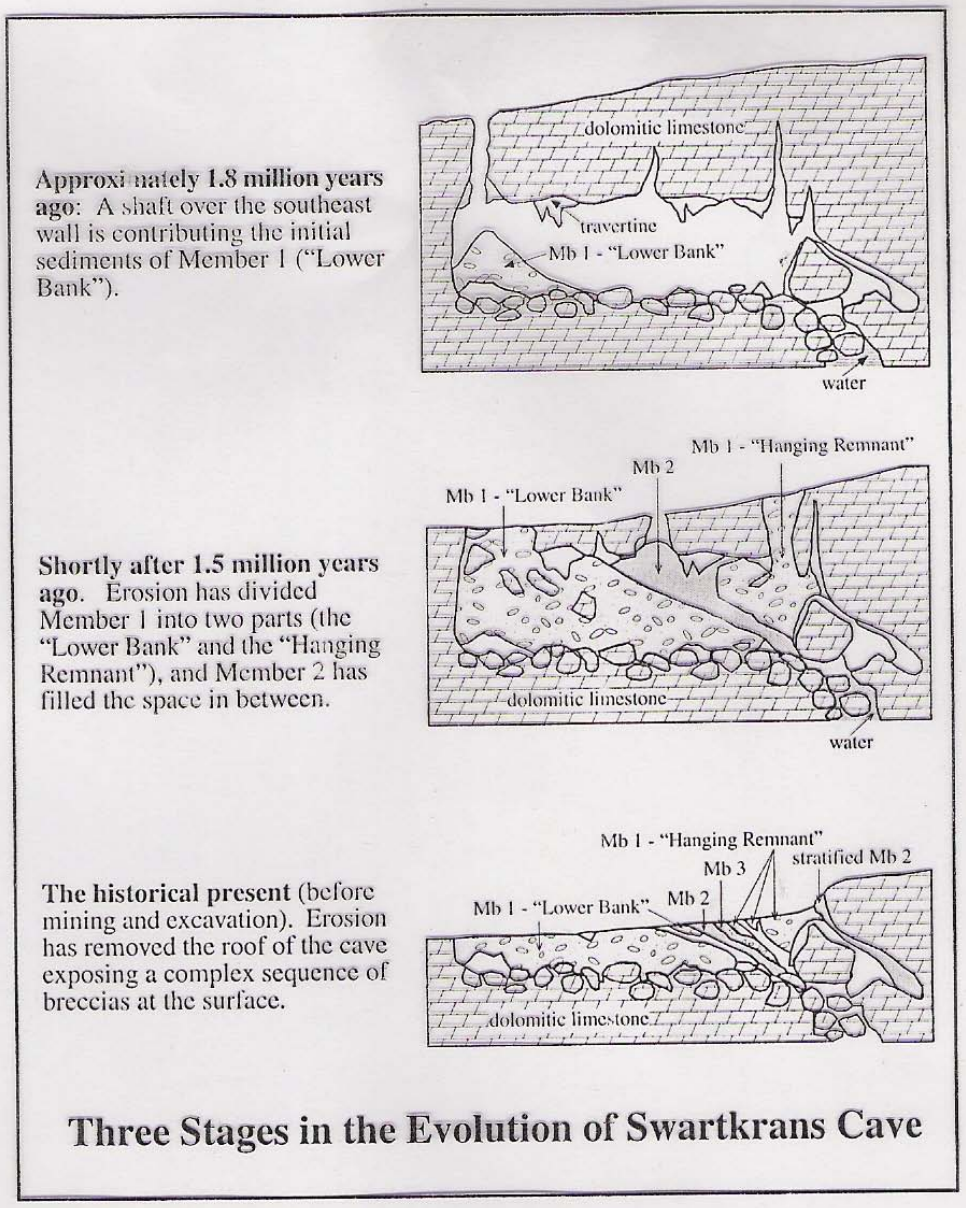

Human Skull Muscles

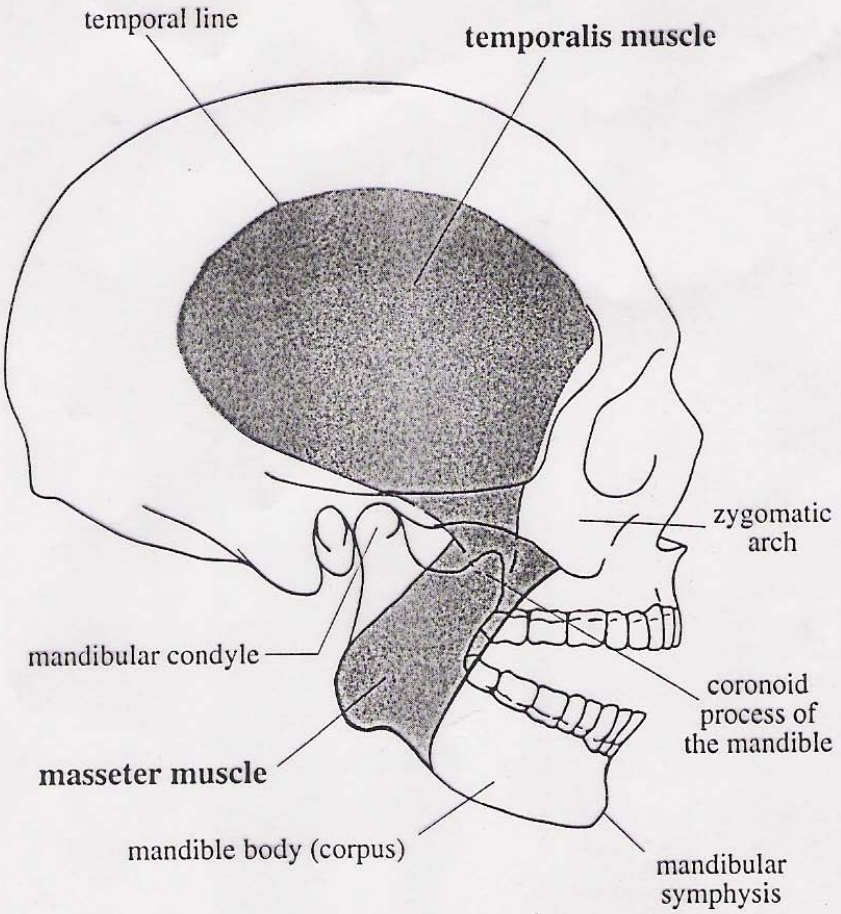

Figure 4.16. Representation of a modern human skull showing the insertion of the masseter and temporalis muscles involved in mastication (adapted from 415, p. 177). In the evolution of the later australopithecines from *Australopithecus afarensis*, the anterior (fore) part of the temporalis muscle became increasingly important relative to the posterior (rear) part. This change was accompanied by a forward shift in the root of the zygomatic arch to which the masseter muscle attaches. The result was an increase in the grinding power of the cheek teeth, also reflected in the teeth themselves.

Tibiae and Femurs of Primates

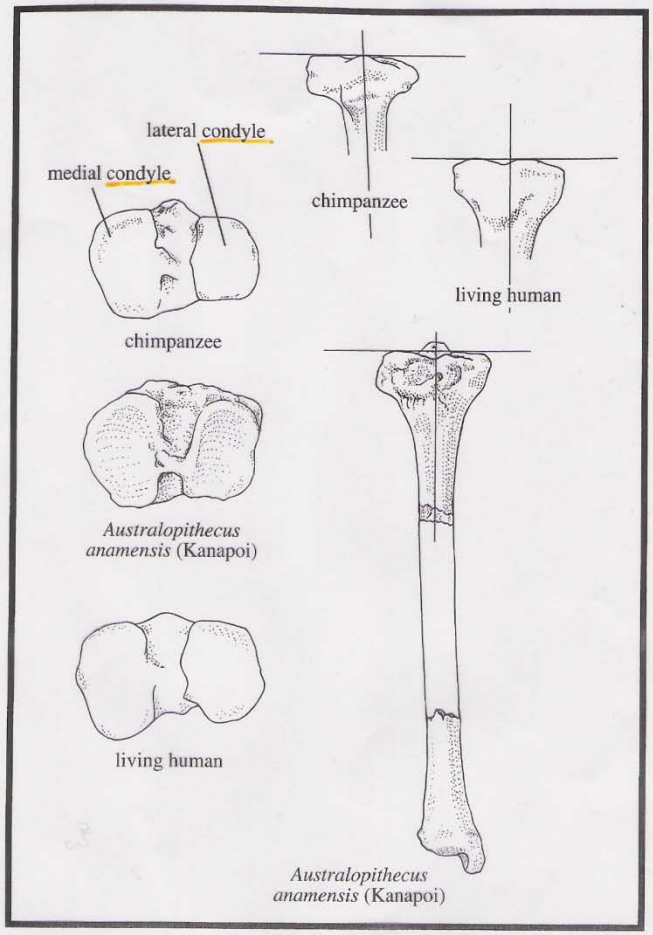

Figure 4.20. *Left:* the proximal tibiae of a chimpanzee, *Australopithecus anamensis* from Kanapoi, and a living human viewed from the surface that articulates with the distal femur. *Right:* The proximal tibiae of a chimpanzee and a living human viewed from the front and compared with the reconstructed tibia of Kanapoi *A. anamensis* (redrawn after 1339, p. 45). The Kanapoi tibia resembles the human one in the subequal size of the lateral and medial condyles and in the right angle between the proximal surface and a line bisecting the shaft. In chimpanzees the medial condyle is conspicuously larger than the lateral one, and the proximal surface meets the shaft at an oblique angle. The shared human and Kanapoi condition reflects the demands of habitual bipedal locomotion.

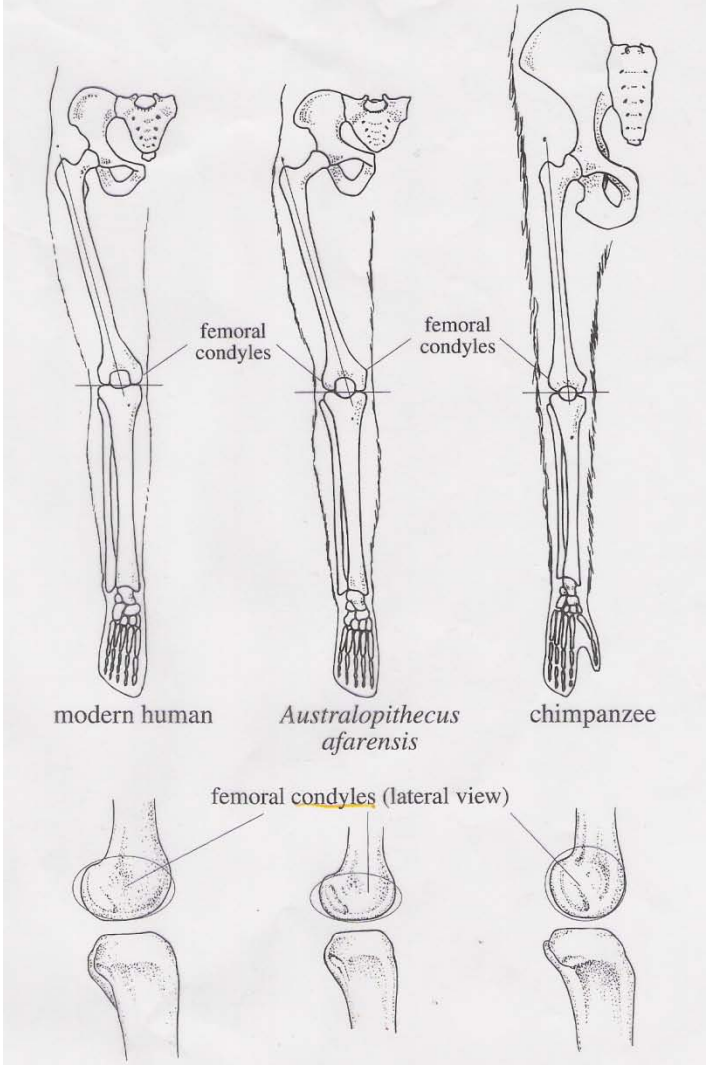

Figure 4.31. *Above:* Lower limbs of a modern human, *Australopithecus afarensis*, and a chimpanzee, with emphasis on the knee joint (redrawn after 1148, p. 157). *Below:* Lateral views of the knee joint (distal femur and proximal tibia) in the same three species. The distinct angle between the distal femur and proximal tibia, as well as the oval femoral condyles shared by modern people and *A. afarensis*,

Australopithecus afarensis

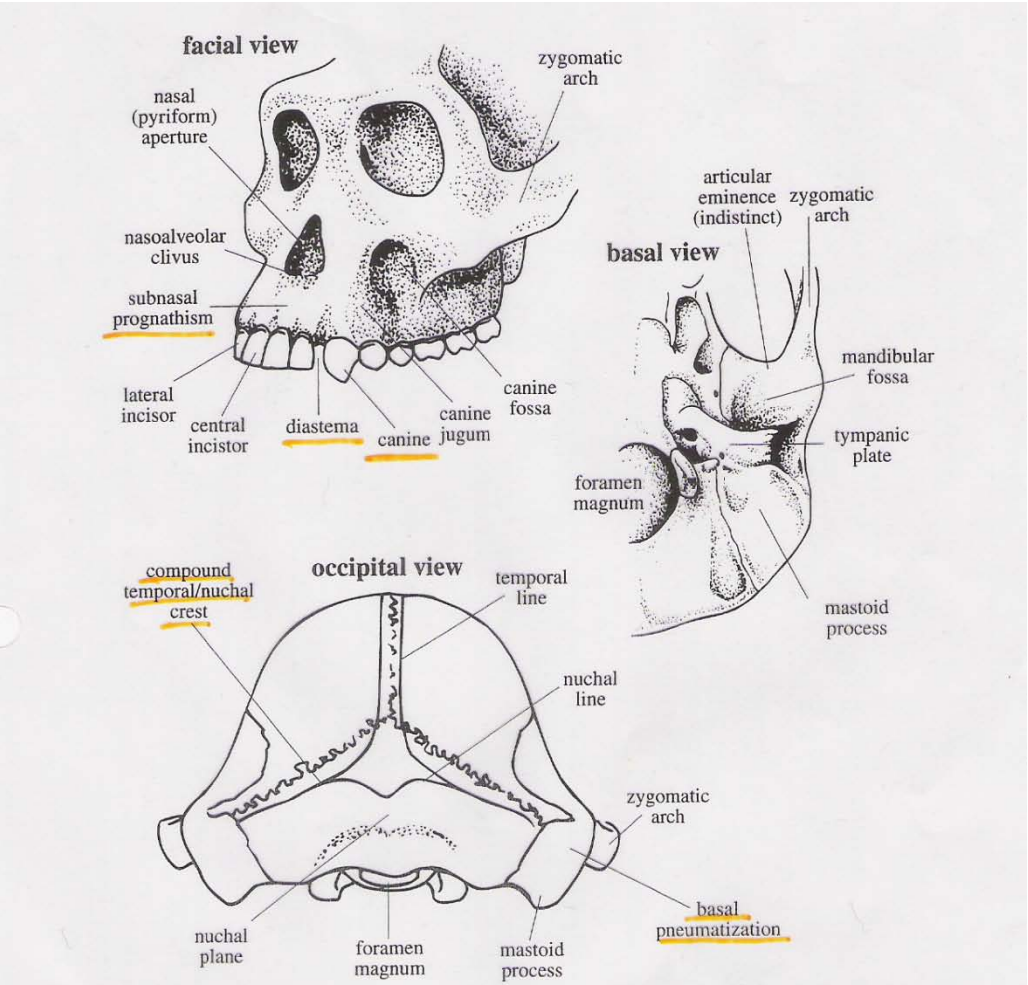

Figure 4.21 Three views of the skull of *Australopithecus afarensis*, showing important features mentioned in the text (redrawn after 2459, figs. 8, 10, 11). *A. afarensis* exhibits many primitive, apelike features, including extensive pneumatization of the cranial base, the presence of a compound temporal-nuchal crest, pronounced subnasal prognathism, the absence of a distinct articular eminence, and a diastema or gap in the upper tooth row between the lateral incisor and the canine.

Australopithecus and *Paranthropus*

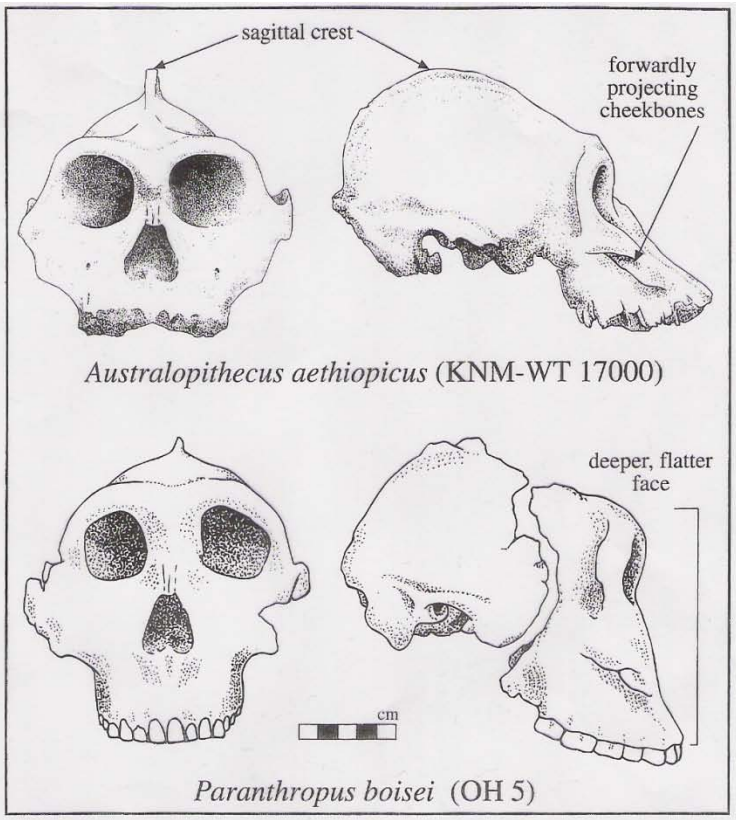

Figure 4.33. *Top:* a skull of *Australopithecus aethiopicus* dated to about 2.5 my ago at West Turkana, Kenya. *Bottom:* a skull of the "robust" australopithecine, *Paranthropus boisei* (= "*Zinjanthropus*"), dated to about 1.8 my ago at Olduvai Gorge (drawn by Kathryn Cruz-Uribe from casts and photos; © 1999 by Kathryn Cruz-Uribe). *A. aethiopicus* combined very primitive features like small endocranial capacity and pronounced alveolar prognathism with specialized "robust" features like a prominent sagittal crest and forward projection of the cheekbones. This suggests that *A. aethiopicus* could have been ancestral to *P. boisei*. Alternatively, the shared specializations may imply only a shared, independently evolved dietary adaptation, emphasizing heavy chewing between the upper and lower cheek teeth. (KNM-WT = Kenya National Museum–West Turkana; OH = Olduvai Hominid.)

analogies or homologies?

Paranthropus boisei

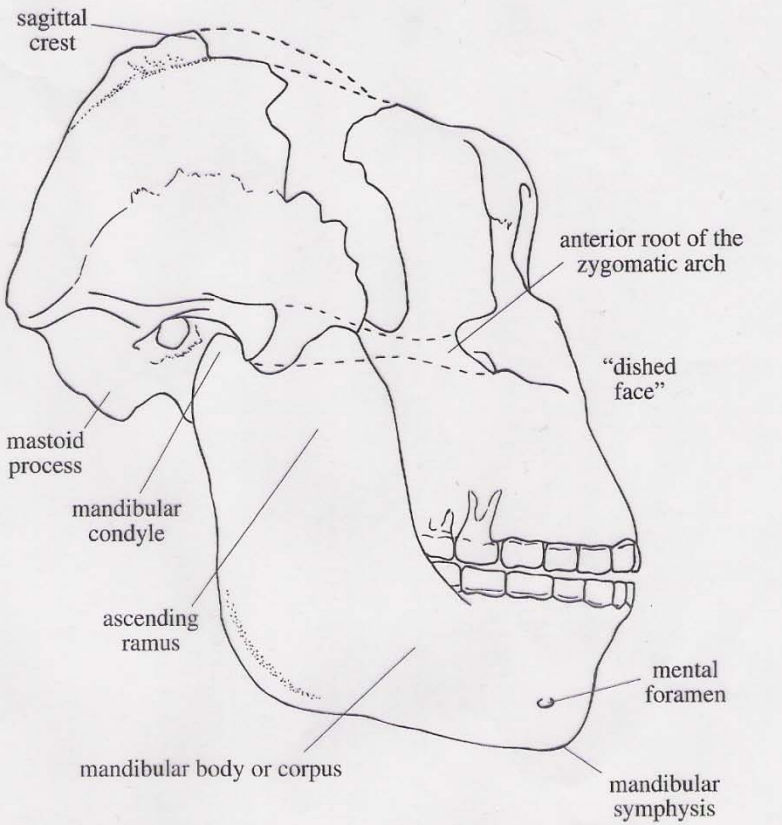

Figure 4.22. *Top:* Lateral view of a mandible from Swartkrans articulated with a reconstructed *Paranthropus boisei* skull fromOlduvai Gorge. *Bottom:* Occlusal view of the mandible (redrawn after 415, fig. 7.8). The occlusal outline has been slightly distorted by pressure in the ground that compressed the horizontal branches inward. Note such characteristic robust australopithecine characters as the anteriorly placed sagittal crest, dish-shaped face, thick, deep mandibular body, and molarized premolars.

Paranthropus robustus

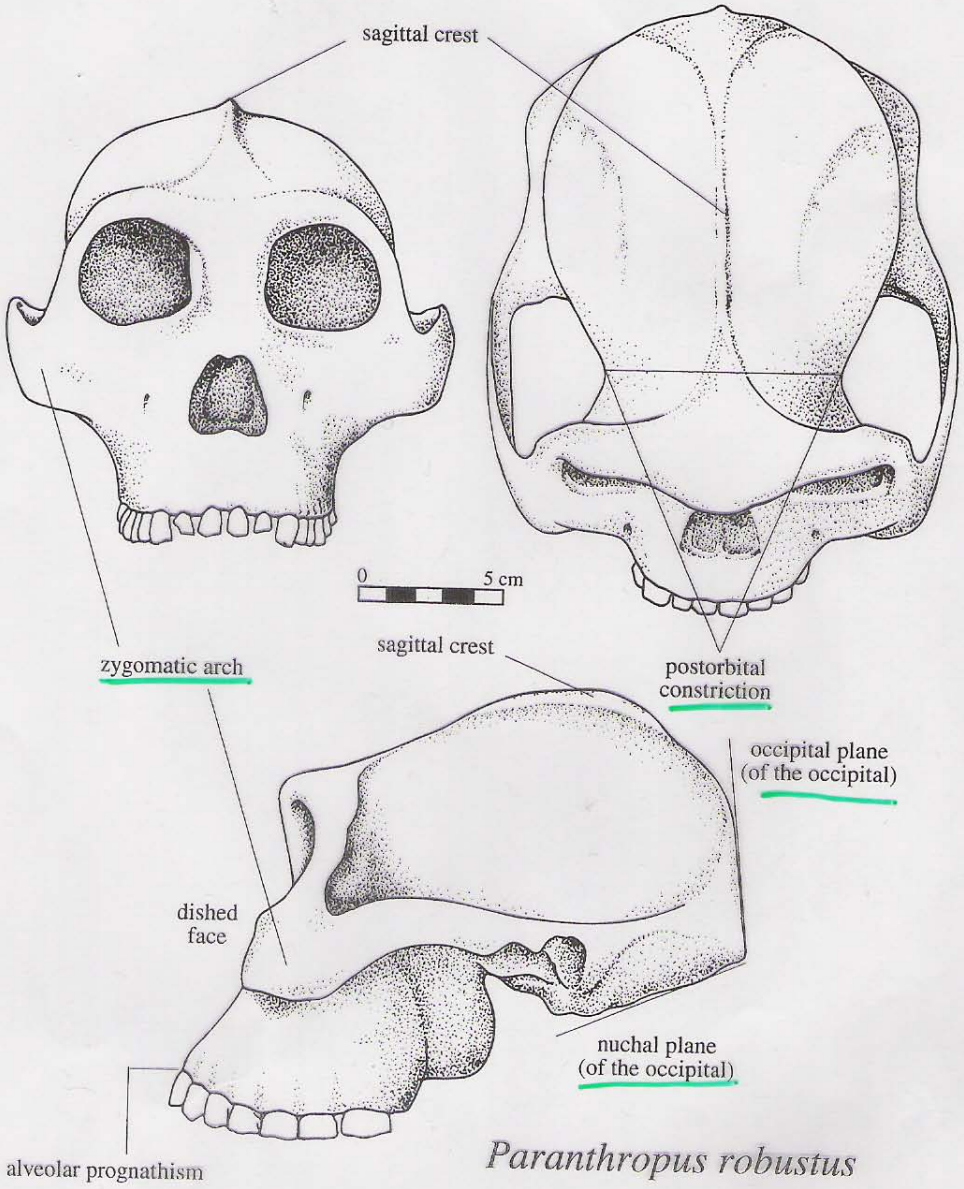

Figure 4.23. Front, top, and side views of a reconstructed skull of *Paranthropus robustus* (redrawn after 1073, fig. 10.7). Note the anteriorly placed sagittal crest, the powerfully built, widely flaring zygomatic arches, pronounced postorbital constriction, dish-shaped face, and sharply angled occipital bone, which singly and together characterize the robust australopithecine skull.

Cranial Variation

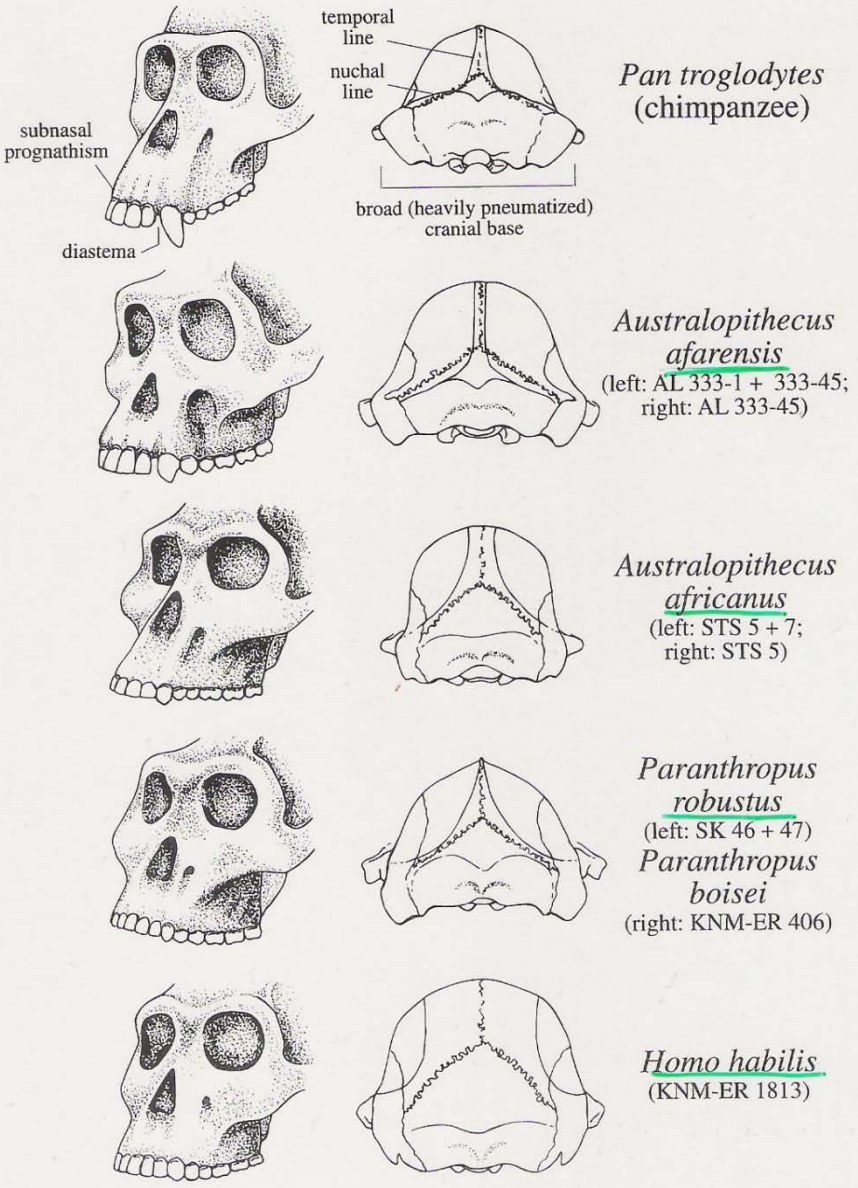

Figure 4.24. Facial and occipital views of *Pan troglodytes* (chimpanzee), *Australopithecus afarensis*, *A. africanus*, *Paranthropus robustus*, *P. boisei*, and *Homo habilis* (redrawn after 2459, figs. 9, 10). Note how *A. afarensis* and the chimpanzee are alike in their pronounced subnasal prognathism, relatively large anterior teeth, diastema between the lateral incisor and the canine, confluence of the temporal and nuchal lines, great breadth of the cranial base, and other features. Note also how *A. afarensis* differs from other hominids in all these respects. (AL = Hadar; STS = Sterkfontein; SK = Swartkrans; KNM-ER = Kenya National Museum–East Rudolf.)

Canines of Primates

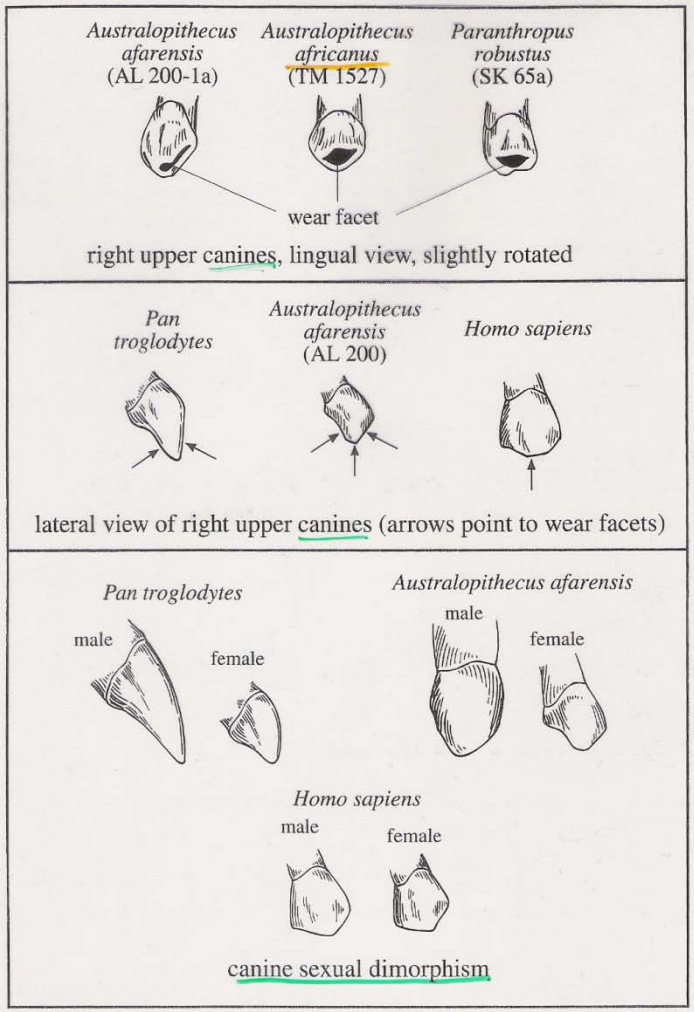

Figure 4.27. Upper canine morphology of various australopithecines, the chimpanzee, and modern humans (top redrawn after 2459, fig. 14; middle and bottom redrawn after 1148, p. 268). In *Australopithecus afarensis* the canine wore not only at the tip, as in later hominids, but also on the fore and rear (mesial and distal) surfaces, as it does in chimpanzees. *A. afarensis* was also more apelike in the degree of canine size difference between the sexes. (AL = Hadar; TM = Transvaal Museum; SK = Swartkrans.)

Palates of Primates

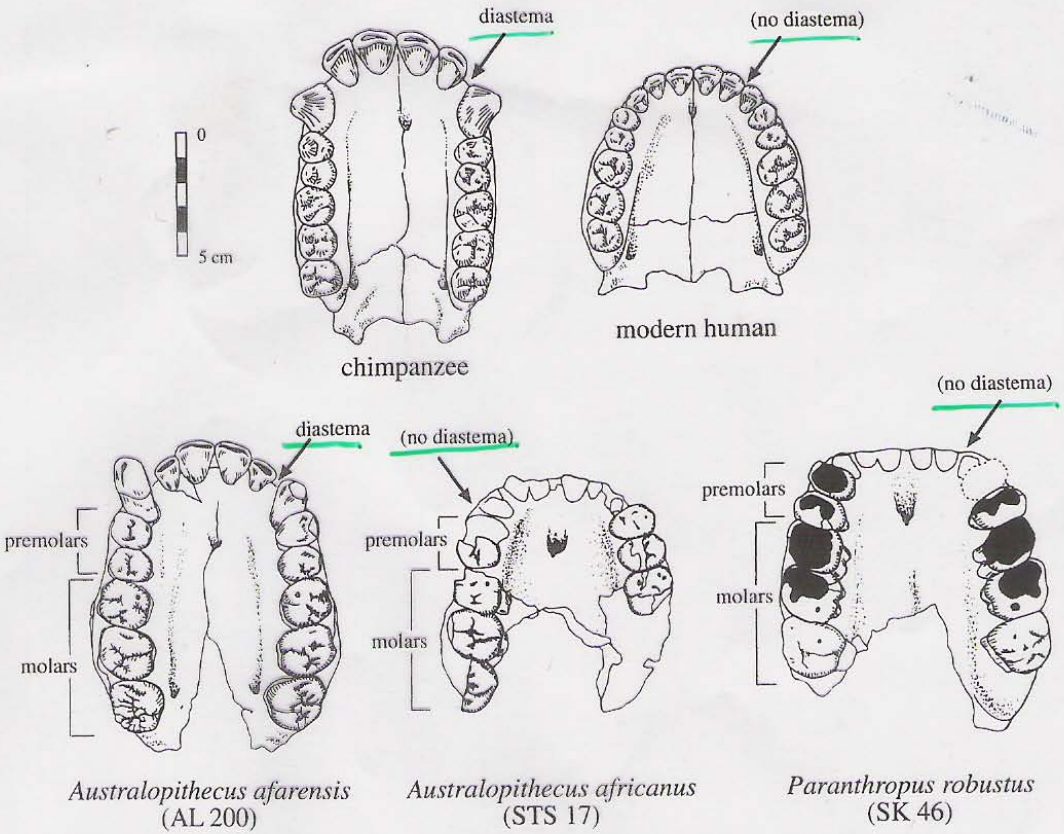

Figure 4.26. Palates of a chimpanzee, various australopithecines, and a modern human (top row redrawn after 1148, p. 367; bottom row redrawn after 2459, fig. 9). Note the presence of a diastema between the lateral incisor and the canine in both the chimpanzee and *Australopithecus afarensis*, and note also the enlargement of the premolars versus the other teeth in *A. africanus* and especially in *Paranthropus robustus*. (AL = Hadar; STS = Sterkfontein; SK = Swartkrans.)

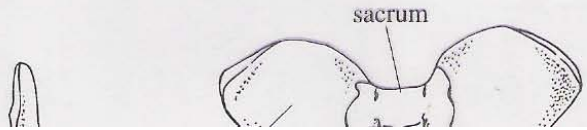

Figure 4.32. Left lateral and full frontal views of

Pelvises of Primates

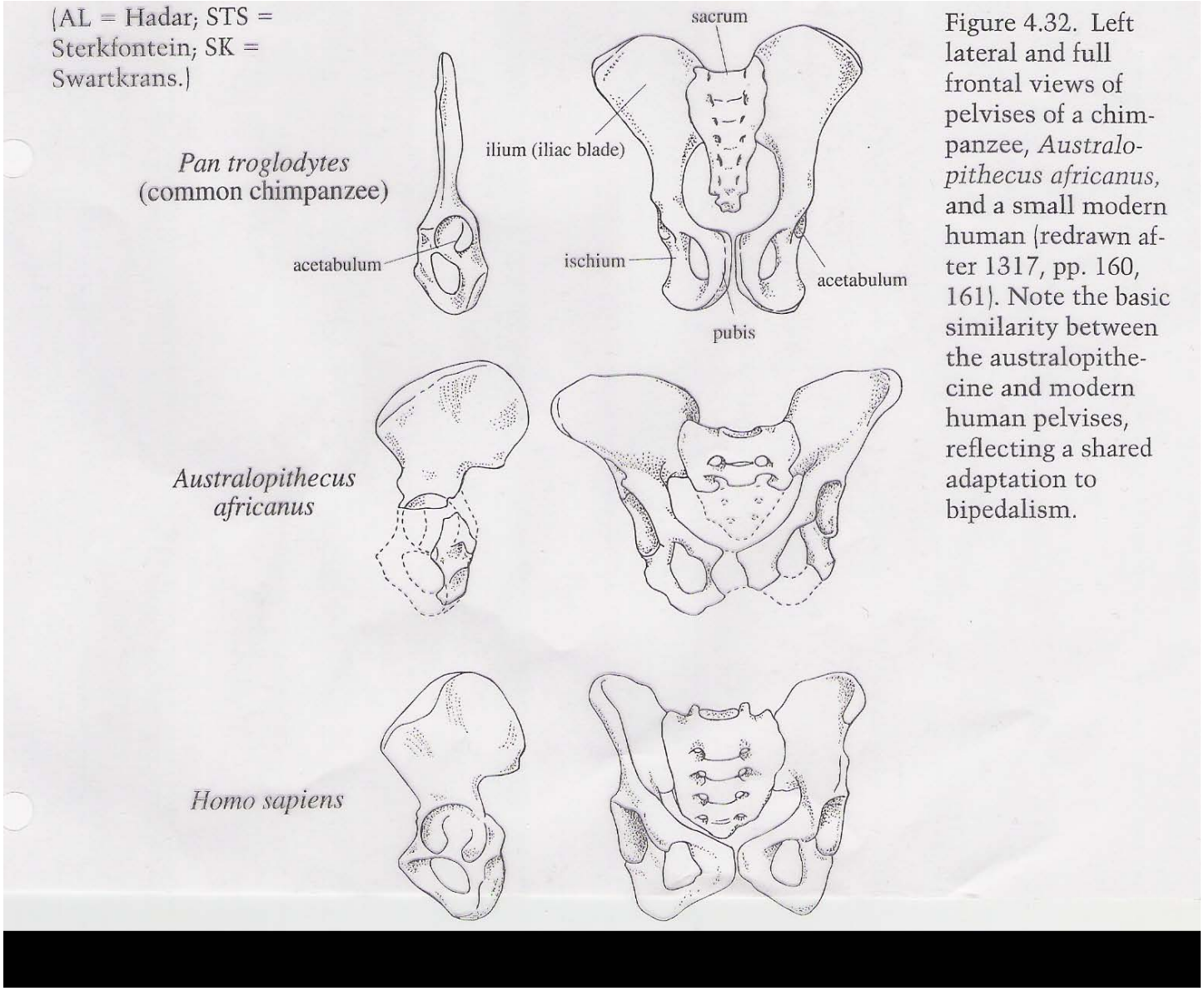

Figure 4.32. Left lateral and full frontal views of pelvises of a chimpanzee, *Australopithecus africanus,* and a small modern human (redrawn after 1317, pp. 160, 161). Note the basic similarity between the australopithecine and modern human pelvises, reflecting a shared adaptation to bipedalism.

Lower Third Premolar Morphology

KNM-ER = Kenya National Museum–East Rudolf.)

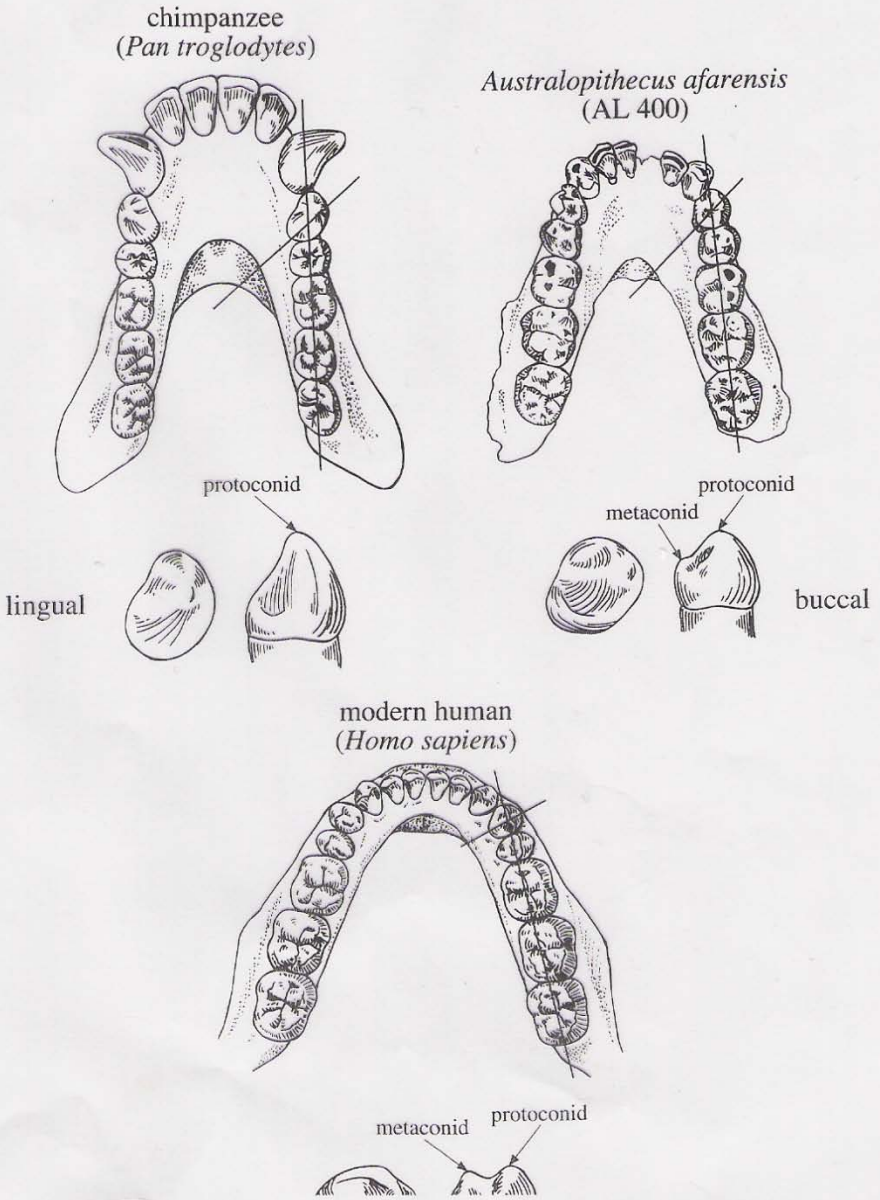

Figure 4.29. Lower third premolar (P_3) morphology in the chimpanzee, in *Australopithecus afarensis*, and in modern humans (redrawn after 1148, p. 269). Note that in its P_3 *A. afarensis* was intermediate between the chimpanzee and modern people. Thus it maintained roughly the same angle between the P_3 axis and the rest of the tooth row as is seen in the chimpanzee, but the P_3 itself was somewhat rounder and sometimes had a small inner or lingual cusp (meta-

Homo Phylogeny

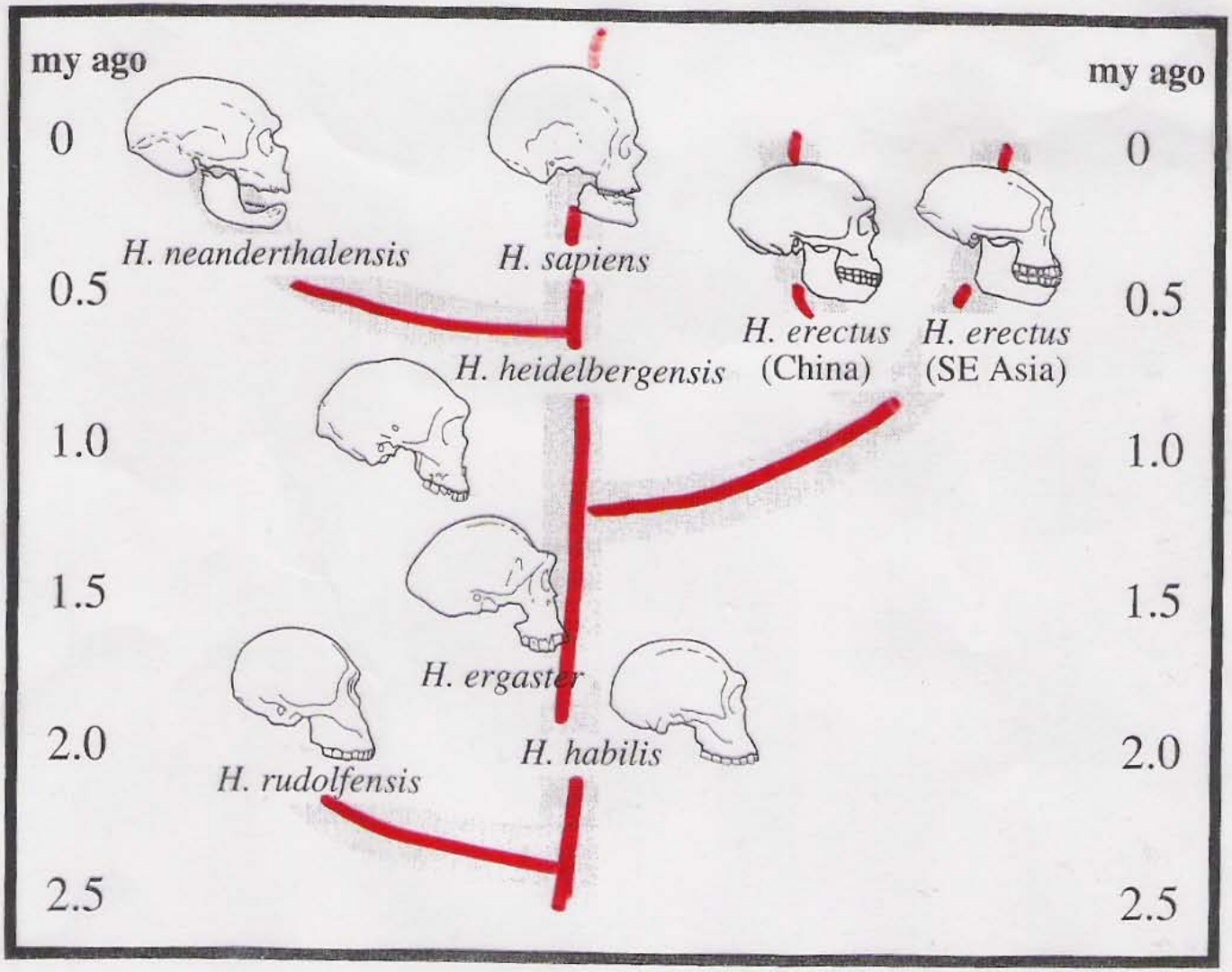

Figure 5.1. The phylogeny of the genus *Homo*.

Homo halibis

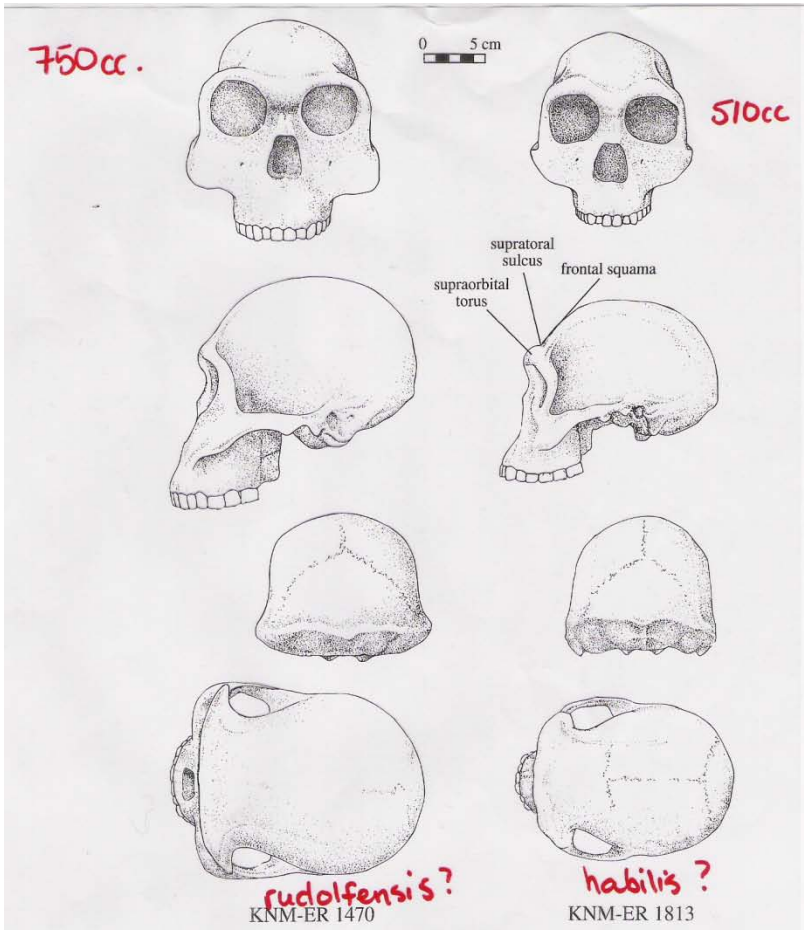

Figure 4.34. Reconstructed skulls of *Homo habilis* (broadly understood) from Koobi Fora (redrawn after 1074, fig 10.9). Both skulls date from roughly 1.9–1.8 my ago, but they differ sharply in size and more subtly in shape. KNM-ER 1470 has an endocranial capacity of about 750 cc and large cheek teeth (inferred from the alveoli). Its face is relatively long (from the bridge of the nose to a point between the upper central incisors), broad across the orbits, and flattened below the nose. KNM-ER 1813 has an endocranial capacity of about 510 cc and much smaller cheek teeth. Its face is shorter, narrower across the orbits, and more projecting below the nose. It also has a more developed supraorbital torus (browridge). Many authorities believe the difference could reflect sexual dimorphism within a single species (male on the left, female on the right) but a growing number think it reflects

Cladograms of the Hominids

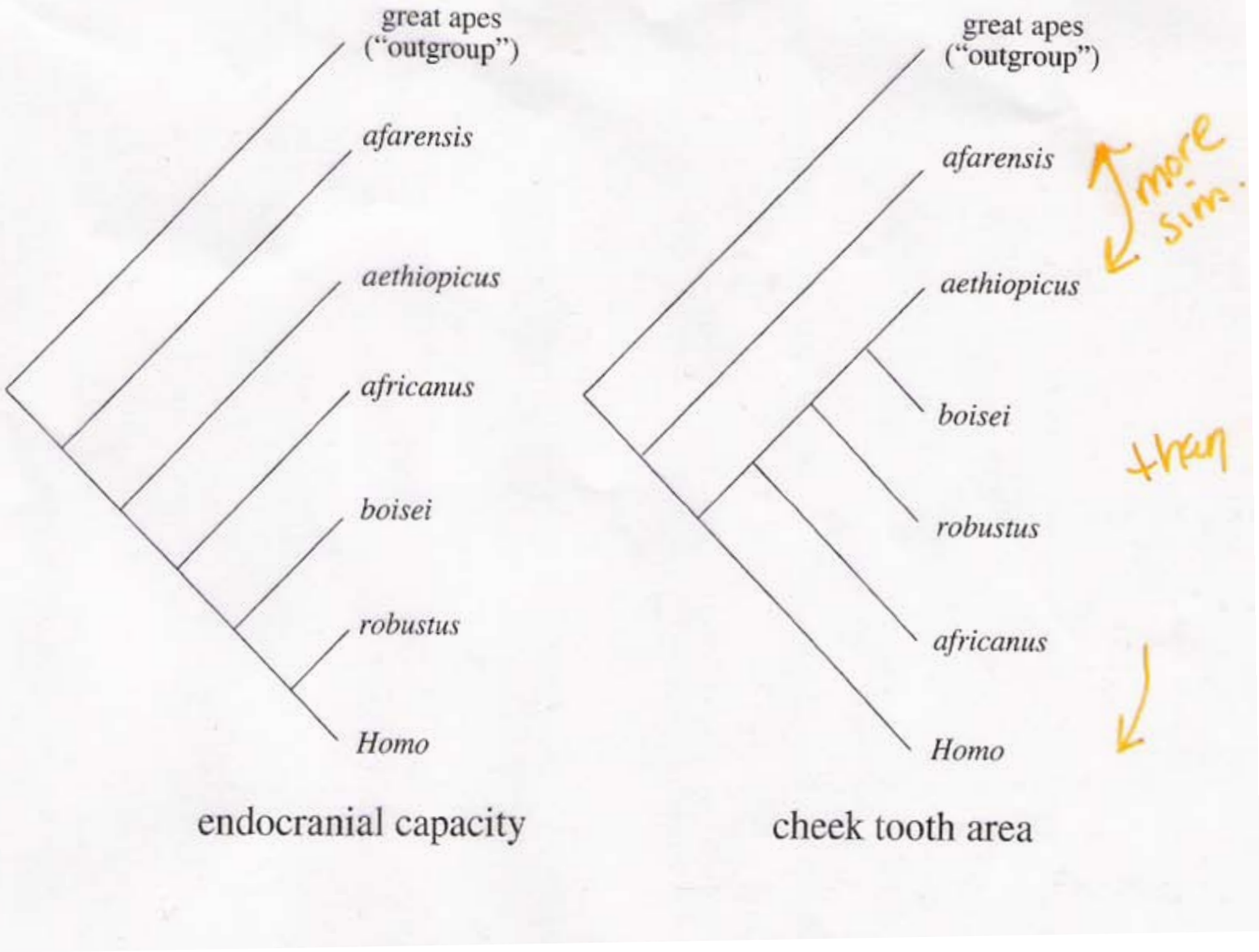

Figure 4.35. Cladograms showing the evolutionary relationships of the australopithecines and *Homo* suggested by endocranial capacity (*left*) and cheek tooth area (*right*). The contrast implies that similarities in endocranial capacity, cheek tooth area, or both must partly or wholly reflect parallel evolution (homoplasy) rather than true evolutionary relationships (redrawn after 1512, p. 83).

Hominid Evolutional Relationships

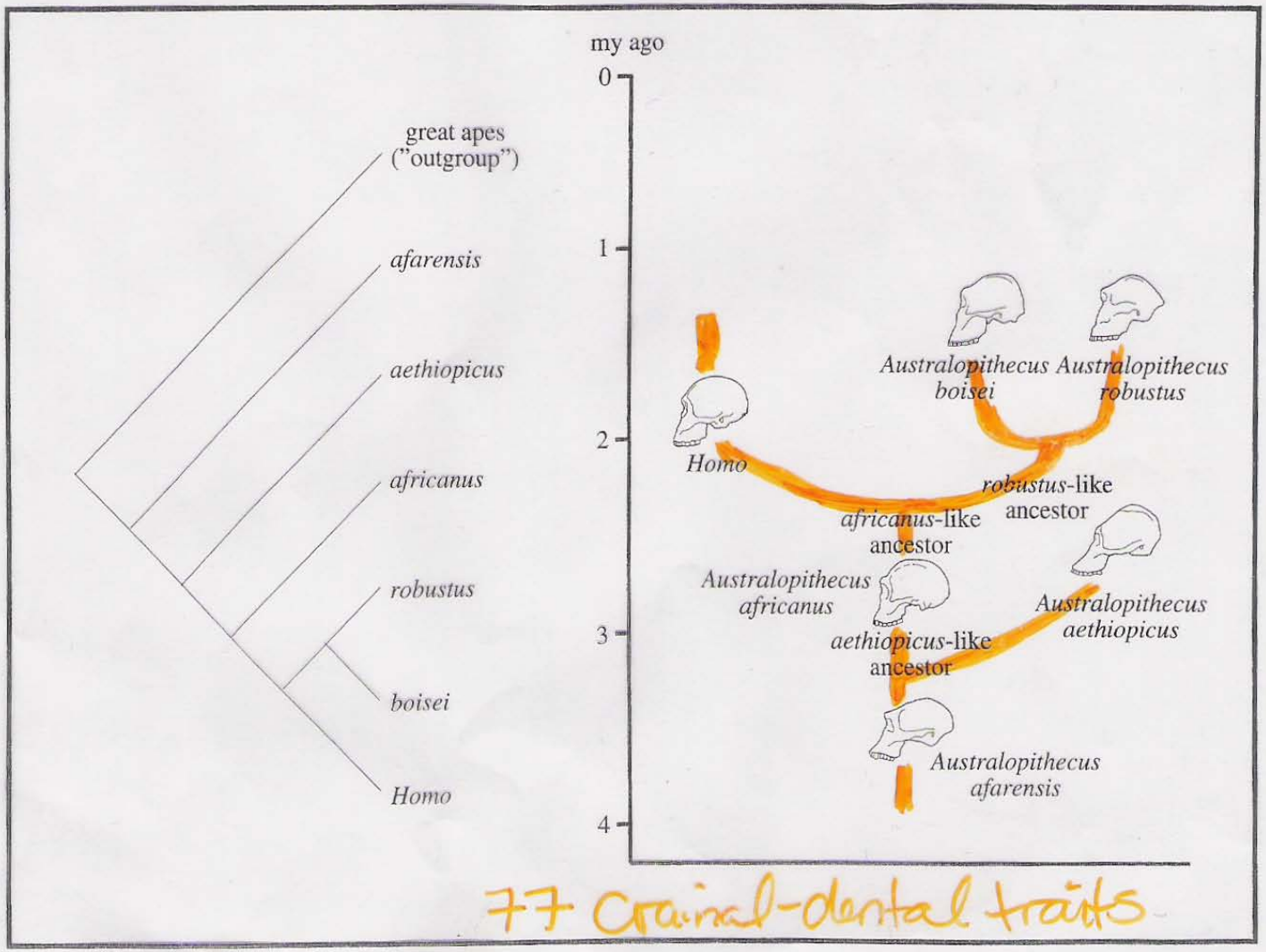

Figure 4.36. The evolutionary relationships among the australopithecines and *Homo* that Skelton and McHenry have inferred from seventy-seven craniodental characters. *Left:* the cladogram requiring the least amount of parallel evolution (homoplasy) in these characters.

Hominid Evolutional Relationships

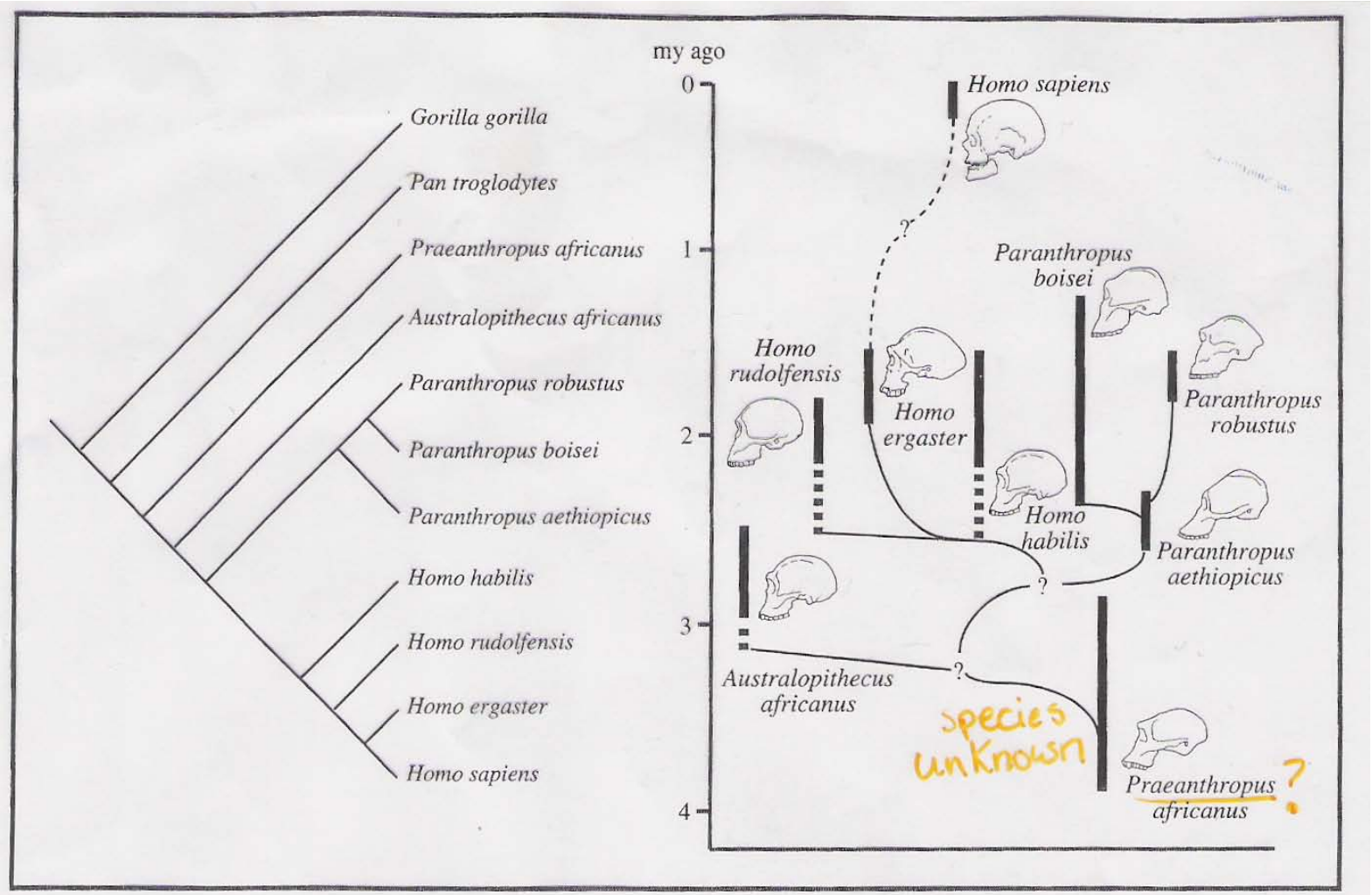

Figure 4.37. The evolutionary relationships among the australopithecines and *Homo* inferred that Strait, Grine, and Moniz have inferred from sixty craniodental characters. *Left:* the cladogram requiring the least amount of parallel evolution (homoplasy) in these characters. *Right:* the most plausible phylogeny that this cladogram implies (redrawn after 2055, p. 55).

Appearance of the Earliest Artefacts

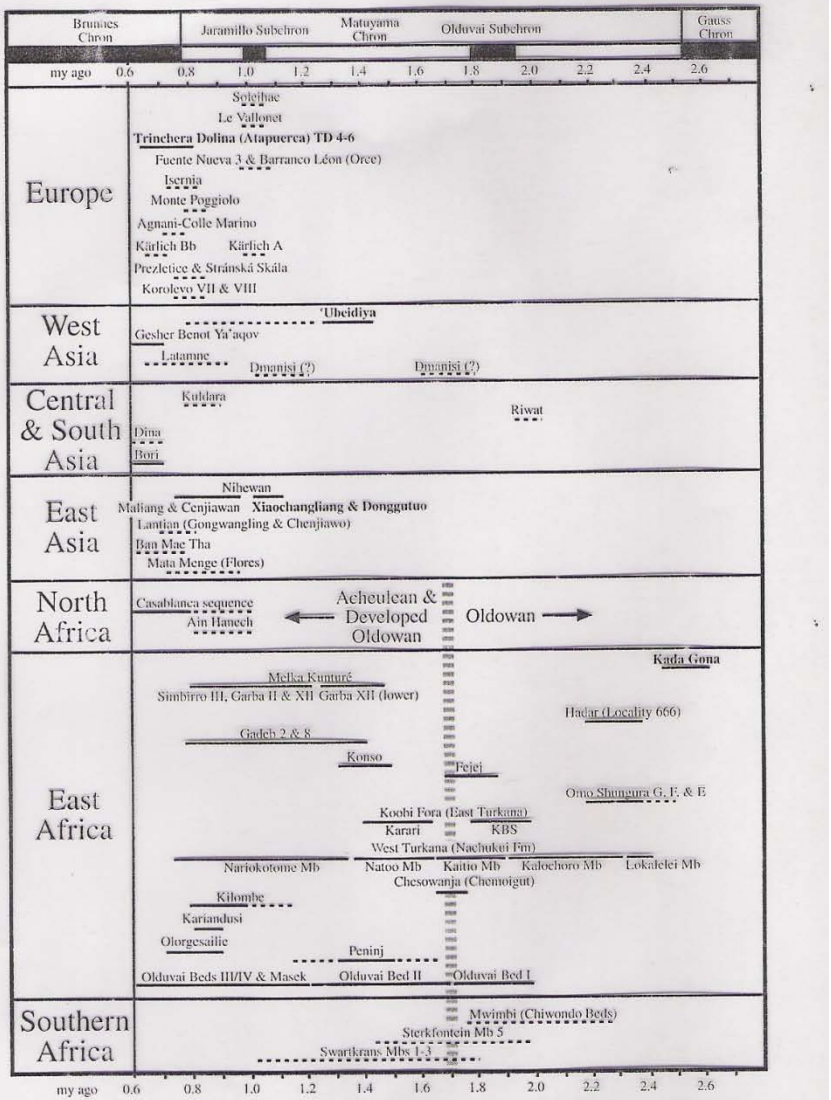

Figure 4.5. Dating of the earliest artifact industries in Africa and Eurasia (in a format suggested by 1119, fig. 13.2). Dotted lines indicate possible or probable dates based mainly on geologic inference or faunal correlations. Boldface marks the oldest secure sites on each continent. The best evidence for people in Eurasia before 1 my ago comes from 'Ubeidiya in Israel, only marginally outside Africa. On the known record, people colonized the farther reaches of Asia and Europe only after 1 my ago.

Flintknapping

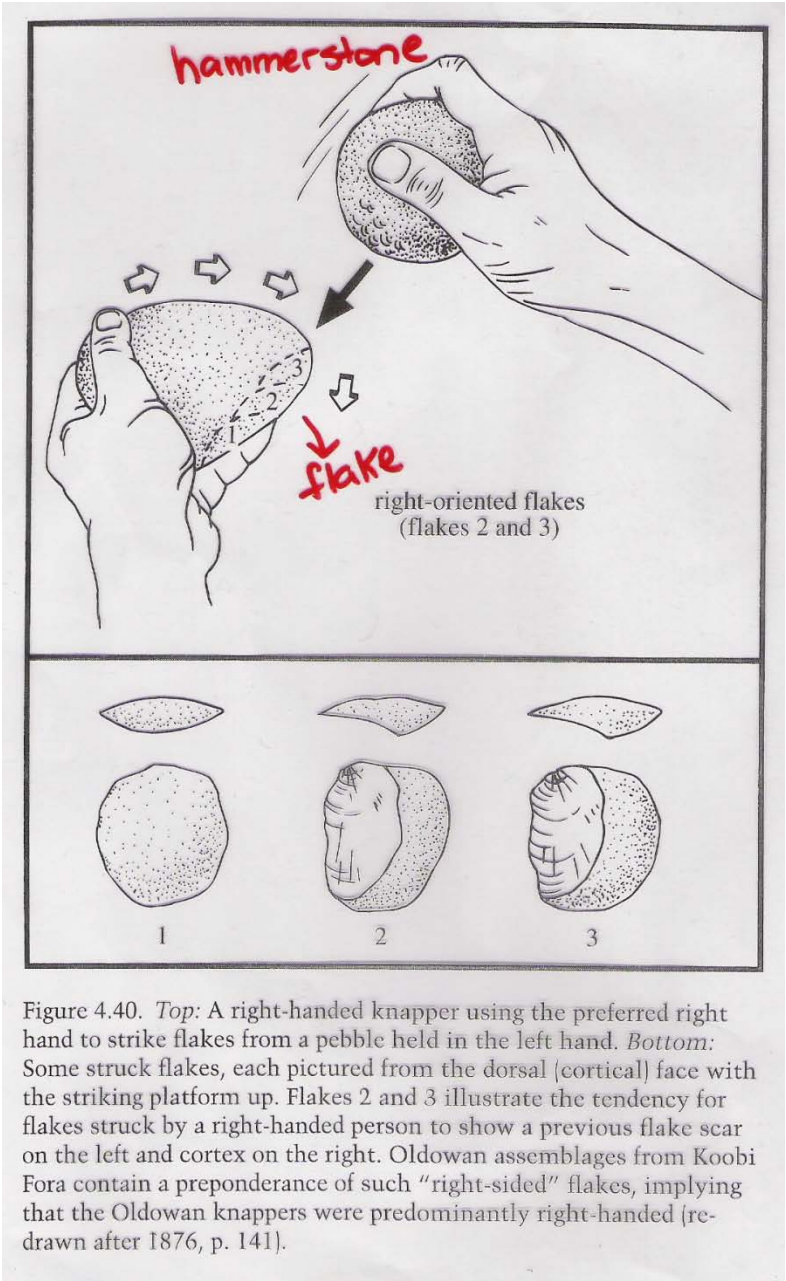

Figure 4.40. *Top:* A right-handed knapper using the preferred right hand to strike flakes from a pebble held in the left hand. *Bottom:* Some struck flakes, each pictured from the dorsal (cortical) face with the striking platform up. Flakes 2 and 3 illustrate the tendency for flakes struck by a right-handed person to show a previous flake scar on the left and cortex on the right. Oldowan assemblages from Koobi Fora contain a preponderance of such "right-sided" flakes, implying that the Oldowan knappers were predominantly right-handed (redrawn after 1876, p. 141).

Oldowan Artefacts

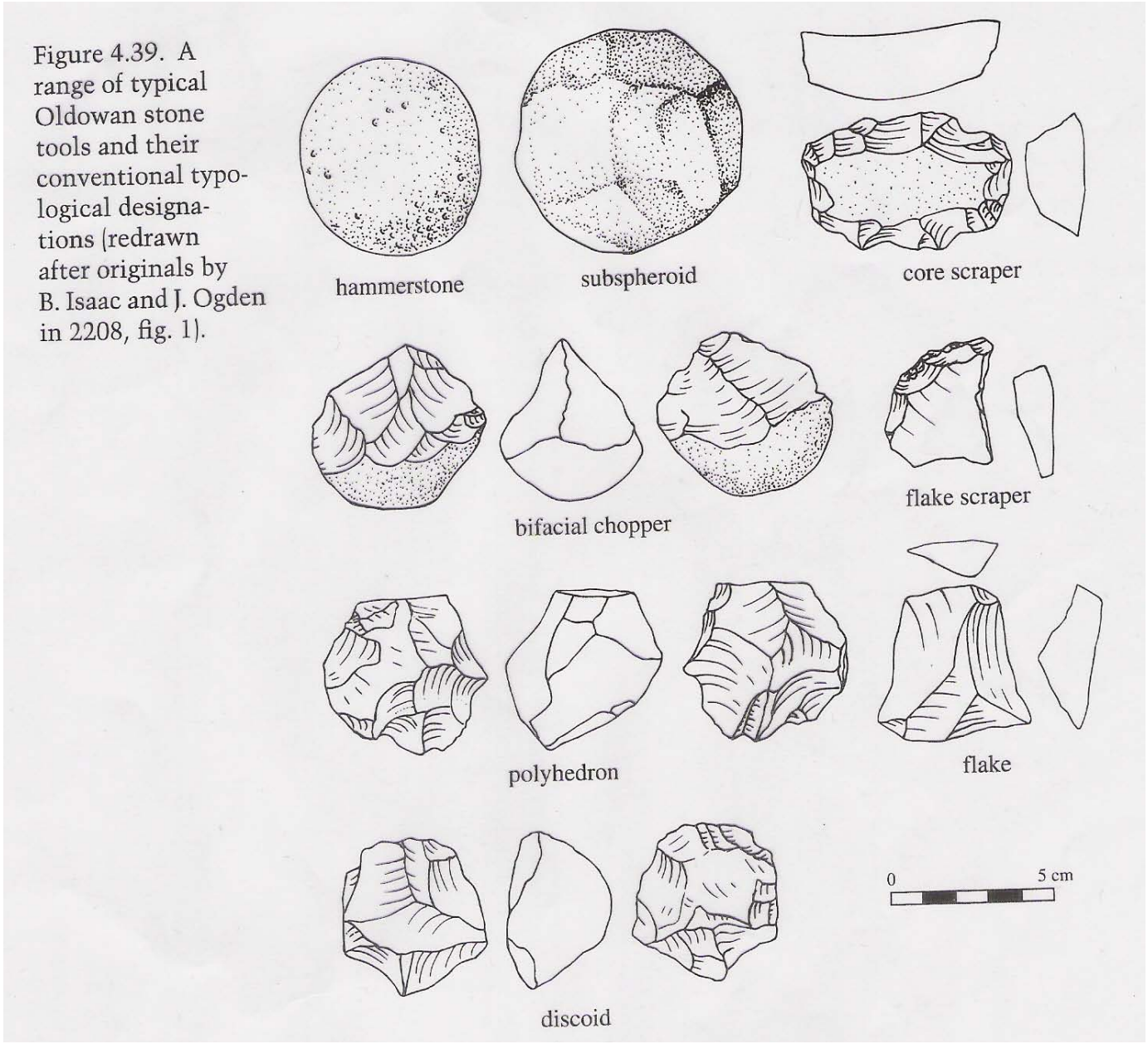

Figure 4.39. A range of typical Oldowan stone tools and their conventional typological designations (redrawn after originals by B. Isaac and J. Ogden in 2208, fig. 1).

Oldowan and Acheulean Artefacts

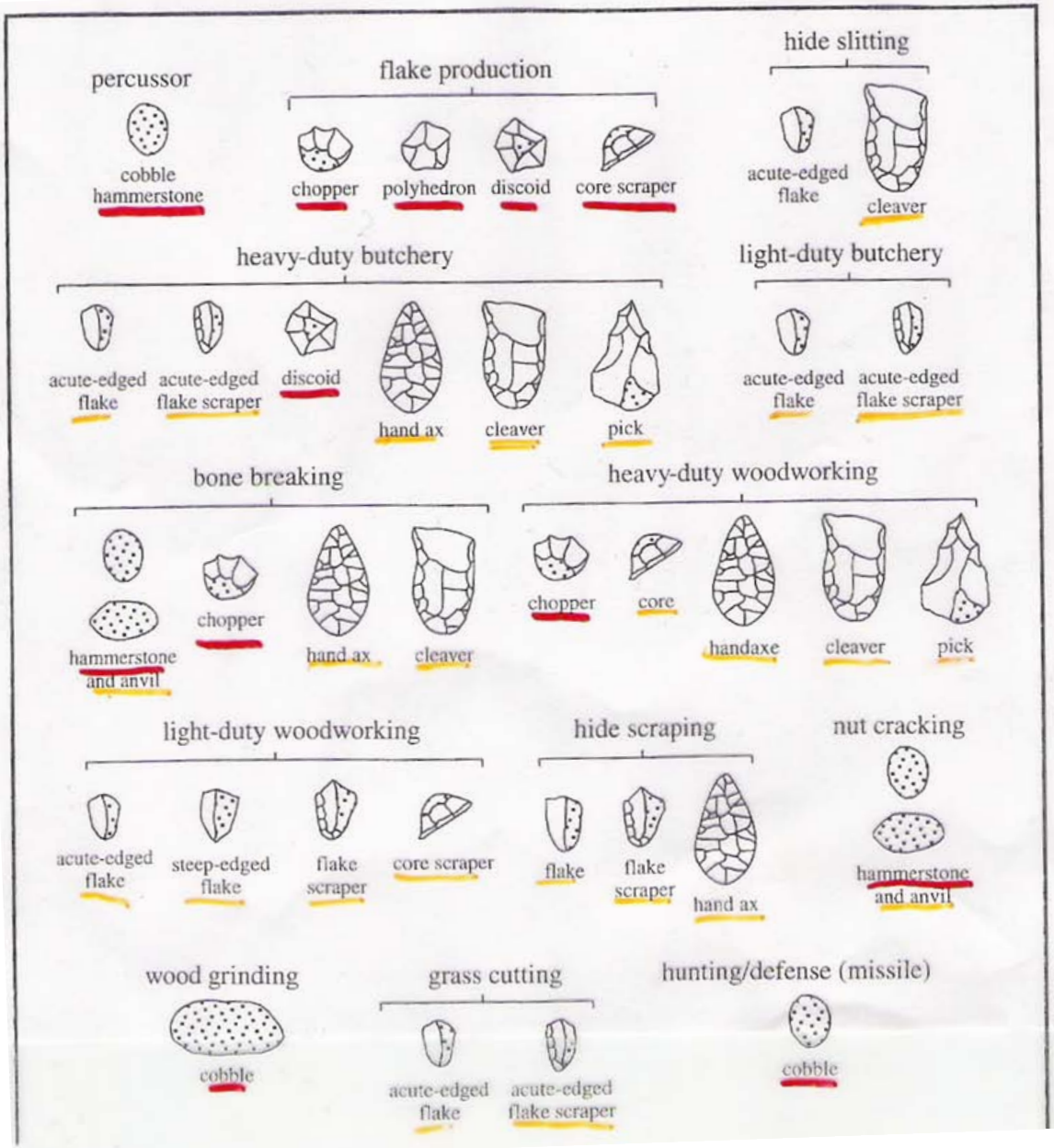

Figure 4.38. The basic types of stone artifacts found at Oldowan and Acheulean sites in Africa (adapted from 2208, fig. 7). The Acheulean is usually distinguished from the preceding Oldowan by the presence of hand axes, cleavers, and other large bifacial tools. Large bifacial tools do, however, occur in some "Developed Oldowan" assemblages. The suggested uses are based on feasibility experiments with replicas.

Structure? At DK 1 in Olduvai Gorge

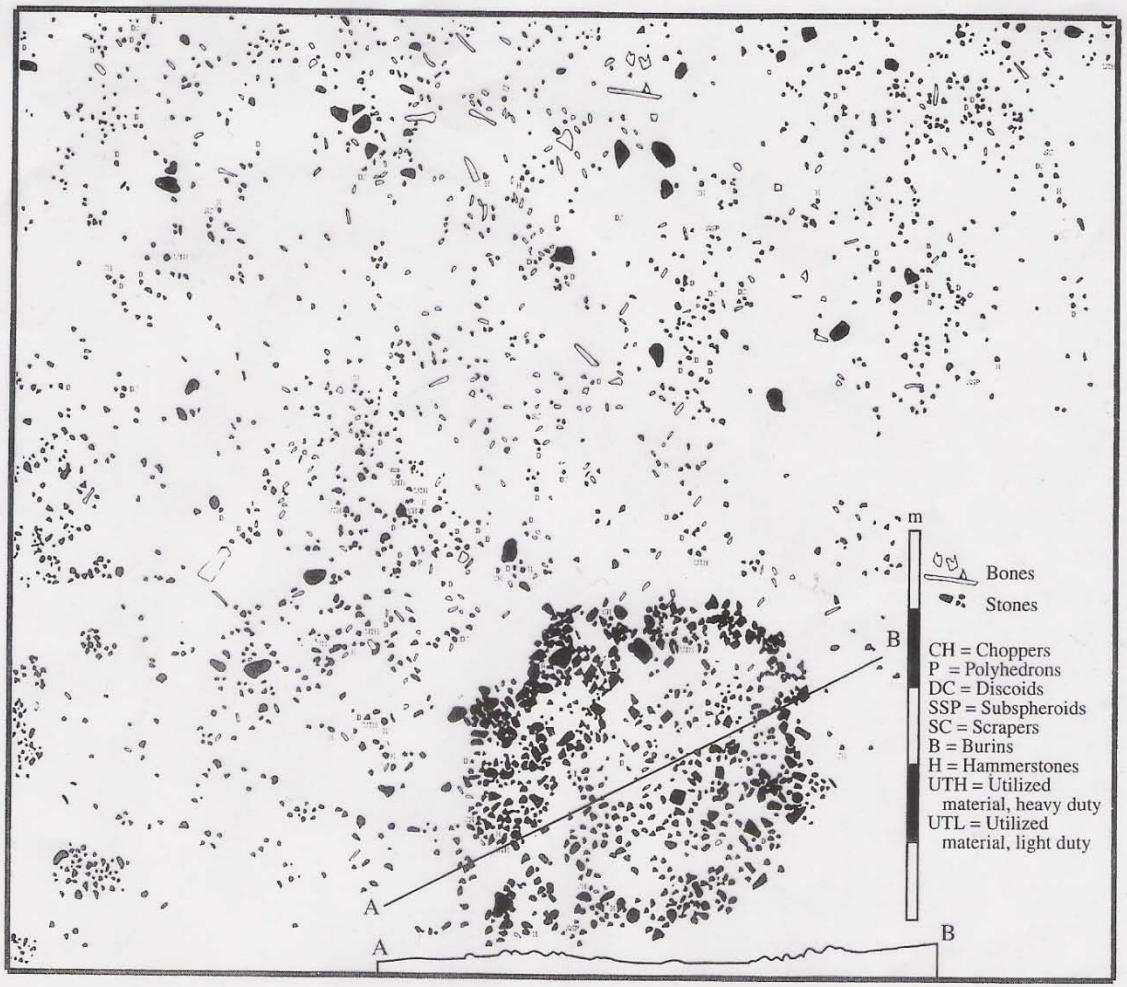

Figure 4.41. A partial floor plan of site DK 1 at Olduvai Gorge (redrawn after 1327, fig. 7). The most striking feature is the large circular concentration of basalt fragments in the right foreground. This may mark the base of the oldest known structure in the world, or more prosaically it may indicate only the location of a tree whose radiating roots fractured pieces of basalt and forced them up from immediately below the occupation surface.

+/- 2mya ?

Faunal Remains at Hominid Sites

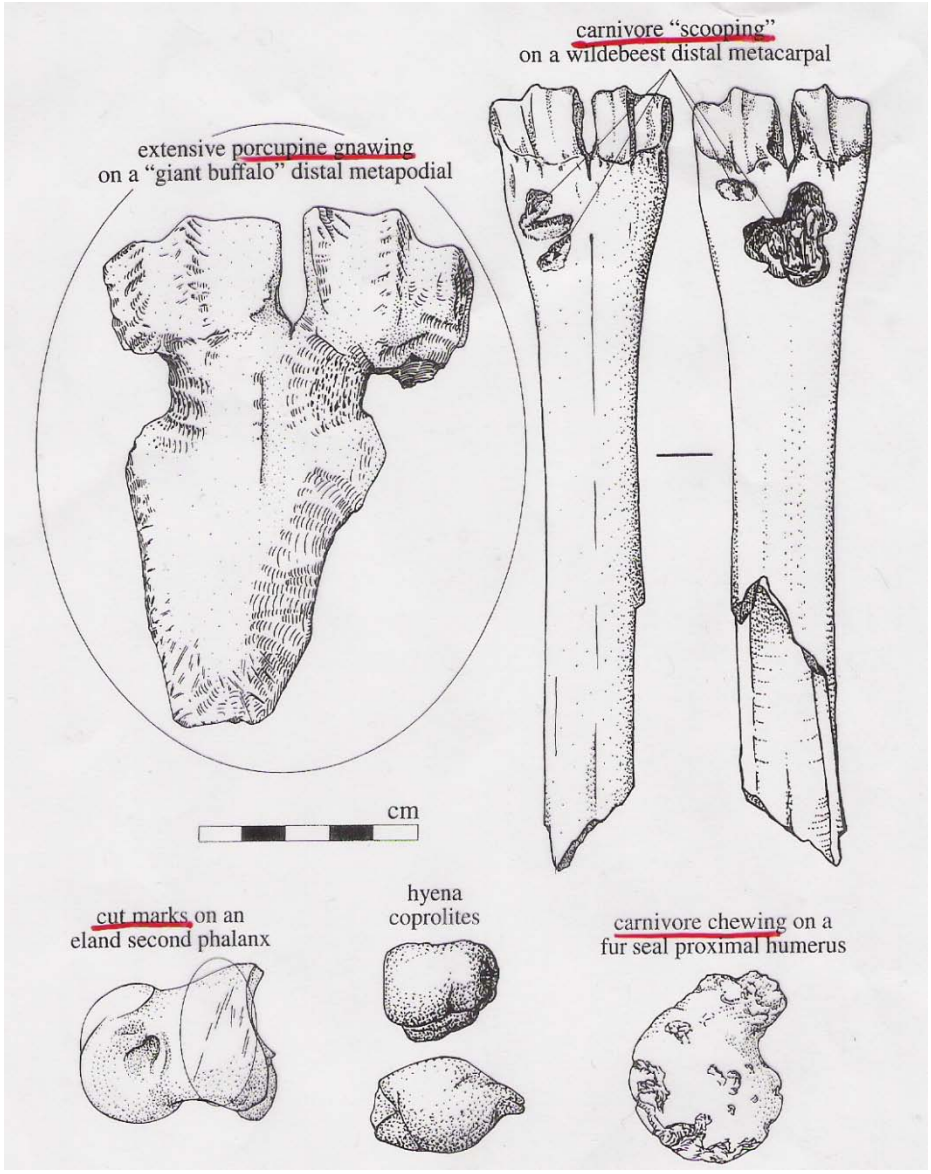

Figure 4.42. *Upper left:* A porcupine-gnawed "giant buffalo" distal metapodial. *Upper right:* A black wildebeest distal metacarpal on which the outer table of the bone has been partially removed ("scooped out") by carnivore gnawing. *Lower left:* Multiple, subparallel cut marks on an eland second phalanx. *Lower middle:* Hyena coprolites (fossilized feces). *Lower right:* A carnivore-chewed fur seal proximal humerus. The buffalo and wildebeest metapodials were originally similar in form, and the current difference shows the extensive remodeling that porcupines can produce. The carnivore-damaged bones closely match specimens in collections produced by recently observed carnivores. Cut marks frequently cluster in a pattern like that on the eland second phalanx. The buffalo metapodial comes from Middle Stone Age layer 16 at Klasies River Mouth Cave 1, Western Cape Province, South Africa; the wildebeest metacarpal and the hyena coprolites come from a fossil hyena lair at Deelpan, Free State Province, South Africa; and the eland and fur seal bones come from the Later Stone Age site of Kasteelberg, Western Cape Province, South Africa. (Buffalo metapodial drawn by Katharine Scott. Re-

FLK Zinj, Olduvai Gorge Large Mammals

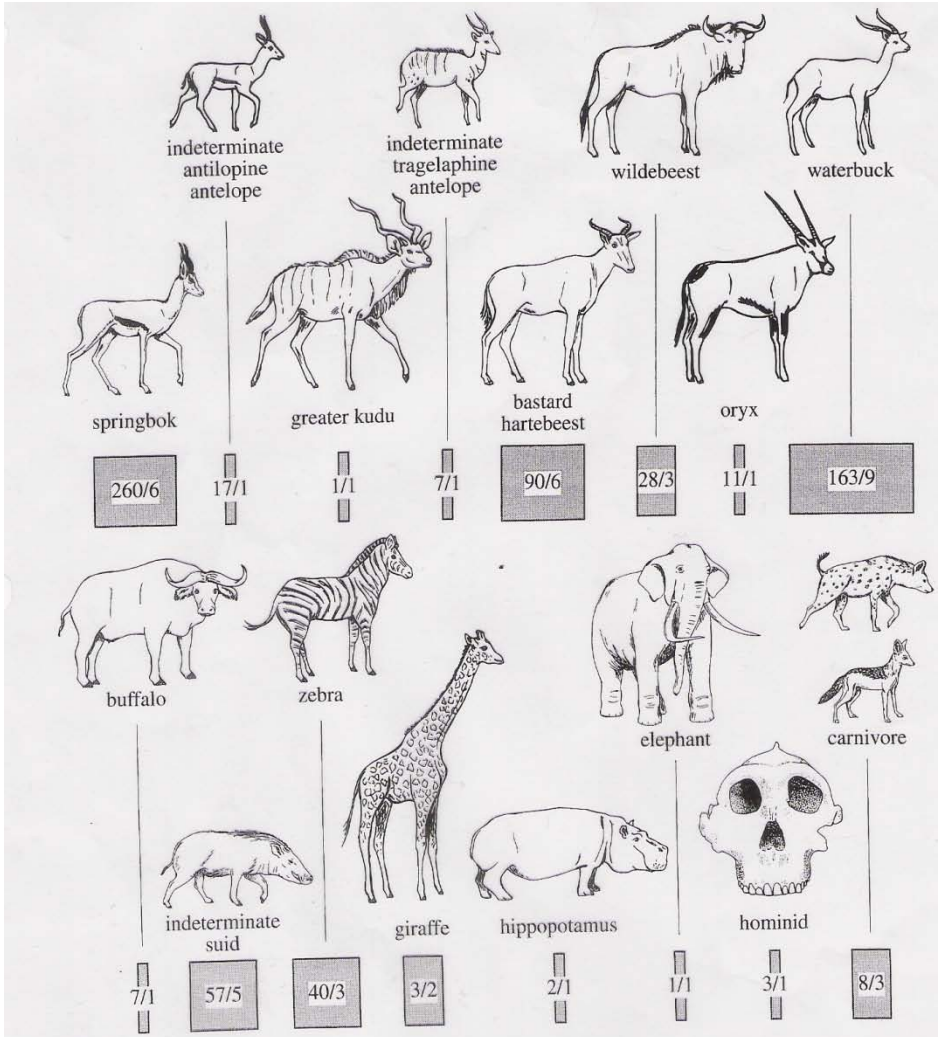

Figure 4.43. The abundance of various large mammals at the FLK Zinj site in Olduvai Gorge Bed I (data from 389). The bars are proportional to the minimum number of individuals by which each species is represented. The numbers superimposed on the bars are the number of bones assigned to each species over the minimum number of individuals. The sample is small, but it still shows the preponderance of antelopes and other medium-sized species that tends to characterize all African Stone Age sites, regardless of age. As discussed in the text, specialists disagree on how the animal bones accumulated at FLK Zinj—whether it was mainly through human activity and, if so, whether the people were hunting or scavenging.

>1.75 mya

Homo Sites

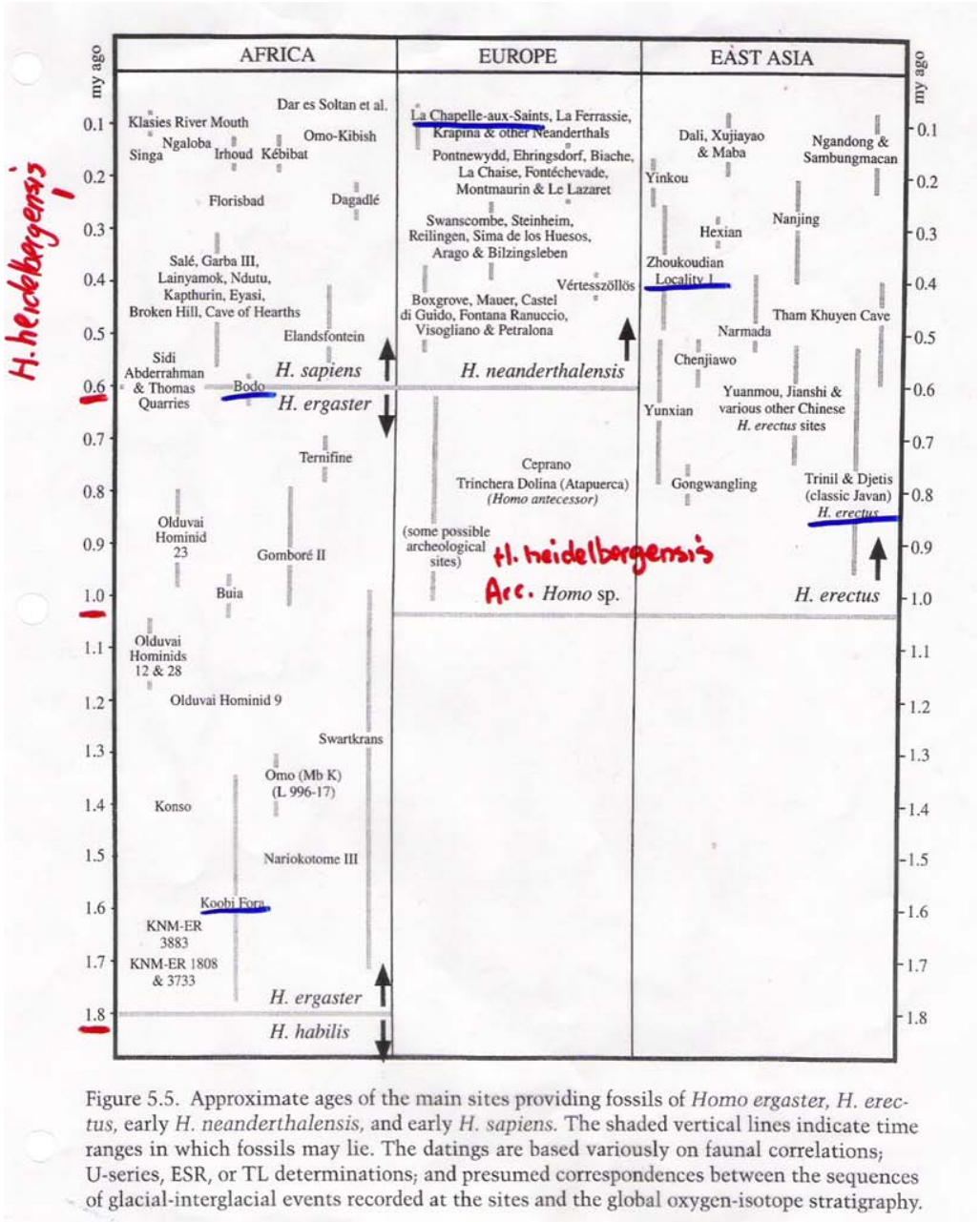

Figure 5.5. Approximate ages of the main sites providing fossils of *Homo ergaster, H. erectus,* early *H. neanderthalensis,* and early *H. sapiens.* The shaded vertical lines indicate time ranges in which fossils may lie. The datings are based variously on faunal correlations; U-series, ESR, or TL determinations; and presumed correspondences between the sequences of glacial-interglacial events recorded at the sites and the global oxygen-isotope stratigraphy.

Homo ergaster KNM-ER 3733

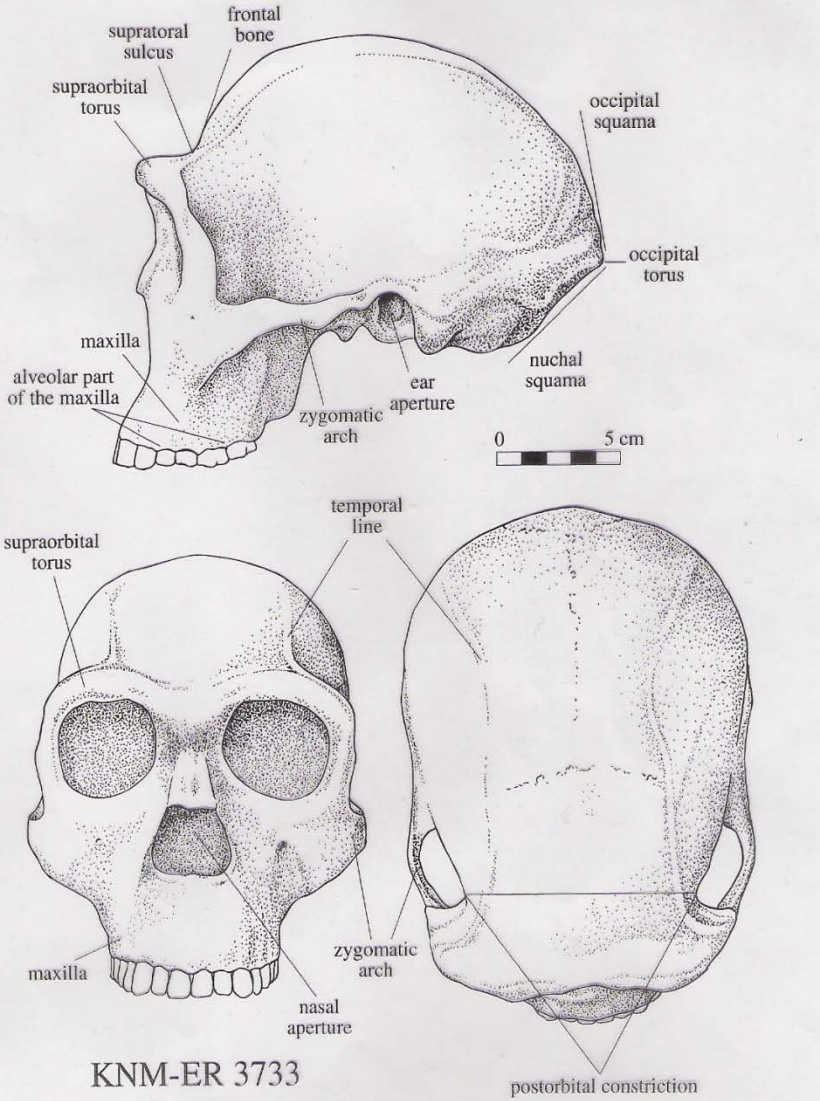

Figure 5.10. Skull KNM-ER 3733 from Koobi Fora, East Turkana (formerly East Rudolf), northern Kenya (redrawn by Kathryn Cruz-Uribe after 1073, fig. 10.10; © 1999 by Kathryn Cruz-Uribe). The skull exhibits several features that distinguish it from preceding *Homo habilis*, including a large, forwardly projecting supraorbital torus, a supratoral sulcus separating the torus from a low, receding frontal, a highly angulated occipital bone with a pronounced occipital torus, and an expanded braincase (with an estimated endocranial capacity of 848 cc). It is one of three north Kenyan fossils documenting the emergence of *Homo ergaster* about 1.7–1.6 my ago. (KNM-ER = Kenya National Museum–East Rudolf.)

Homo ergaster KNM-WT 15000

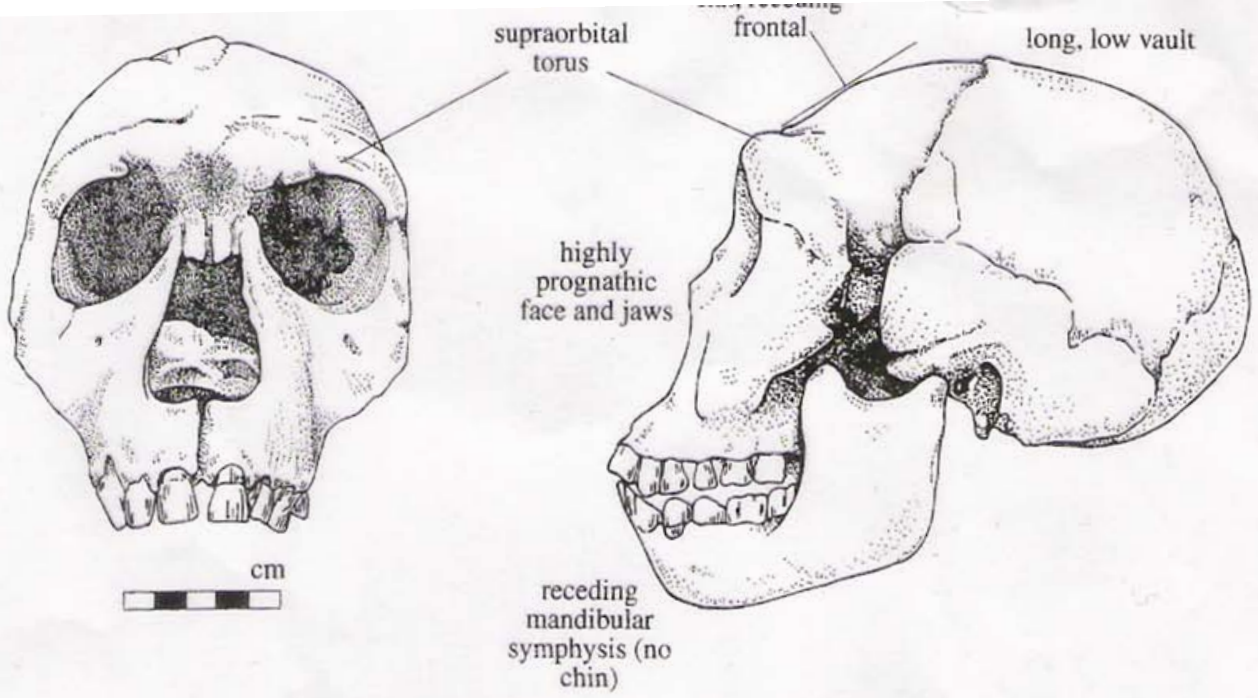

KNM-WT 15000 (Nariokotome III)

Figure 5.11. Skull of KNM-WT 15000 from Nariokotome III, West Turkana, northern Kenya (drawn by Kathryn Cruz-Uribe from photos in 2362; © 1999 by Kathryn Cruz-Uribe). The skull is roughly 1.5 my old, and it exhibits the same features that distinguish other skulls of *Homo ergaster* (or early African *H. erectus*) from those of *H. habilis*, including a distinct supraorbital torus, an enlarged braincase (with an endocranial capacity of 880 cc), and a reduction in the postcanine dentition. (KNM-WT = Kenya National Museum–West Turkana.)

Homo ergaster Olduvai Hominid 9

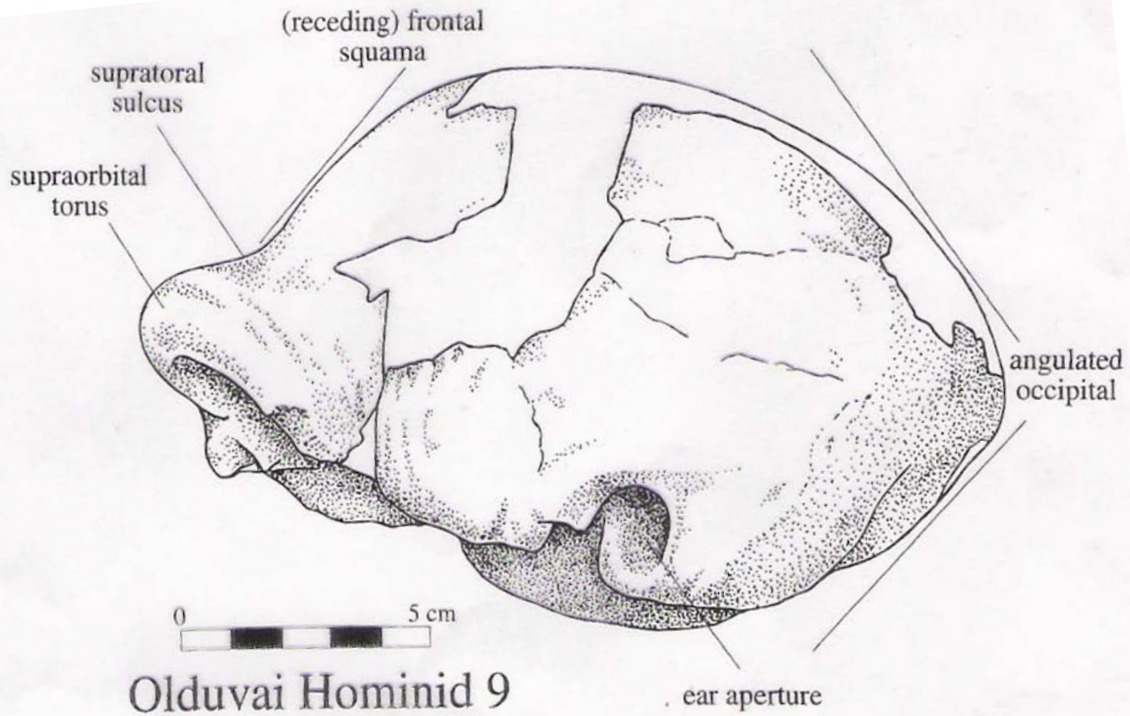

Figure 5.14. Skullcap of Olduvai Hominid 9 from Upper Bed II, Olduvai Gorge (drawn by Kathryn Cruz-Uribe from a cast and slides; © 1999 by Kathryn Cruz-Uribe). The skullcap is roughly 1.2–1.1 my old. It is assigned here to *Homo ergaster*, but among all African fossil skulls, it is the most difficult to separate from skulls of classic Far Eastern *H. erectus*. Conspicuous features it shares with *H. erectus* include a massive, forwardly projecting supraorbital torus, a low, receding frontal bone, a highly angulated occipital, and thick cranial walls.

Homo ergaster vs. A. afarensis Skeletons

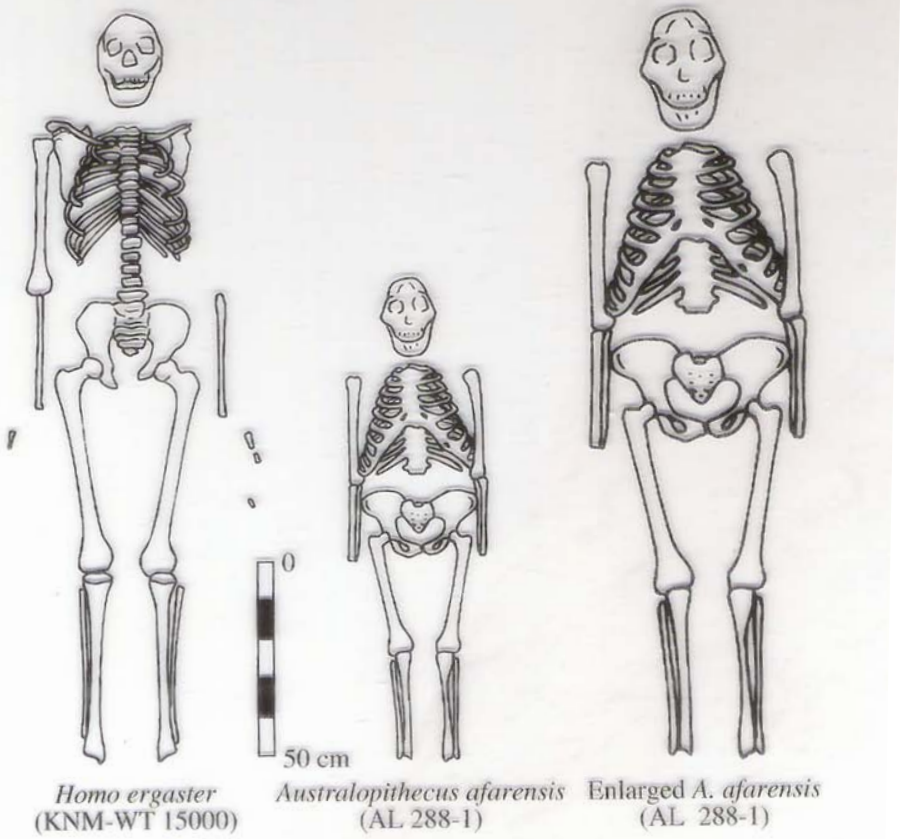

Figure 5.13. *Left:* Skeleton of *Homo ergaster* from Nariokotome, West Turkana, northern Kenya. *Middle:* Skeleton of *Australopithecus afarensis* (AL 288-1, "Lucy") from Hadar, Ethiopia. *Right:* The *A. afarensis* skeleton scaled to the height of the *H. ergaster* skeleton (redrawn after 1843, p. 55). *H. ergaster* was the first hominid species to achieve the stature and bodily proportions of living humans. The *H. ergaster* individual whose skeleton is pictured was probably an eleven- to twelve-year-old boy who stood about 1.60 m (5′ 3″) tall and who might have reached 1.85 m (6′ 1″) at adulthood (1846). His body was long and linear like the bodies of living humans who inhabit similar hot, dry savanna environments. (KNM-WT = Kenya National Museum–West Turkana; AL = Hadar.)

Fossil sites in Java and China

Figure 5.3. Major Quaternary fossil localities of Java (redrawn after 2168, fig. 1).

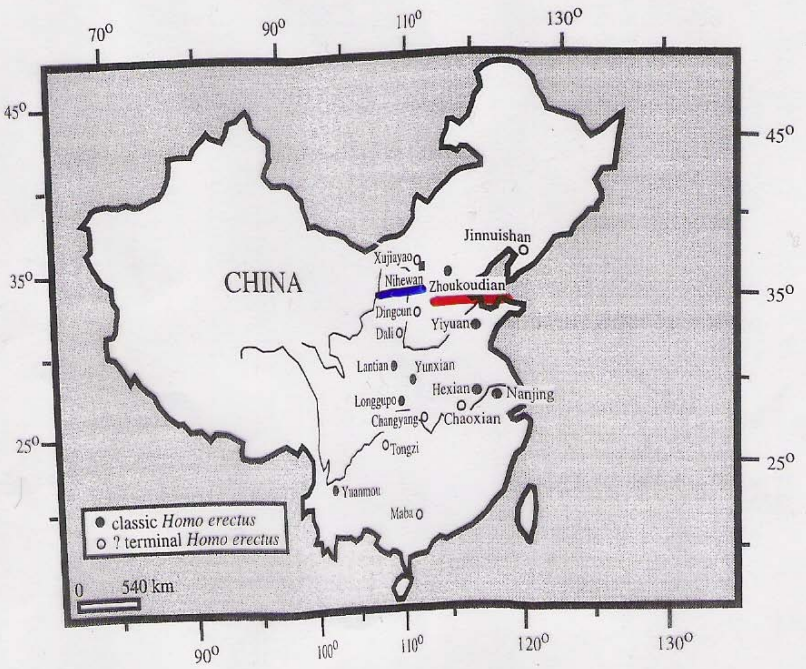

Figure 5.4. The main Chinese sites with fossils of primitive *Homo* (modified after 2533, fig. 1, and 695, fig. 2).

Homo erectus Skulls

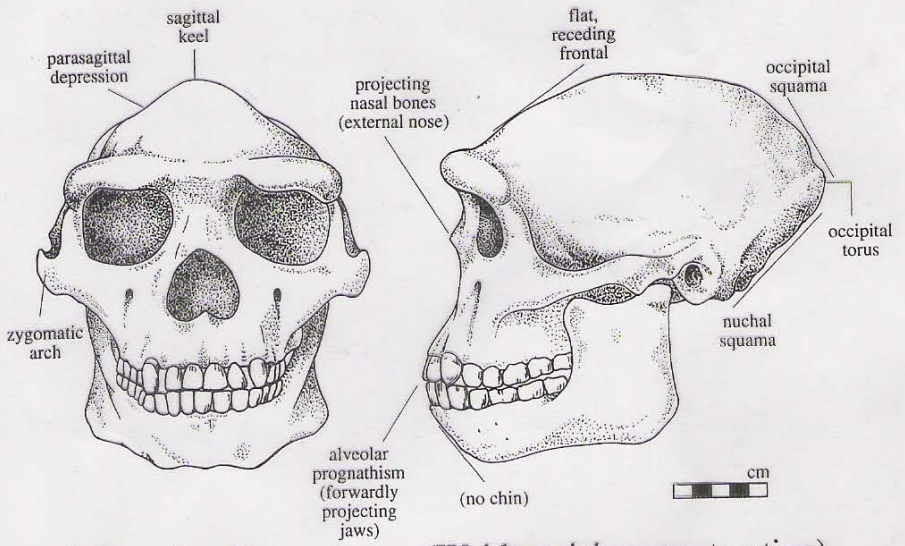

Indonesian *Homo erectus* (Weidenreich reconstruction)

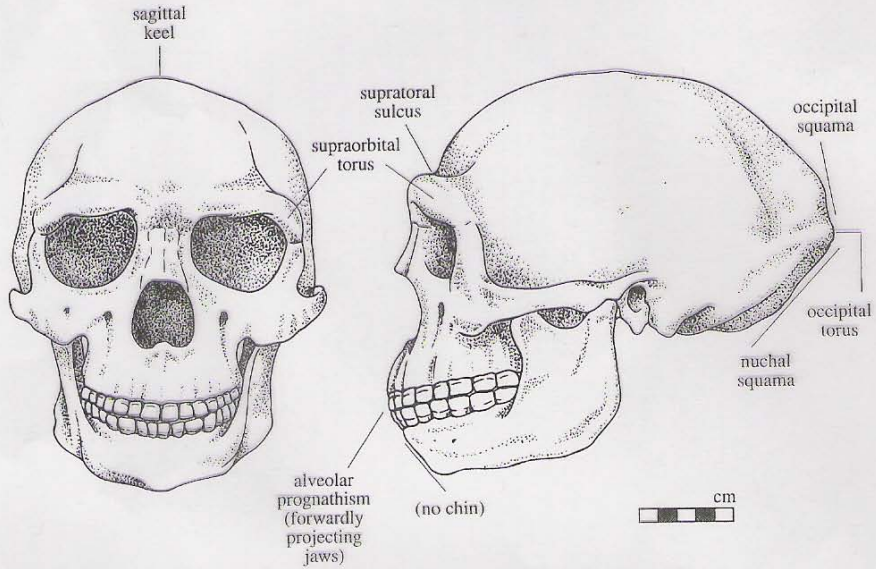

Zhoukoudian *Homo erectus* (Weidenreich reconstruction)

Figure 5.6. Franz Weidenreich's restorations of *Homo erectus* skulls from Sangiran in Java and Zhoukoudian Locality 1 in China (redrawn by Kathryn Cruz-Uribe partly after originals by Janis Cirulis in 1081, pp. 156, 169; © 1999 by Kathryn Cruz-Uribe). Typical *H. erectus* features that are visible in both restorations include a large forwardly projecting, shelflike supraorbital torus, a distinct supratoral sulcus, a low, receding frontal bone, sagittal keeling, a highly angulated occipital with a very prominent occipital torus, and pronounced alveolar prognathism.

Homo erectus and *H. sapiens* Skulls

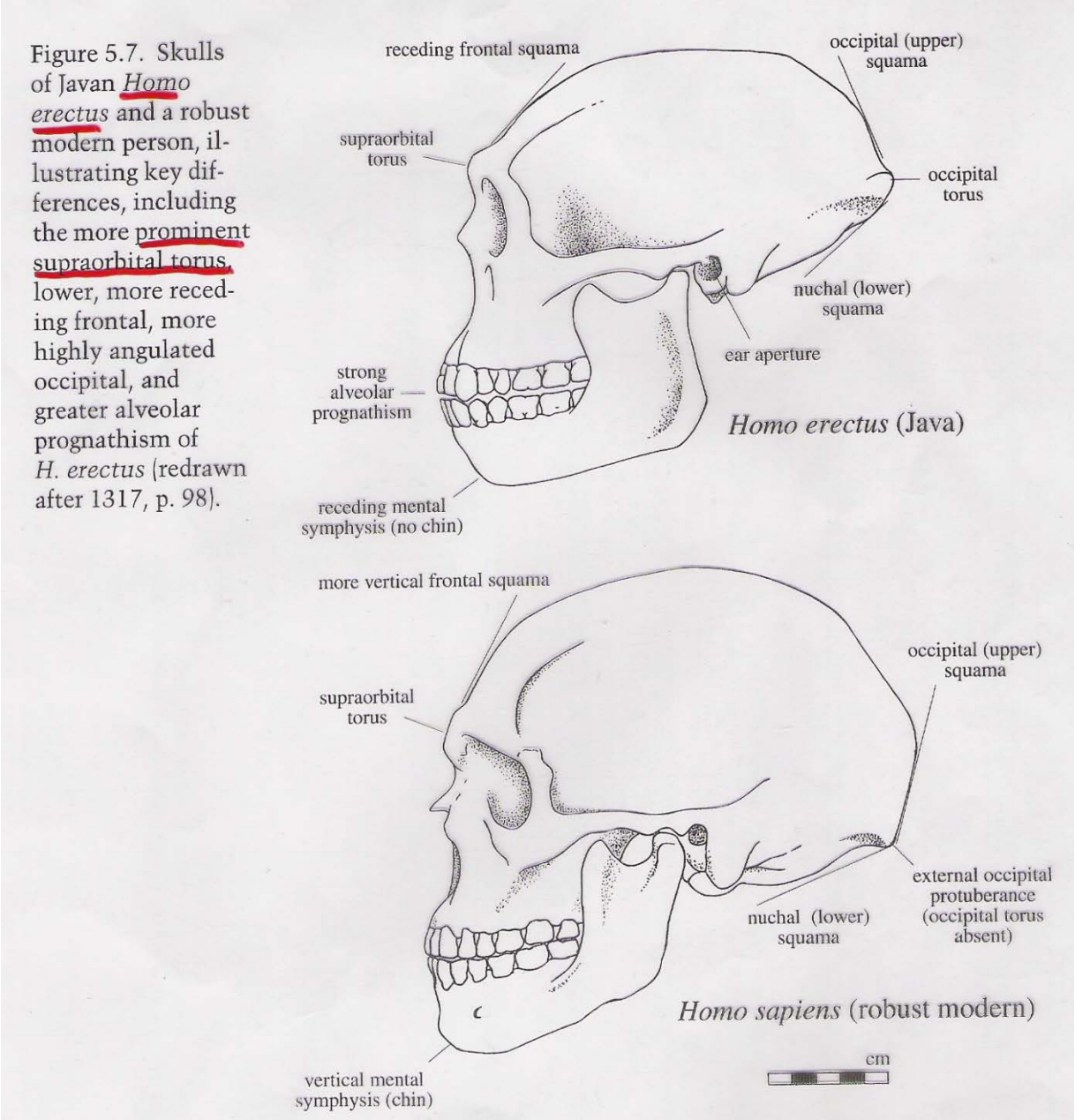

Figure 5.7. Skulls of Javan *Homo erectus* and a robust modern person, illustrating key differences, including the more prominent supraorbital torus, lower, more receding frontal, more highly angulated occipital, and greater alveolar prognathism of *H. erectus* (redrawn after 1317, p. 98).

Homo erectus and *H. sapiens* Mandibles

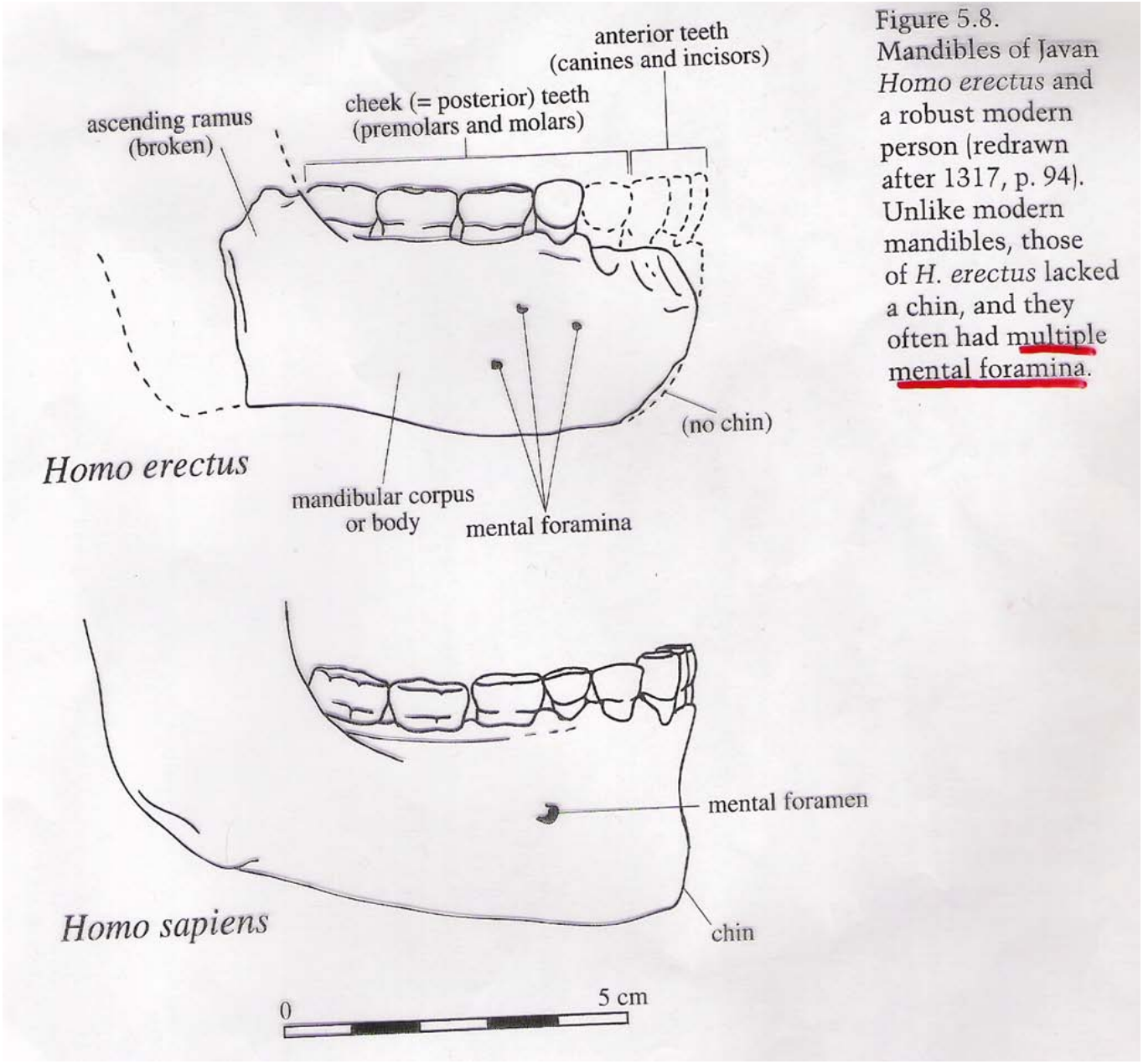

Figure 5.8. Mandibles of Javan *Homo erectus* and a robust modern person (redrawn after 1317, p. 94). Unlike modern mandibles, those of *H. erectus* lacked a chin, and they often had multiple mental foramina.

Narmada Skull (India)

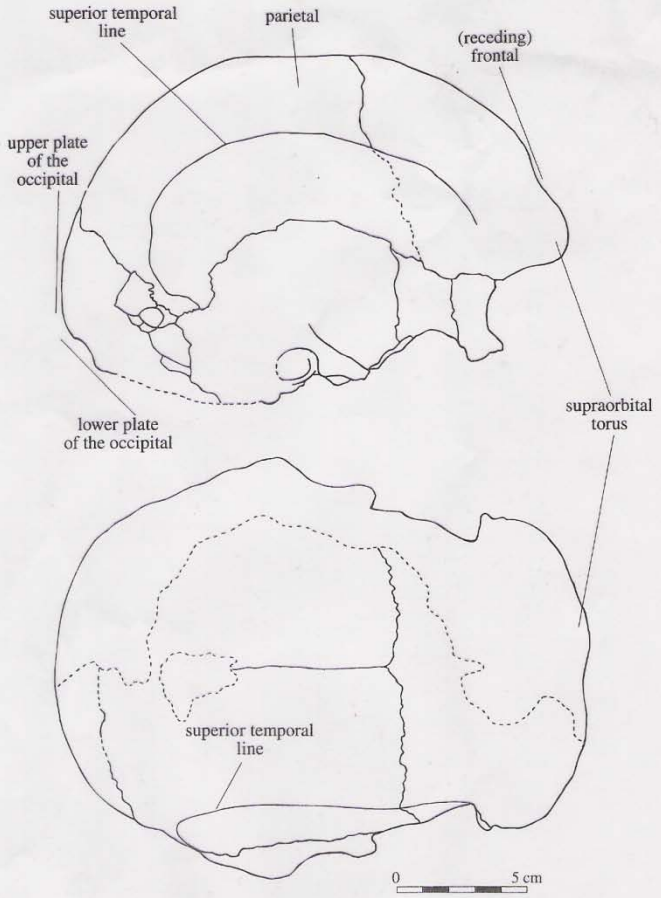

Narmada Skull

Figure 5.15. Skullcap of primitive *Homo* from the Narmada Valley, north-central India (redrawn by Kathryn Cruz-Uribe after 1409, pp. 26, 30; © 1999 by Kathryn Cruz-Uribe). Associated animal bones and "Upper" Acheulean artifacts imply the skull is between 600 and 400 ky old. It combines primitive features like a thick, forwardly projecting supraorbital torus, thick cranial walls, and great basal breadth with advanced features like expanded parietals, a less angulated (flexed) occipital, and a relatively large endocranial capacity (> 1,200 cc). In its mix of primitive and derived characters, it recalls like-aged African and European specimens that are variably assigned to early *Homo sapiens*, early *H. neanderthalensis*, or *H. heidelbergensis*.

Homo Skulls

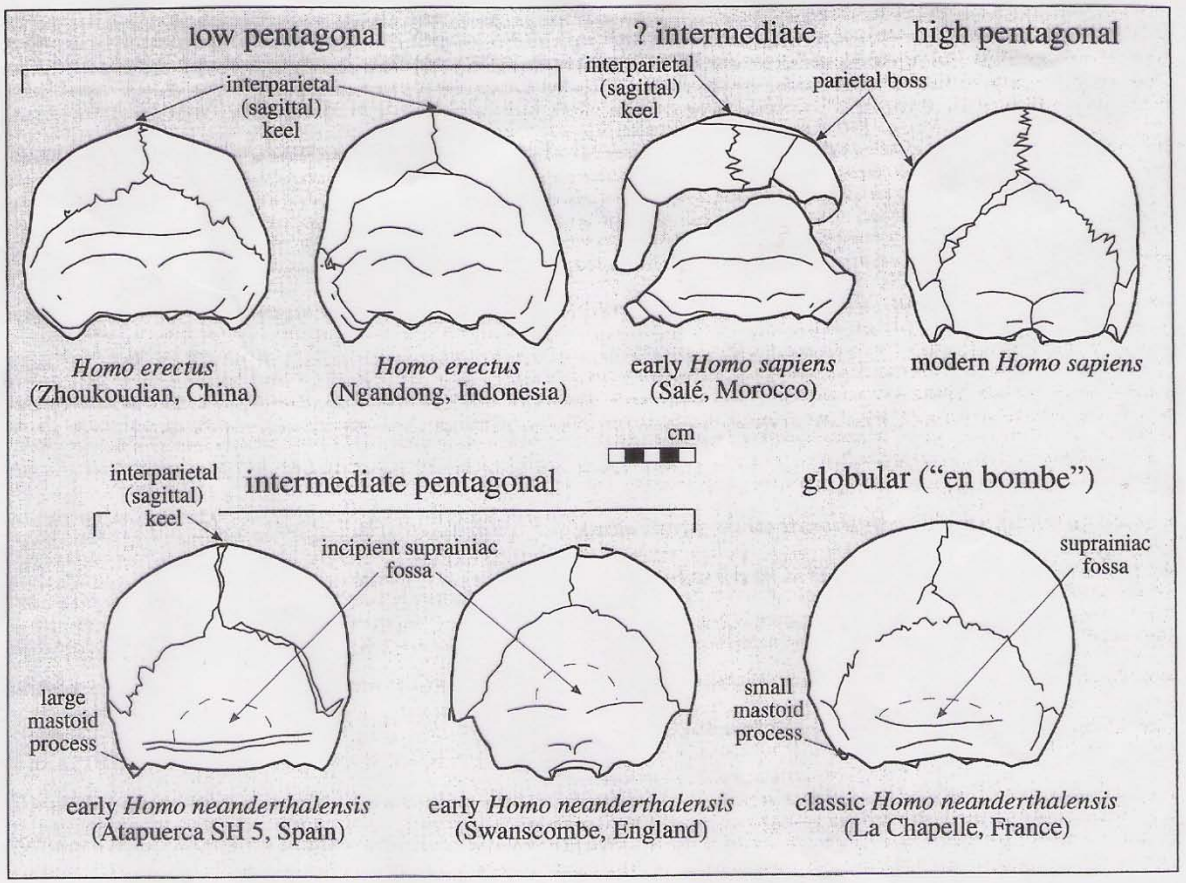

Figure 5.17. Skulls of *Homo erectus*, early *H. sapiens*, modern *H. sapiens*, early *H. neanderthalensis*, and classic *H. neanderthalensis* viewed in occipital (rear) view (redrawn after 1096, p. 41, and 79, photo on p. 224). From this perspective, skulls of *H. erectus* are pentagonal with sidewalls that slope sharply inward from near the base ("low pentagonal"); skulls of early *H. sapiens* and early *H. neanderthalensis* are pentagonal with walls that tend to rise more vertically; skulls of classic *H. neanderthalensis* are globular with walls that bulge outward at midparietal level; and skulls of modern *H. sapiens* are pentagonal with walls that rise vertically to a point high on the parietals before sloping inward ("high pentagonal"). Skulls of modern *H. sapiens* also tend to show a boss or bulge at the point where the parietals turn inward. Arguably, the early *H. sapiens* skull from Salé, Morocco, shows an incipient boss.

Homo neanderthalensis

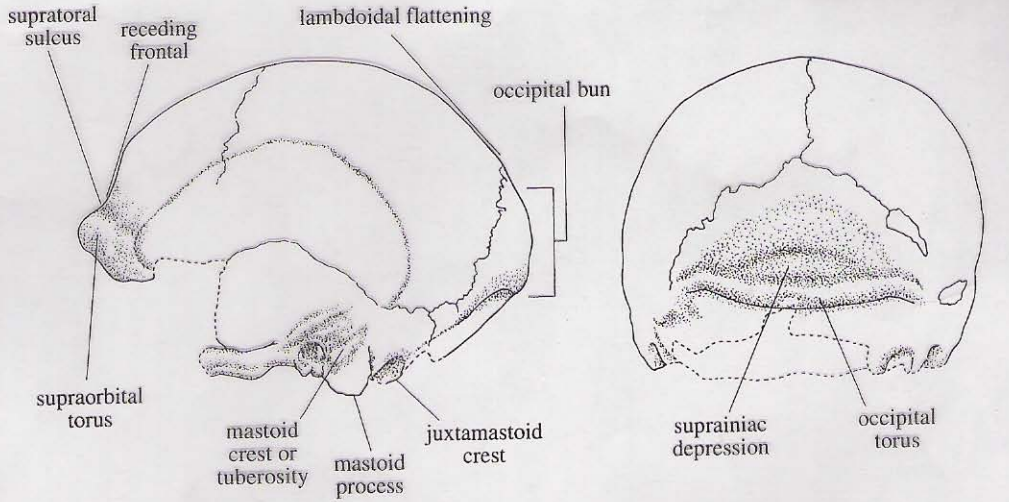

Spy 2 (Neanderthal)

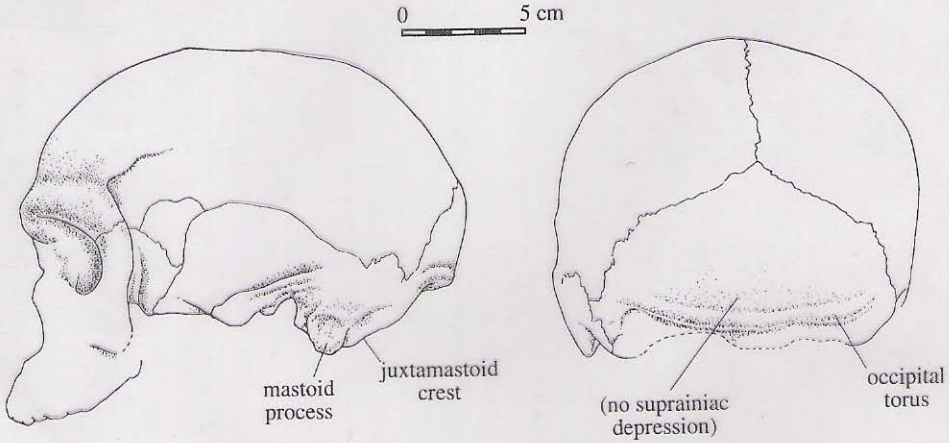

Jebel Irhoud 1 (non-Neanderthal)

Figure 6.5. One of the Neanderthal skulls from Spy Cave, Belgium, compared with the somewhat older non-Neanderthal skull from Jebel Irhoud, Morocco (redrawn after 1863, pp. 624, 627). The Irhoud skull has sometimes been labeled Neanderthal, but it differs from typical Neanderthal skulls in several crucial features, including its shorter and flatter face, its more rectangular orbits, its more parallel-sided (less globular) braincase, and its lack of a suprainiac fossa or depression. In most of these features it anticipates anatomically modern people, near whose ancestry it may lie.

Homo neanderthalensis

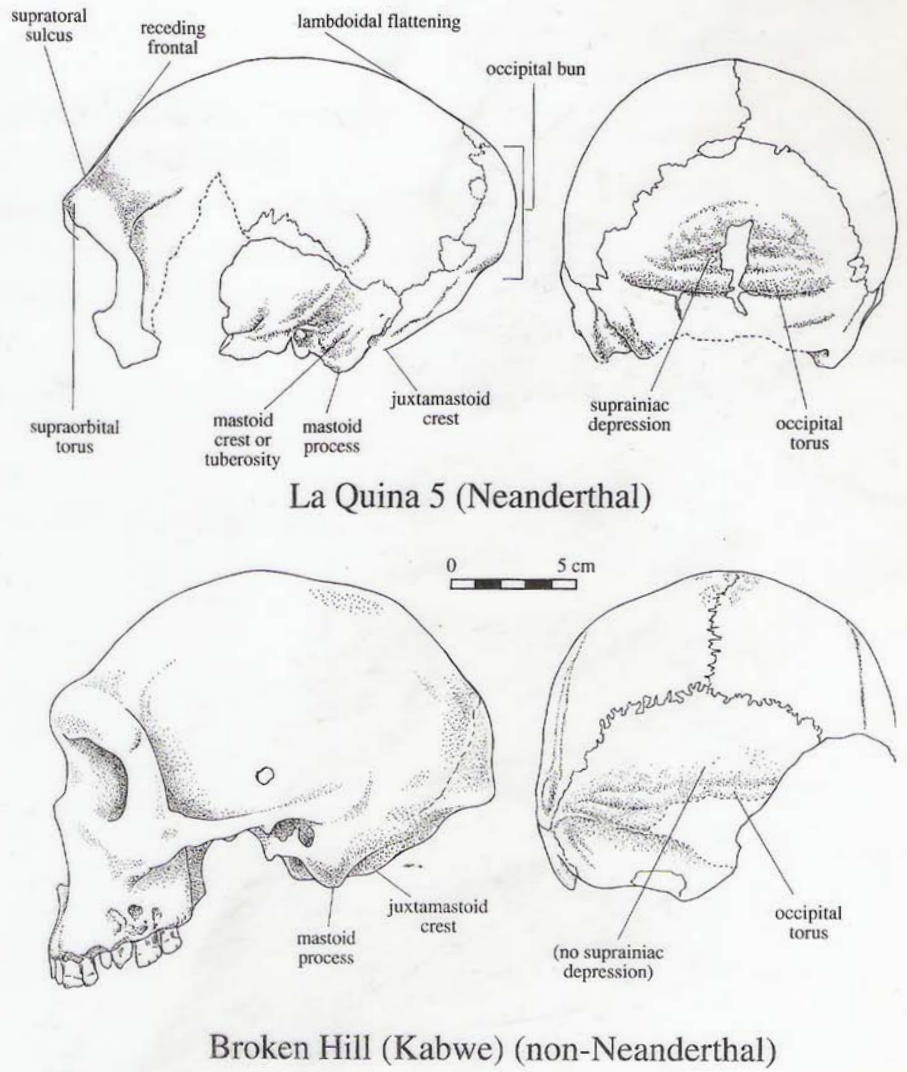

Figure 6.6. Neanderthal skull from La Quina in France compared with the non-Neanderthal skull from Broken Hill (Kabwe), Zambia (redrawn after 1863, pp. 623, 626). The Broken Hill skull has sometimes been identified as an African Neanderthal, but it lacks such characteristic Neanderthal features as the suprainiac depression and the globular shape in rear view (it is more angular from behind and has its maximum breadth nearer the cranial base). It also antedates the Neanderthals by a substantial interval and is now widely regarded as a representative of mid-Quaternary African *Homo sapiens*, as discussed in chapter 5.

Homo neanderthalensis Mandibles

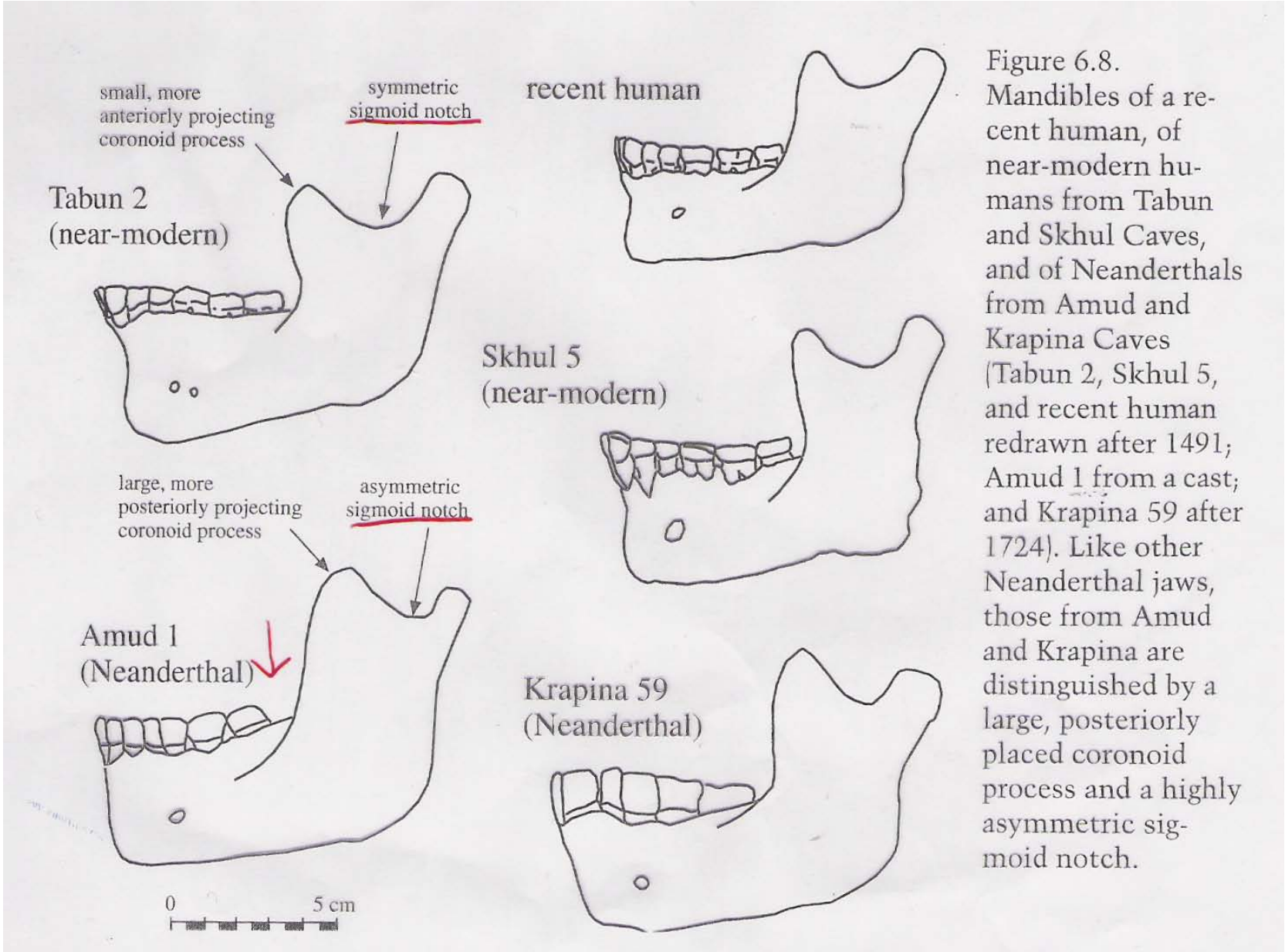

Figure 6.8. Mandibles of a recent human, of near-modern humans from Tabun and Skhul Caves, and of Neanderthals from Amud and Krapina Caves (Tabun 2, Skhul 5, and recent human redrawn after 1491; Amud 1 from a cast; and Krapina 59 after 1724). Like other Neanderthal jaws, those from Amud and Krapina are distinguished by a large, posteriorly placed coronoid process and a highly asymmetric sigmoid notch.

Shanidar Skull

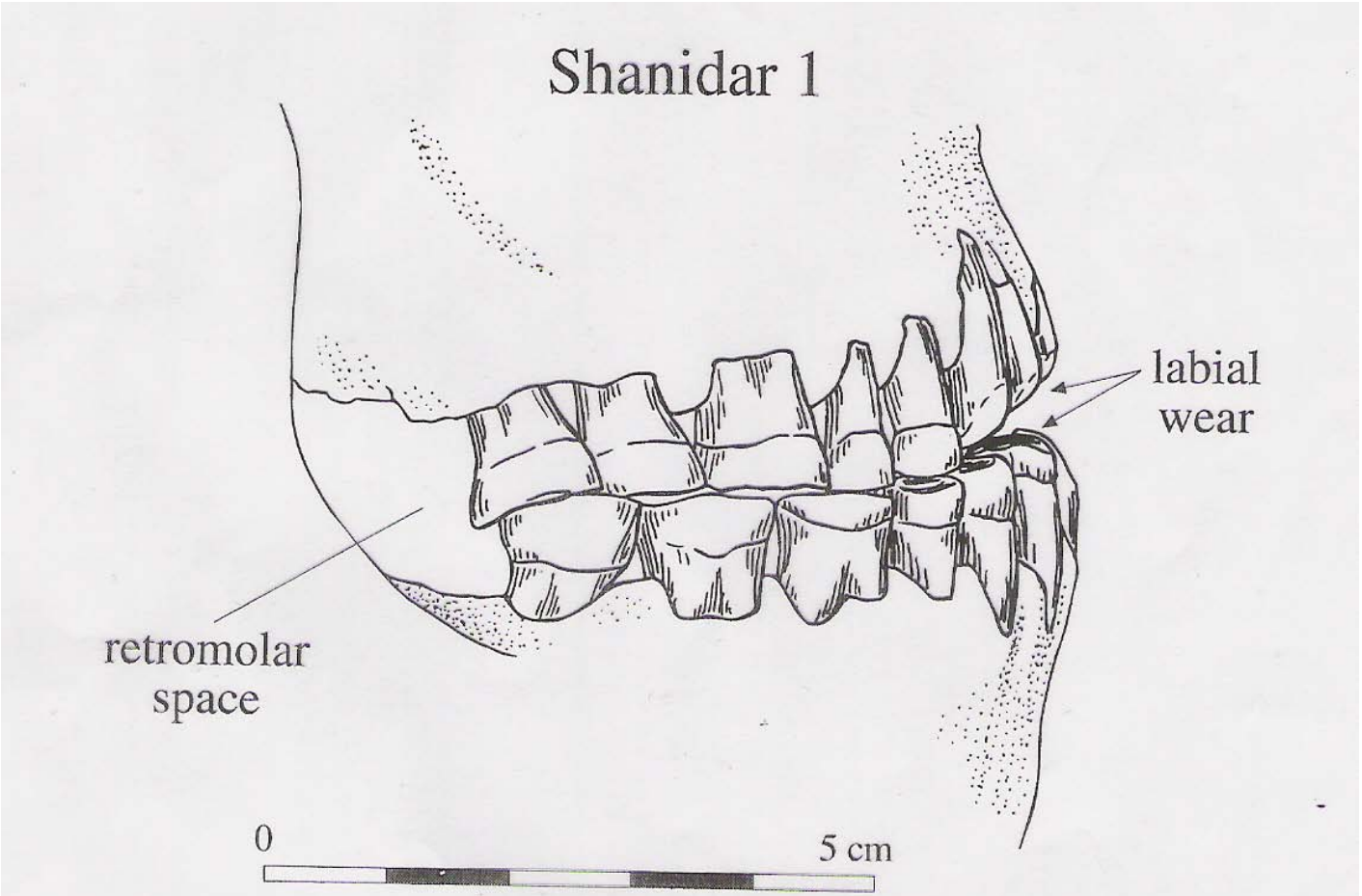

Figure 6.10. Enlarged view of the dentition of Shanidar skull 1 showing the retromolar space and the rounded wear on the labial surface of the incisors that are characteristic Neanderthal features (drawn by Kathryn Cruz-Uribe from a photograph; © 1999 by Kathryn Cruz-Uribe). The wear resulted from exceptional use of the incisors, perhaps for clamping or gripping skins or other objects.

Homo Phylogeny

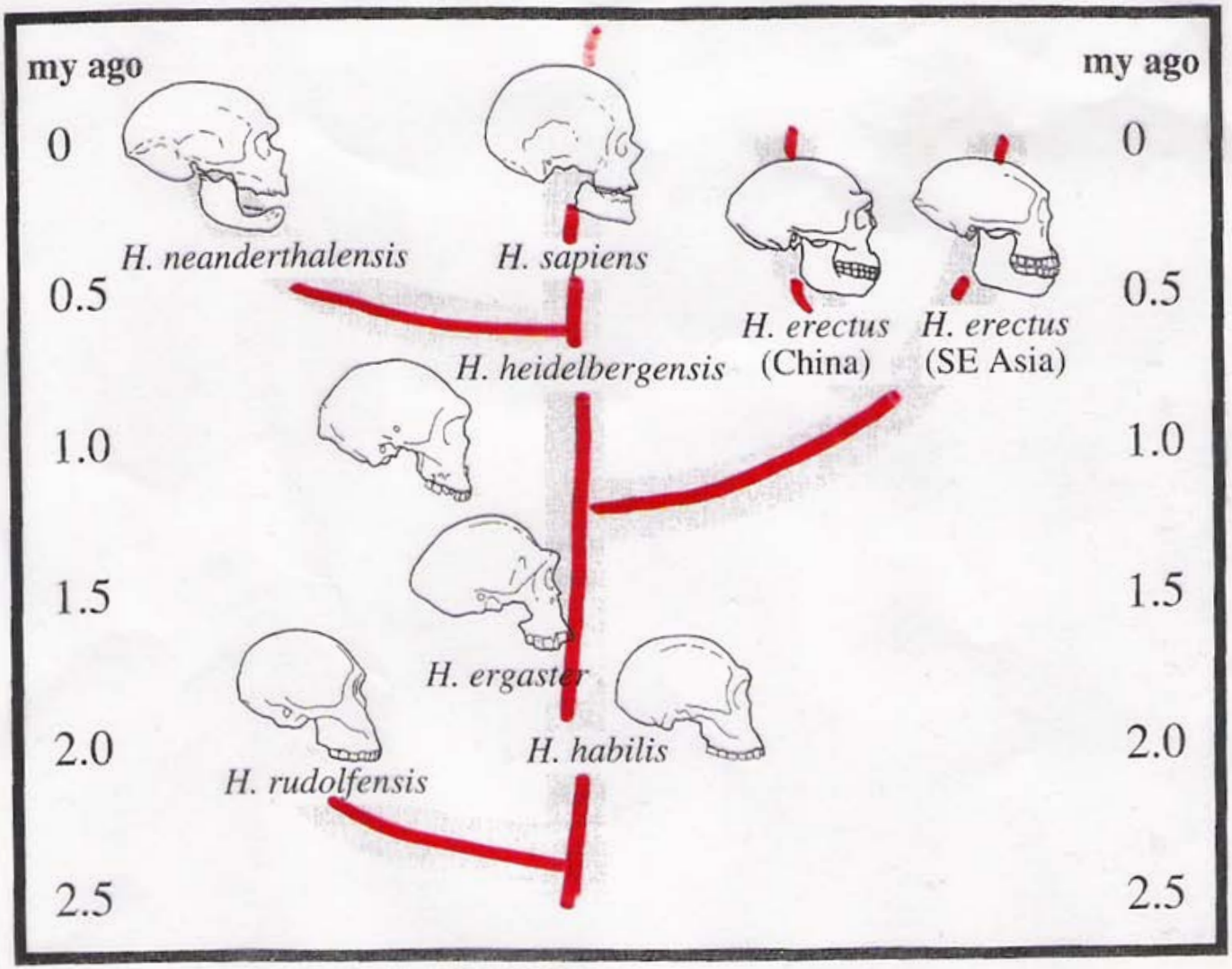

Figure 5.1. The phylogeny of the genus *Homo*.

Movius Line

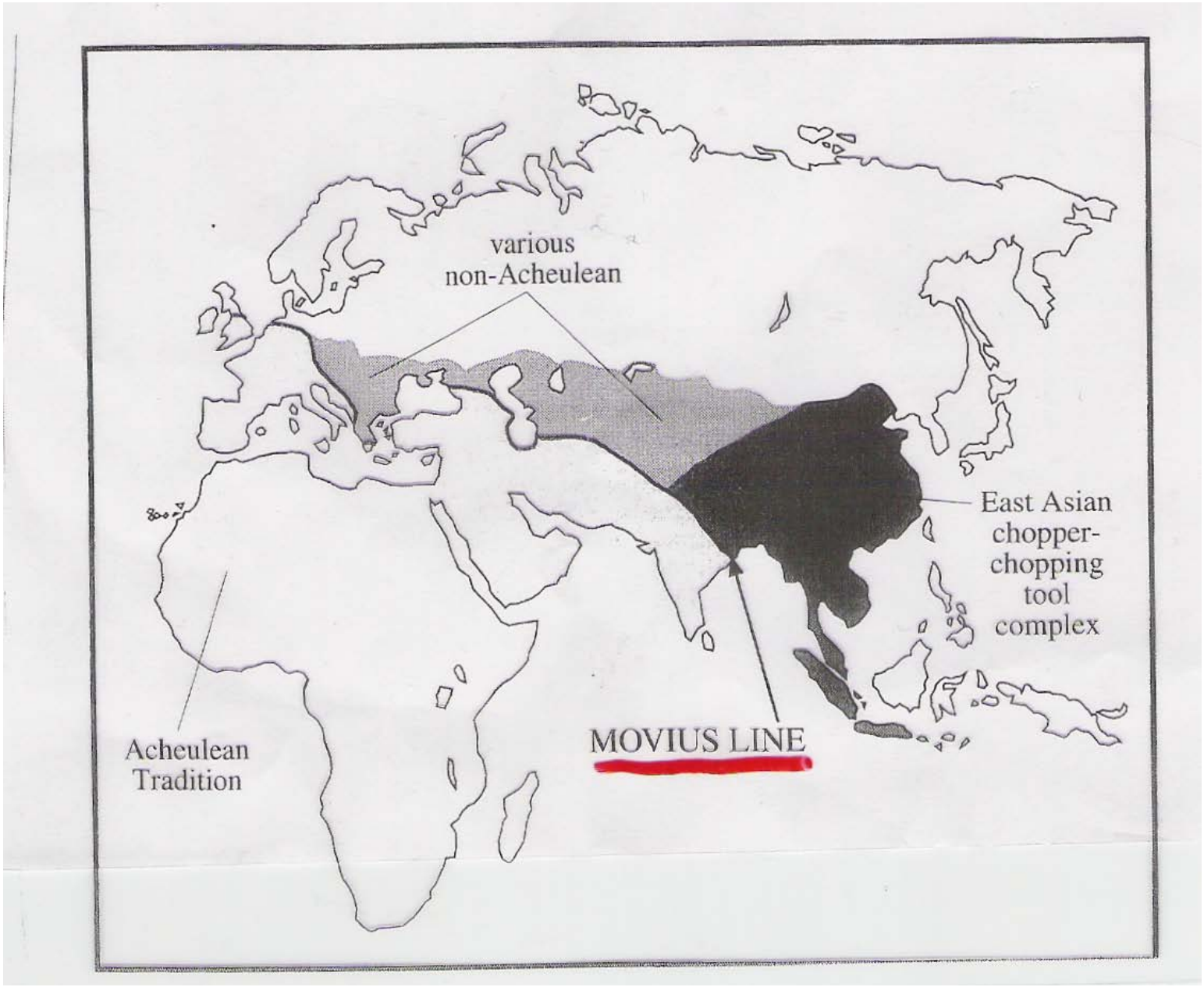
various
non-Acheulean
East Asian
chopper-
chopping
tool
complex
Acheulean
Tradition
MOVIUS LINE

African Acheulean Sites

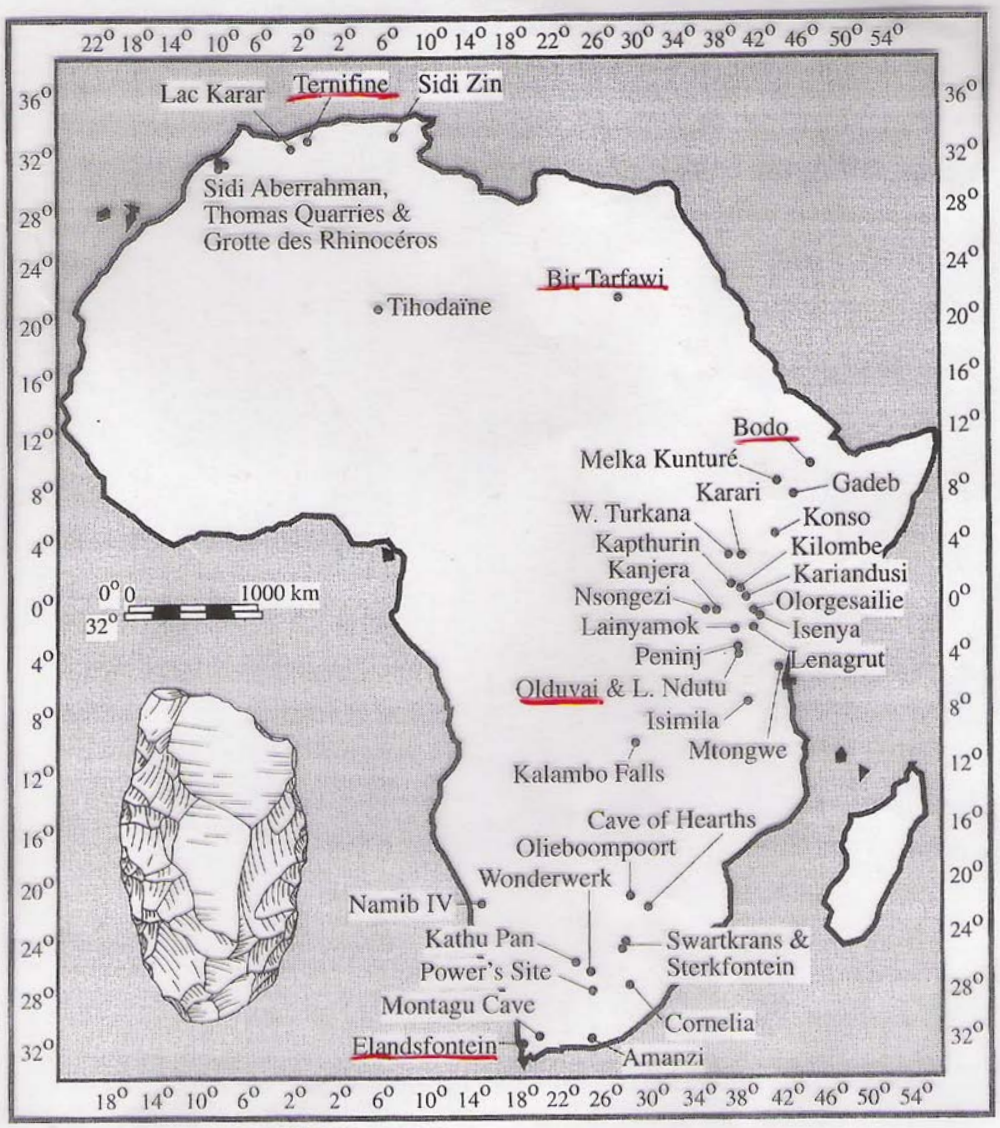

Figure 5.40. Map showing the approximate locations of major African Acheulean sites.

Chopper and Chopping Tool Industry

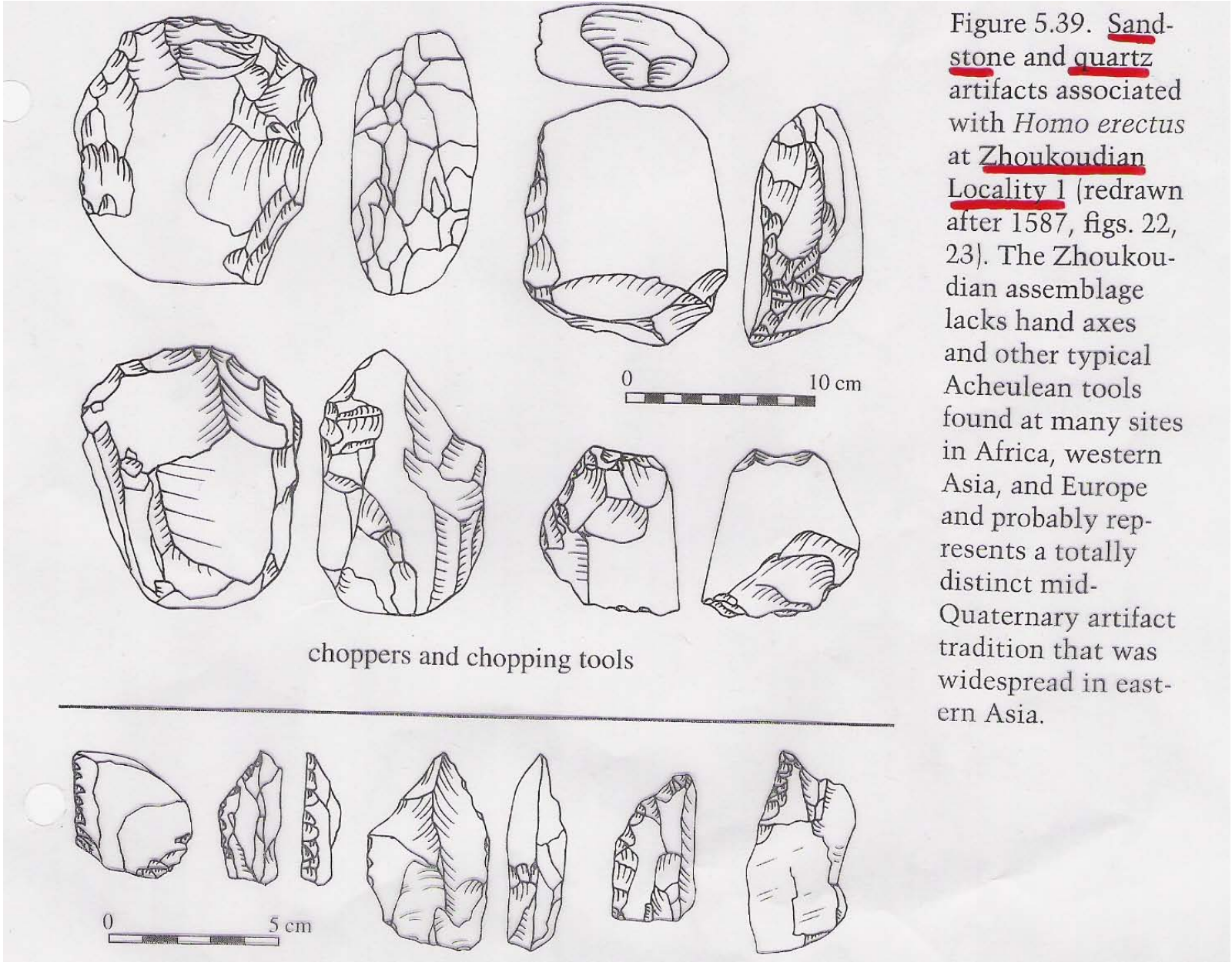

Figure 5.39. Sandstone and quartz artifacts associated with *Homo erectus* at Zhoukoudian Locality 1 (redrawn after 1587, figs. 22, 23). The Zhoukoudian assemblage lacks hand axes and other typical Acheulean tools found at many sites in Africa, western Asia, and Europe and probably represents a totally distinct mid-Quaternary artifact tradition that was widespread in eastern Asia.

European Sites

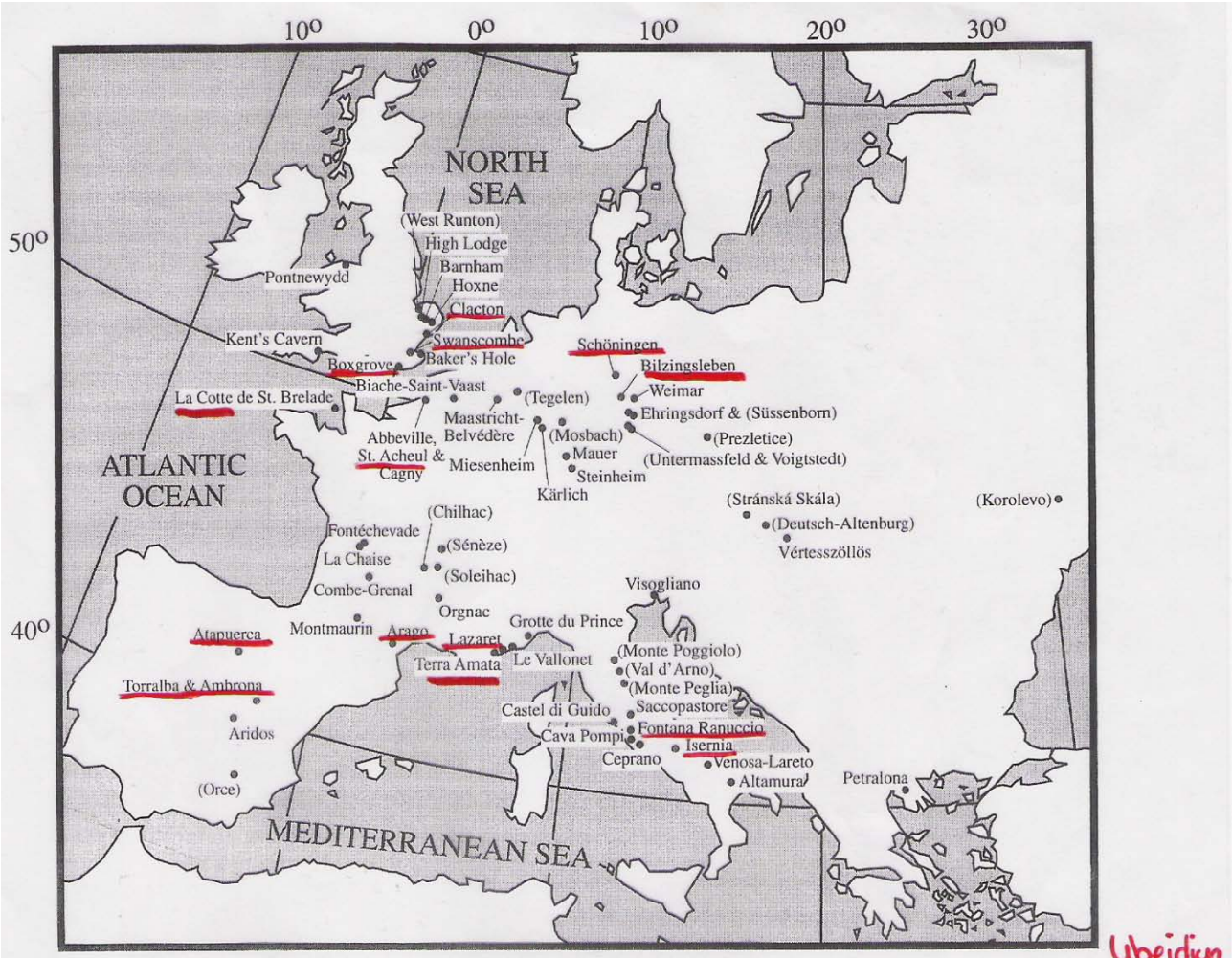

Figure 5.36. The approximate locations of early and mid-Quaternary archeological and human fossil sites in Europe. Some specialists believe that Korolevo in Ukraine, Stránská Skála and Prezletice in the Czech Republic, Kärlich in Germany, Le Vallonet, Chilhac, and Soleihac in France, Isernia and Ceprano in Italy, and Atapuerca and Orce in Spain all document human presence before 500 ky ago, but the case is truly compelling only for Atapuerca (Trinchera Dolina). Sites shown in parentheses are older than 500 ky ago but lack firm evidence for human presence.

Ubeidiya Israel

Late Acheulean Artefacts from Boxgrove

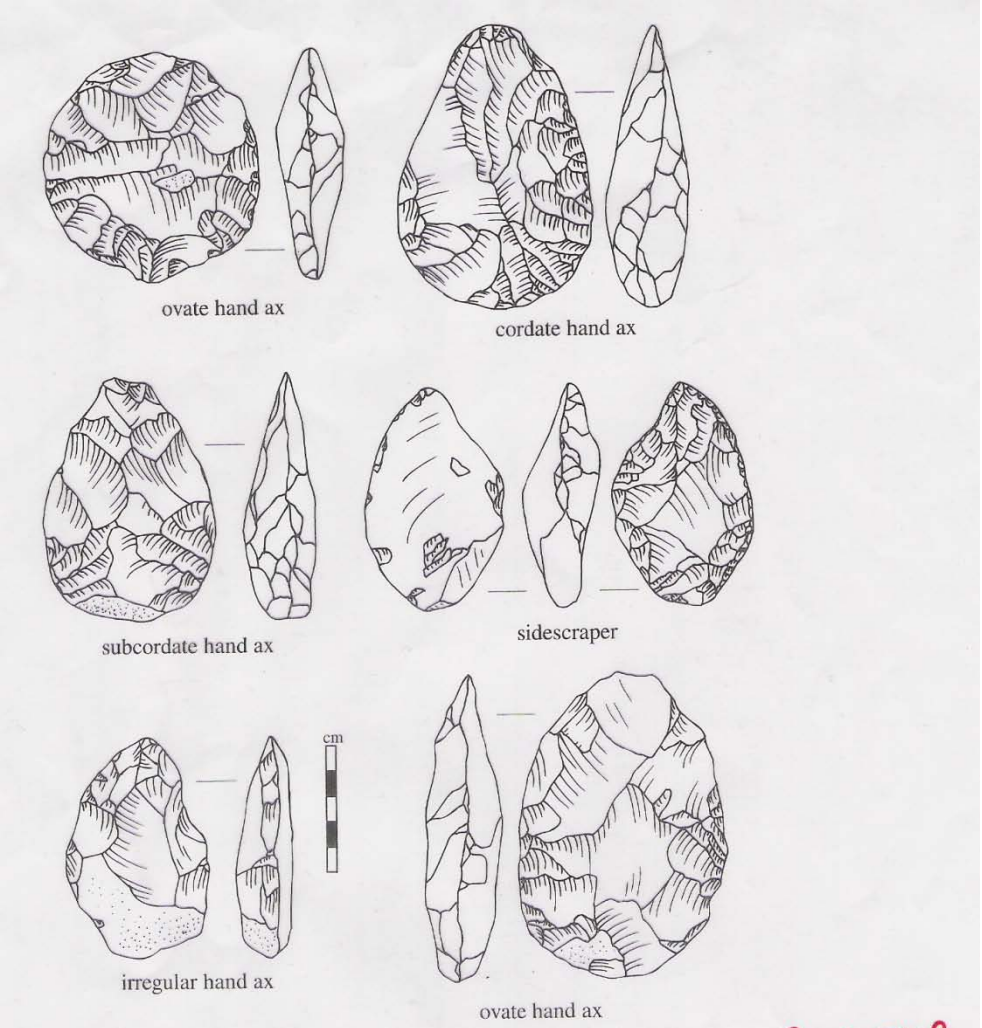

Figure 5.44. Late Acheulean artifacts from southern England (redrawn after 2519, p. 147). Finely crafted hand axes of various shapes and sizes are the hallmark of the late Acheulean in Europe, but biased collection probably artificially raised their frequency in most assemblages obtained in the later nineteenth and early twentieth centuries. Fine hand axes tend to be much less abundant in samples that have been carefully excavated in more recent decades.

Boxgrove

Bone Tool from Bilzingsleben

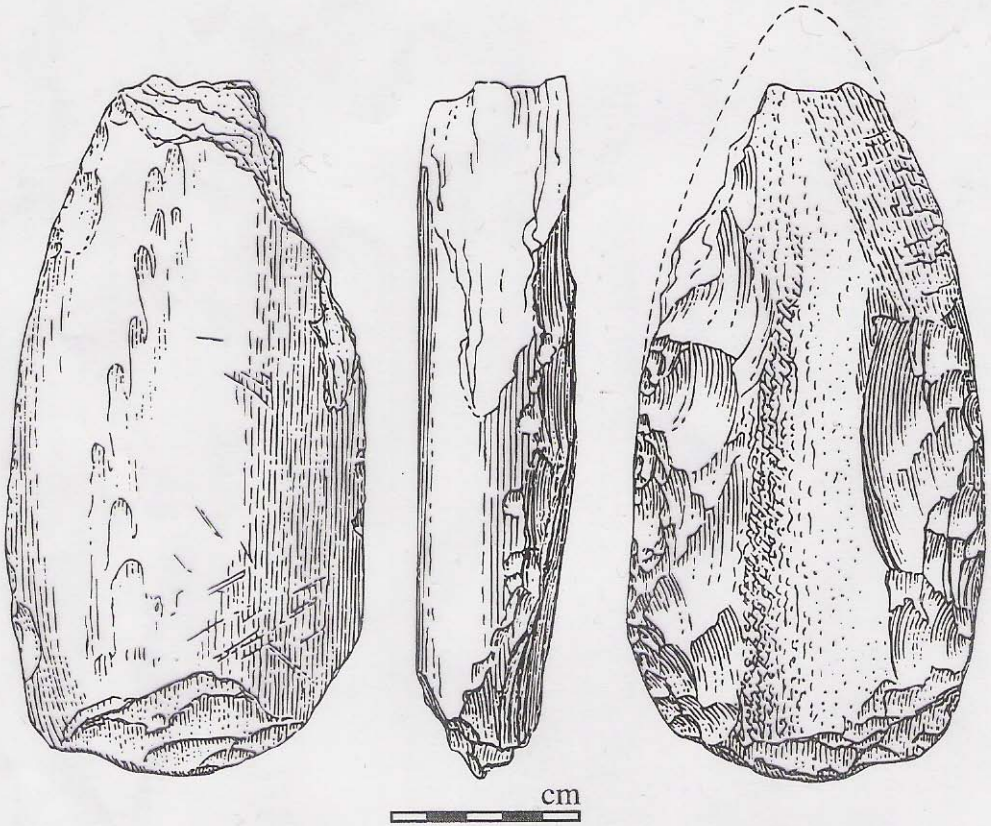

Figure 5.46. A flaked fragment of elephant bone from Bilzingsleben, Germany (after 1434, fig. 4). The Bilzingsleben site is probably about 350 ky old, and it has provided other flaked bone artifacts in addition to numerous stone artifacts and some fragmentary human remains. The Bilzingsleben bone artifacts and similar ones from other sites (particularly in Italy) show that early people sometimes flaked bone in the same way they flaked stone. However, only people after 50 ky ago routinely carved or ground bone to produce formal artifacts.

Spears from Schoningen

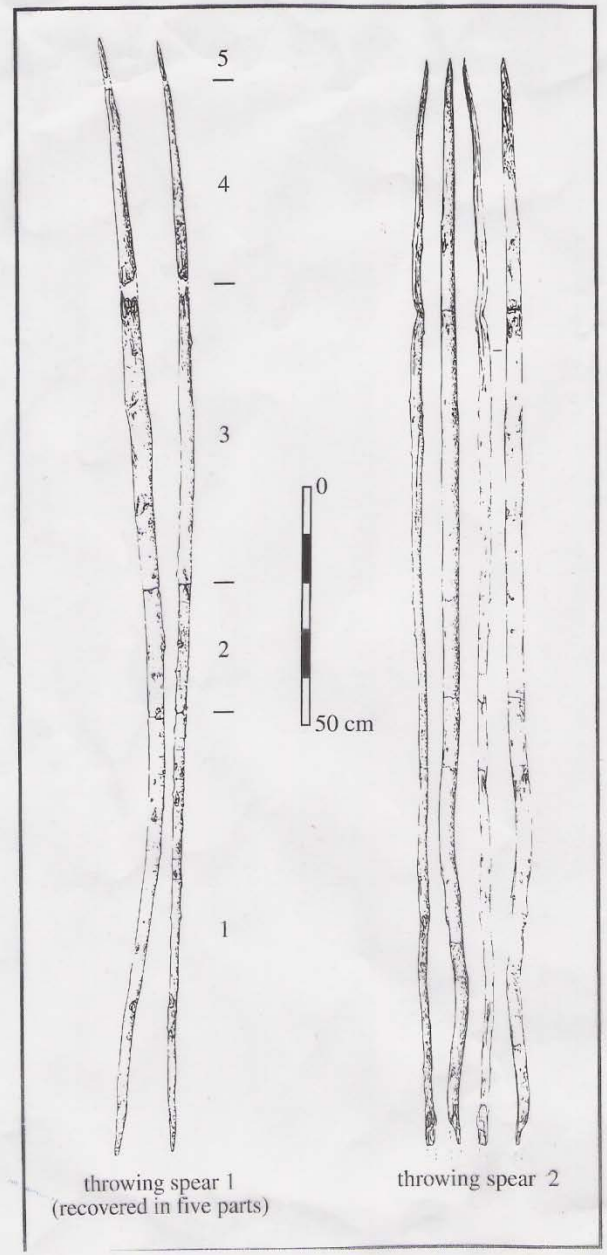

Figure 5.47. Multiple views of two of the three wooden throwing spears recovered from 400 ky old lakeside deposits at Schöningen, Germany (redrawn after 2170, fig. 9). The spears are the oldest known unequivocal human hunting weapons. They were probably used to hunt wild horses, whose bones abound in the same deposits.

Hominid Phylogeny

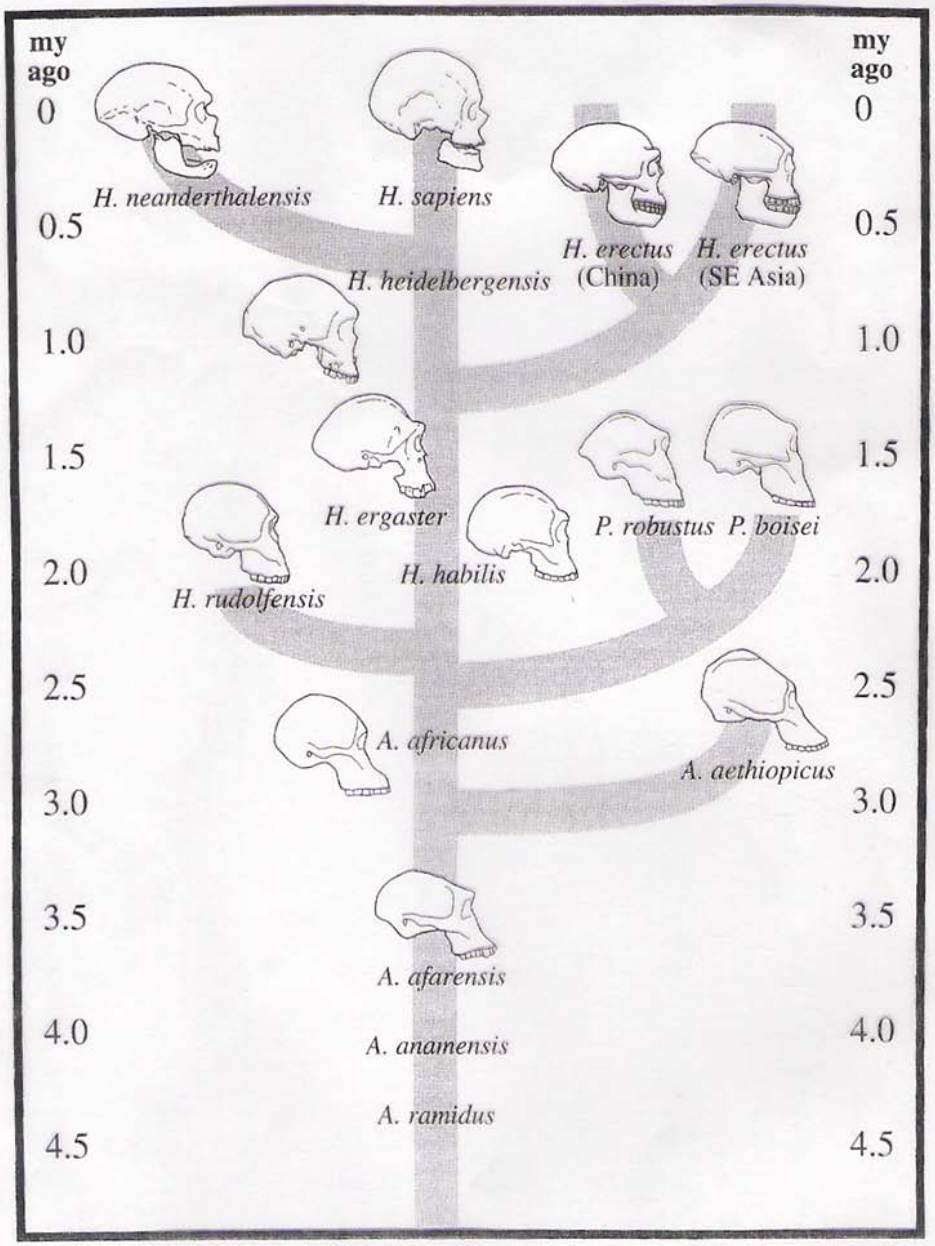

Figure 8.1. A working phylogeny linking the human species discussed in the text. (*A.* = *Australopithecus*; *P.* = *Paranthropus*; *H.* = *Homo*). The postulated branching events within *Homo* after 2–1.5 million years ago are particularly controversial.